

An Evaluation of Seeding Effectiveness in the Central Colorado Mountains River Basins Weather Modification Program

Submitted to
Grand River Consulting Corporation
by
Research Applications Laboratory of the
National Center for Atmospheric Research (RAL/NCAR)

Contributors: Daniel Breed, Duncan Axisa, Changhai Liu, and Xinyuan Feng

15 April 2015



(Northerly view from Berthoud Pass)

Executive Summary

Introduction

Cloud seeding of winter orographic storms follows a conceptual model that was established in the mid 1950's. The concept is based on the fact that the development of snow is hindered or delayed, under certain cloud conditions, by the lack of natural ice nuclei (IN). IN are those atmospheric particles onto which water vapor condenses and subsequently freezes to start the growth into ice particles and snow. Natural IN that activate or start the freezing process in layer clouds at temperatures warmer than about $-15\text{ }^{\circ}\text{C}$ ($+5^{\circ}\text{F}$) are sparse. Introducing large numbers of artificial IN (i.e., cloud seeding) that activate at warmer temperatures can “jump start” the snow growth process and presumably make it more efficient.

The conceptual model of seeding winter orographic clouds has been refined over several decades as our understanding of the complexities of mountain flows and precipitation processes advanced. In simplified terms, the following chain of events is hypothesized for seeding from the ground. Seeding material, usually in the form of silver iodide (AgI) particles, is released from a ground-based generator and carried by the wind toward the target area. The plume of AgI rises and disperses such that it can effectively mix into cloudy air. The AgI particles nucleate ice in cloudy conditions at temperatures colder than about $-5\text{ }^{\circ}\text{C}$ ($+23^{\circ}\text{F}$) but are much more effective as temperatures cool to about $-8\text{ }^{\circ}\text{C}$ ($+18^{\circ}\text{F}$). The ice crystals then grow, forming precipitation-sized particles and falling to the ground as snow.

One of the critical steps necessary for cloud seeding to be effective, and one of the most difficult to assess, is getting the seeding material into cloud conditions susceptible to seeding. These conditions are the regions in clouds where liquid cloud droplets exist at sub-freezing temperatures (super-cooled liquid water) warmer than about $-15\text{ }^{\circ}\text{C}$ ($+5^{\circ}\text{F}$). Seeding plumes in the Colorado programs are generated by ground-based generators. Therefore, the first step in evaluating the effectiveness of an operational cloud seeding program is to determine when “seedable” conditions exist, and another important step is to assess the likelihood that seeding plumes are reaching seedable conditions and affecting snowfall in the areas of interest (i.e., target areas).

There are currently seven wintertime cloud seeding programs in Colorado spanning the state from the San Juan's in the southwest to the Winter Park area of the central Rockies. These programs involve more than 100 ground-based generators. The focus of this study was limited to Target Area 2, shown in Figure A, of the Central Colorado Mountains River Basins program (CCMRB), which includes 27 ground-based generators. Several avenues of study were to be addressed in this work, much of which included numerical modeling efforts. As the study evolved however, two major tasks were identified and completed as a proof-of-concept in evaluating the effectiveness of the CCMRB program:

Task 1. Develop a climatology of conditions relevant to seeding, using criteria such as temperature, cloud water content, and winds at various levels, liquid water path, stability, and snow water equivalent or snowfall, for precipitation events across Target Area 2. The climatology

utilized numerical model output (re-analysis of actual conditions) from eight winter seasons (2000-2008) at points every 4-km.

Task 2. Simulate conditions during a seeding case to assess the utility and improvement of using a higher resolution model (≤ 1 -km grid spacing) to simulate seeding events compared to the 4-km model output. The high-resolution model run was used to assess seeding plumes using a transport and diffusion modeling tool called HYSPLIT.

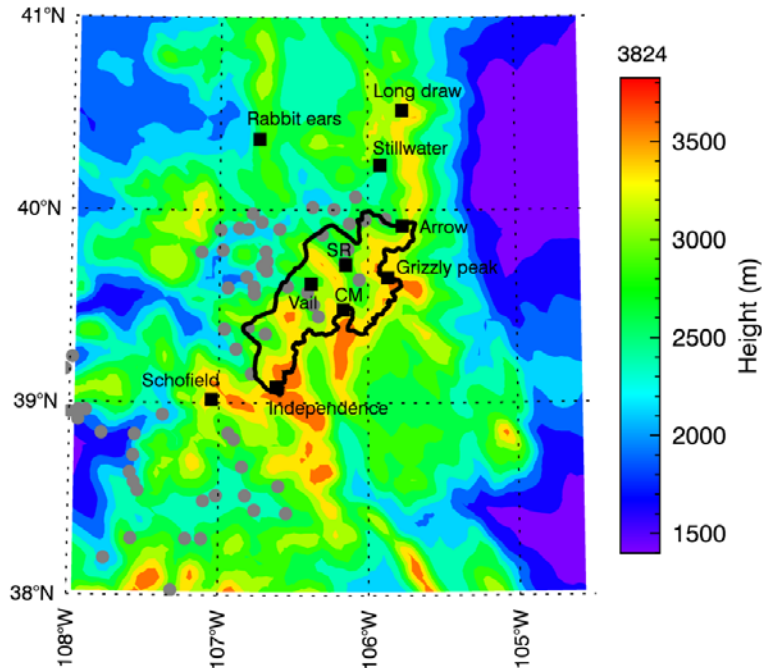


Figure A. Plot of terrain height over the numerical model domain. All cloud seeding generator locations identified by the CWCB are indicated by the gray dots, but not all of them are part of the CCRMB program. The highlighted polygon denotes Target Area 2. A selection of SNOTEL sites are identified by black square symbols (abbreviations: SR - Summit Ranch, CM - Copper Mountain).

This report includes background on potential extra-area effects and on operational seeding criteria to provide context for the CCMRB programs. A detailed climatology of winter conditions in Target Area 2 is presented and combined with seeding criteria to highlight areas of seedable conditions, specific during northwesterly flow. A high-resolution model simulated one storm period known to meet operational seeding criteria, targeting the Winter Park area, and was compared to the coarser 4-km WRF model simulation. HYSPLIT was used to investigate plume behavior for ten seeding generators close to Winter Park, not all of which were used in this seeding event. Results from past studies and the limited results of this study led to preliminary recommendations on generalized seeding generator locations and operations, and outlined the next steps to better assess the seeding assumptions and operations in the CCMRB program.

Background – Extra-area Effects and Seeding Criteria

A potential change in precipitation due to seeding in regions outside of primary target areas or during periods beyond what might be expected from seeding operations is an issue frequently raised by water users, stakeholders, and the general public. These potential extra-area effects are also important scientifically in evaluating seeding projects. Here we focus on two approaches to address potential extra-area effects: 1) water balance estimates in the hydrologic cycle, which is a large-scale approach; and 2) a review of past studies concentrating on winter orographic storm projects.

During storm passage over a mountain, the vast majority of the total water in the atmosphere (water vapor, cloud water-ice, precipitation) remains in the water vapor state. Typically, only about 20% of the water is converted into cloud. Generally, about 30% of the cloud gets converted into precipitation, or 6% of the total atmospheric water (0.2 times 0.3). If cloud seeding enhanced precipitation by 15% in the storm, that equates to converting an additional 0.9% of the total atmospheric water (0.15 times 0.06) into precipitation. In terms of extra-area effects, the approximate 1% change in atmospheric water components (vapor to cloud condensate to precipitation) due to precipitation increases from seeding is negligible and impossible to measure at the time scales and areal scales covered by standard observations. Hence, in this context the argument that increased precipitation due to seeding measurably decreases precipitation downwind is without merit. However, over short time periods or small areas, precipitation changes or re-distribution due to seeding may have enhanced effects that reach measurable amounts.

Typical cloud-seeding efforts focus on increasing the precipitation efficiency in seeded clouds such that their precipitation falls within a target area. However, even for mountain clouds, which dissipate downwind of the barrier, the plume of seeding material will advect some distance beyond the target area. Therefore, seeded precipitation could conceivably fall beyond the boundaries of the target area, and the seeding material (usually silver iodide) could also advect beyond the target – so-called “extra-area” effects.

Several studies have documented seeding material or tracer concentrations, released with seeding material, being transported downwind of seeding sites many tens of kilometers (60 miles or more). There have also been many studies that looked at precipitation data downwind of target areas. While these studies have generally shown a positive impact on precipitation downwind of target areas, the results have not been statistically significant because of the small impact and large natural variability in precipitation. Nonetheless, a comprehensive summary of studies on extra-area effects has shown fairly consistent evidence of downwind effects of precipitation *enhancement* by cloud seeding. The spatial extent of the positive extra-area seeding effects may extend to a hundred miles. The extra-area effects did not appear to produce regional impacts on the water balance, nor on the natural precipitation on a regional scale. However, the results require more verification, which is not likely to come from observations but may benefit from numerical modeling studies.

Criteria for seeding wintertime orographic clouds can be simplified to just three conditions, according to the seeding conceptual model: super-cooled liquid water (SLW), cold-enough cloud temperatures for the seeding material to be effective, and a form of delivery that puts sufficient seeding material into the “seedable” parts of clouds. Corollary conditions are that the cloud is not naturally efficient, which is akin to requiring seedable conditions, and that precipitation trajectories impact the desired target, which is an extension of the delivery requirement.

The seeding criteria are best determined from direct observations of SLW, temperature, winds, and possibly precipitation. Recent programs in Australia, Idaho, and Wyoming have demonstrated the utility of radiosondes, microwave radiometers, icing meters, and numerical models in directly determining seeding conditions. Advances in remote sensing technology, such as wind profilers, acoustic sounders, cloud-sensing radars, as well as microwave radiometers, allow for better determination of seeding criteria than in past programs. Making direct measurements is highly recommended for operational programs, but some of these instruments are economically or logistically impractical for some operations. Hence, proxies for many of these observations/criteria are generally used in determining when to seed. One of the challenges for both direct observations and particularly for proxy variables is determining a value or a threshold for a seeding criterion.

Climatology of Seeding Conditions

The model data used in the climatology study were output from numerical model runs at a 4-km grid spacing from October 2000 through September 2008. These output data were generated as part of another NCAR project called the Colorado Headwaters Program, which covered a large area of the Rocky Mountain region. A subset of the data covering the CCRMB area (see Figure A) at specific altitude levels were used in the climatology to make the analysis more tenable. The seeding criteria used by operators in the CCMRB program are heavily weighted toward the use of proxy variables. For the climatology, the numerical model output was formulated or “translated” into proxy variables that mimicked the criteria for seeding decisions. This was done to provide continuity in the climatology compared to seeding criteria used in practice.

Seeding conditions were analyzed two ways: by periods or time-steps during which seeding criteria were met over Target Area 2, and by sub-areas within Target Area 2 where seedable conditions occurred. The latter also required a wind direction criterion, and for this initial analysis, a NW wind was chosen since it was one of the seeding criteria used by DRI in the Winter Park area. Seedable periods were stratified by monthly and seasonal time frames and by each seeding criterion. These helped assess whether 1) the eight-year model data actually represented a climatology, 2) there were consistent monthly differences, and 3) certain seeding criteria were limiting the determination of seedable conditions. A summary of the overall frequency of seedable conditions is graphically displayed in Figure B. The month with the lowest frequency of seeding conditions is April and the highest is February, with a mean over all seasons of 20%. Other analysis show that temperature is the most limiting criterion, which is evident in the graph with April being the warmest month and hence meeting seeding conditions less often. The frequency or percentage is in relation to the total time in a month.

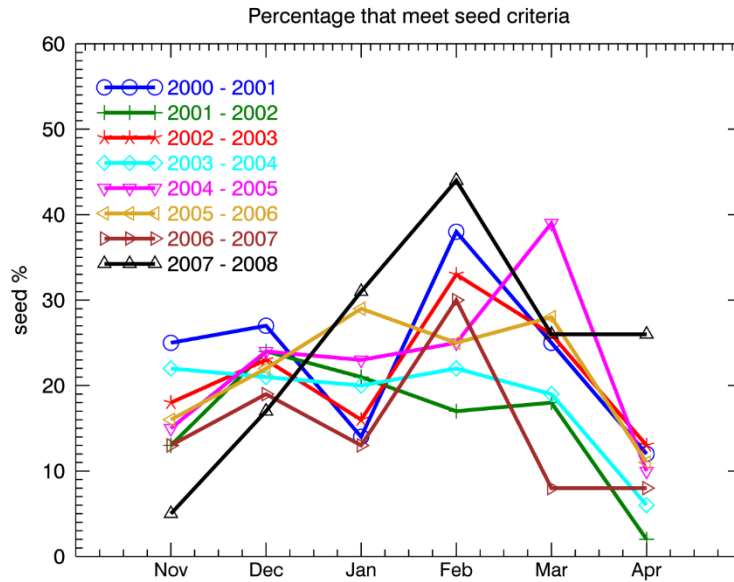


Figure B. Percentage of time during each month that seeding criteria are met, plotted by season.

The spatial analysis of the seeding criteria was done by applying the criteria at each grid point, allowing for a comparison of sub-areas within the target area. Regions of higher frequencies of seedable conditions can be further “normalized” by the presence of snowfall, representing an enhanced potential for seeding. We combined these conditions into a variable called “seed potential”. The frequency distribution for 2000-2008 plotted in Figure C shows relative “hot spots” of seed potential in and around Target Area 2. While the higher seed potential frequencies roughly correspond to areas of higher snowfall, which in turn are related to higher terrain, there are differences in the areas and their frequencies that could be important for targeting. Bear in mind however that the seeding conditions are only for NW winds, and a range of wind regimes would better highlight regions of significant seed potential. Overall, the formulation of the seed criteria and seed potential provide an opportunity to confirm that existing target areas have good seeding opportunities and to identify new target areas.

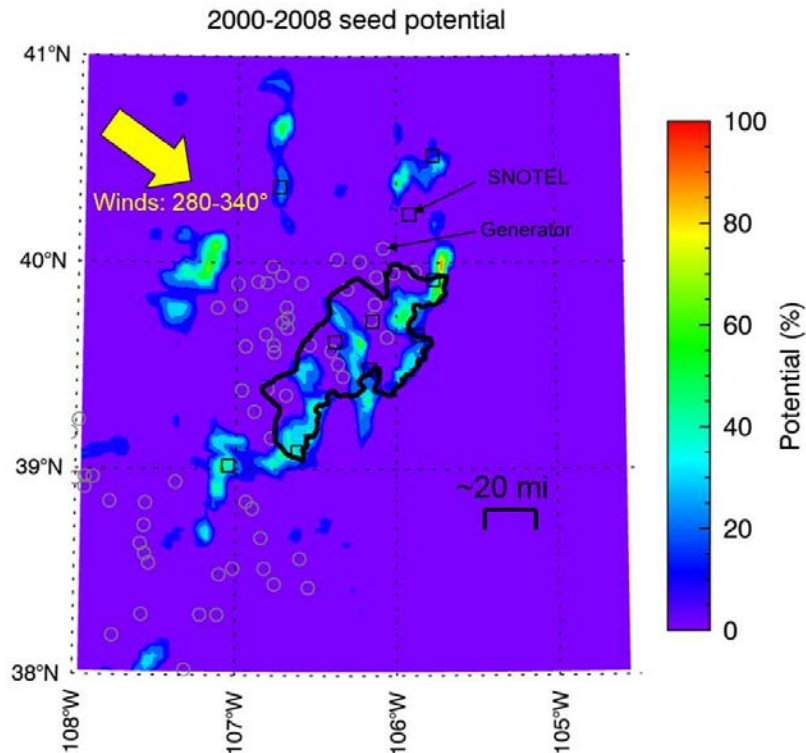


Figure C. 2000-2008 normalized distribution of ‘seed potential’. Symbols for SNOTELs and seeding generators are denoted. The NW wind criterion is also noted.

Numerical Model Results

Resources (time and computer availability) allowed for only one high-resolution numerical model simulation in the CCMRB area. Seeding events when the DRI remote generators operated were examined because of the additional observations at Winter Park. The 28-29 January 2013 period was chosen for the model simulation since it included a major snow event and two closely spaced seeding periods. The focus of the model-observational comparisons has been on the first seeding period (~2100-0200 UTC), because both DRI remotely-operated generators ran during that period and the snow rate was greatest during that period. A plot of the model output and observational data near Winter Park is shown in Figure D. Without going into details, the model generally simulated the trends and changes in most variables reasonably well for such a small time period and small area. However, a critical difference was in the modeled wind direction, which was consistently southwesterly versus the mostly northwesterly observed flow. Therefore, the model does not adequately represent the wind criteria for seeding with the DRI remotely-operated generators. But, the seeding trajectories would be applicable to a southwesterly flow event, with the variations in speed and direction that were modeled during this period. This flow regime is fairly typical for the Winter Park target area, although the speeds are slightly weaker than average.

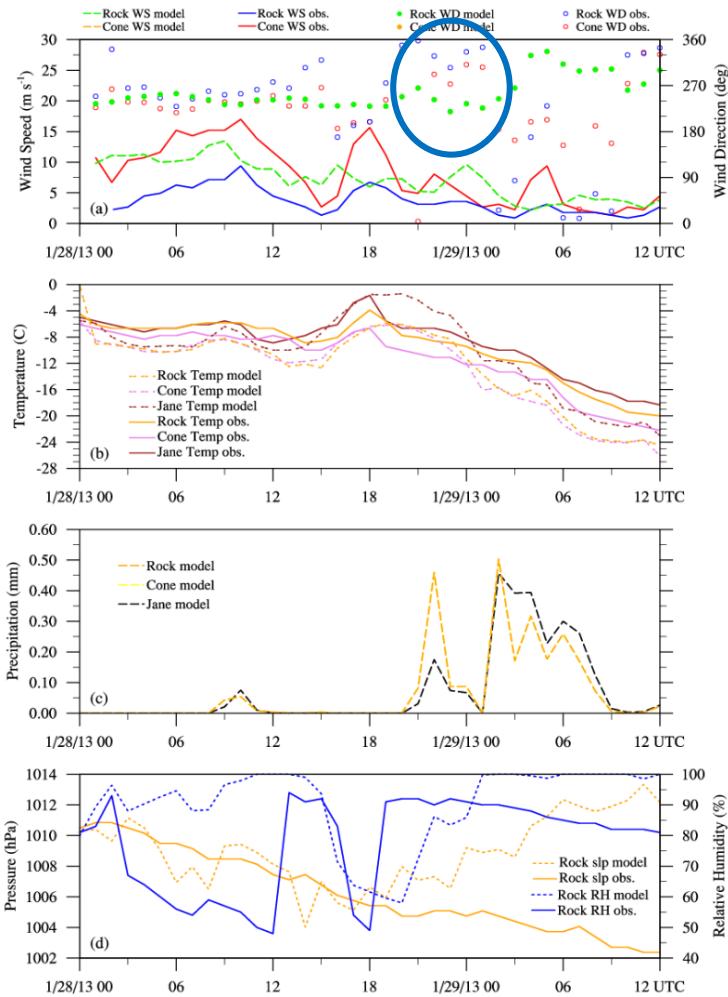


Figure D. Time-series plots of observational data from the Winter Park sites: Jane, Rock and Cone, and WRF model data from the nearest gridpoints to these sites. Each panel has a legend for observations and model data. Rock and Cone model data are often from the same gridpoint and hence not distinguishable from each other. Not all parameters were observed at the three sites. The circled area on the top plot denotes the seeding period and the difference between modeled and observational wind direction.

Locations of ten ground-based generators, two of which were the remotely-controlled generators operated by DRI and closest to the target area, were input into the HYSPLIT model - a transport and diffusion model developed and distributed by NOAA's Air Resources Laboratory. Six-hour trajectories were calculated from each generator during the 2100-0200 UTC seeded period. The first 2-3 hours of the trajectories are the most applicable for interpreting the potential path of the seeding plume. The example output in Figure E shows that three of the generator trajectories are clearly impacted by valley flows, with one or two others stagnant during the 1-2 hours. The general path of the trajectories show the predominance of southwesterly flow, contrary to the NW flow that actually occurred during this period. Consequently, the trajectory results indicate that

southwesterly flow does not target the Winter Park area very well (with the ten chosen generators), nor was it expected to.

Forward trajectories starting at 2300 UTC 28 Jan 13

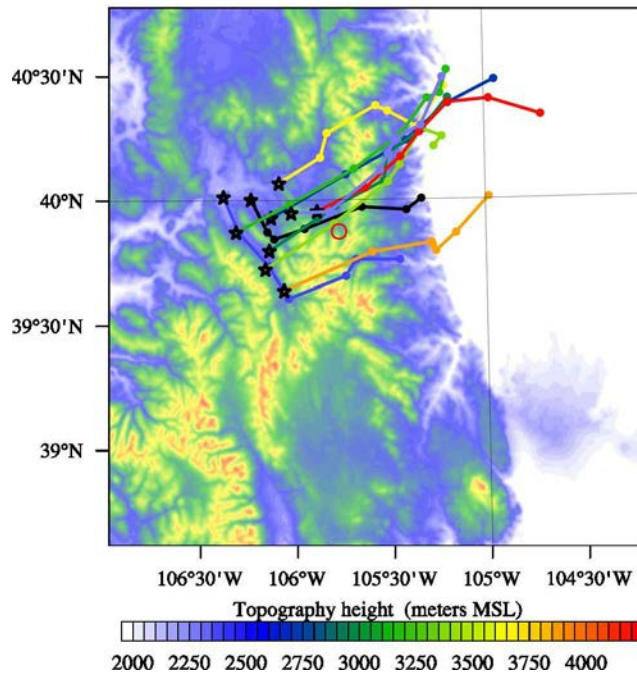


Figure E. HYSPLIT trajectories from the WRF model output, starting at 2300 UTC, 28 January 2013. Plan view showing 6-hr trajectories (dot at each hour) from 10 nearby generators to Winter Park – marked as a red circle. Background shows the topography with color code at the bottom.

The results of the modeling portion of the study show its utility in assessing seeding trajectories from generator sites. For example, several of the lower elevation generators clearly showed funneling in valley flows. There is also a high sensitivity to the elevation or location of the various generators, and several observational studies have found that high elevation releases are regularly effective in transporting seeding material into orographic clouds. Past studies have criticized the use of valley-placed generators, and emphasized the need for remote-controlled generators for effective operations. As mentioned earlier, the transport and diffusion characteristics of the seeding plumes are difficult to assess, and the modeling study is extremely limited. Nonetheless, the trajectory model results, while still uncertain, tend to support these past studies.

Recommendations

The following recommendations, based on this study, should not be considered “well-established”. The climatology work, while fairly comprehensive, would benefit from more extensive analysis of various seeding criteria. The modeling work can best be described as “proof of concept”, and several more simulations representing different flow regimes, temperature ranges, and stability profiles are needed to begin to generalize results and to specify potential changes to operational programs (i.e., generator locations, seeding criteria). Therefore, the following points should be viewed cautiously, knowing that further study is generally required.

- Studies of extra-area or downwind seeding effects tend to show *enhanced* precipitation but the results are generally negligible, to the point of being unmeasurable.
- Operational seeding criteria are heavily reliant on proxy variables, those not directly measuring the relevant seeding conditions according to the seeding conceptual model. Using observations, such as from rawinsonde releases, microwave radiometric sensing, a ceilometer (measuring cloud base), and/or strategically-placed surface observations (including high-resolution precipitation gauges), is highly recommended.
- Regular seeding evaluation also relies on observational data, some of which is similar to that needed operationally. In particular, cloud/precipitation radar and high-resolution precipitation gauges or snow-depth sensors would be useful and are recommended. Leveraging this instrumentation with other weather programs may be possible.
- Stability layers in valleys during storm events that limit seeding material from being transported into cloud are still not well-documented. Yet they are very important to locating effective generator sites and ensuring proper targeting. There are past studies and examples from this study that show valley floor generators can be affected by such conditions. One season of measuring temperature profiles over a valley would go a long way toward settling this issue. Such measurements can be made by radiosondes or remote sensors (e.g., acoustic sounder, radiometric retrievals).
- Running a high-resolution numerical forecast model could provide consistent and objective seeding periods. The model-derived seeding conditions and trajectories would need to be verified with observations to instill confidence in the results.
- The month with the lowest frequency of seeding conditions is April and the highest is February, with a mean over all seasons of 20%. This frequency is related to total time, which includes clear-skies and other non-storm periods.
- Several iterations of varying seeding conditions, determining frequencies compared to snowing periods (versus total time), mapping seed potential for different flow regimes, and other climatological-based results are needed. To facilitate the multiple scenarios and to allow third-party users to conduct their own analysis, combining the climatological data with GIS tools should be investigated.
- A more comprehensive map of seeding potential should guide future seeding operations – new target areas and generator locations.

- Several more model simulations, based on general climatological results, are needed to specify potential seeding impacts under different storm conditions.
- Running a specialized version of HYSPLIT or possibly another transport and dispersion model is needed to characterize the plume dispersion and hence effectiveness of each current generator.

This study provided a proof-of-concept in the use of model-derived re-analysis data for a climatological seeding-conditions assessment and in the application of a high-resolution numerical model for simulating seeding conditions and assessing plume behavior. While the initial project scope was overly ambitious, being based on its feasibility without a good estimate of the amount of work entailed, the ground-work has been laid for a second phase that is better defined in its goals and the work required to achieve them. Instrument deployment and observational studies recommended above would require additional planning and funding.

Contents

<i>Executive Summary</i>	iii
1 Introduction.....	1
2 Background.....	4
2.1 Conceptual model.....	4
2.1.1 Randomized experiments	4
2.1.2 Physical studies	5
2.1.3 Numerical modeling - targeting	6
2.2 Extra-area seeding effects	8
2.2.1 Atmospheric water balance in the hydrologic cycle	8
2.2.2 Past studies of AgI persistence and extra-area effects.....	9
2.3 Operational seeding criteria	10
3 Climatology of seeding conditions in CCMRB target area	13
3.1 Objective.....	13
3.2 Methodology	13
3.2.1 Colorado Headwaters WRF data set.....	13
3.2.2 Formulating seed criteria	15
3.2.3 Implementing the seed criteria	17
3.3 Example model comparison with one SNOTEL site	19
3.4 Climatology of seedable and non-seedable <i>periods</i>	21
3.5 Climatology of seedable and non-seedable <i>areas</i>	24
3.6 Seedability and seeding potential.....	27
4 WRF model simulation at 800-m resolution – one example.....	34
4.1 Choice of storm event	34
4.2 Model setup and simulations.....	35
4.3 Comparisons of model output with observations	36
4.4 HYSPLIT model results.....	38
4.4.1 Trajectories from all generators near Winter Park target	38
4.4.2 Relative concentrations from the DRI remotely-operated generators	42
5 Conclusions and Recommendations	46
5.1 Climatology results.....	46
5.2 WRF (800-m) model results	46
5.3 Recommendations	47

REFERENCES	48
Appendix A: WRF model configuration and data set	53
Appendix B: Text output data of seed times.	55
Appendix C: Climatology plots and statistics	57
Appendix D: High-resolution WRF Model Setup.....	73

1 Introduction

Cloud seeding of winter orographic storms fundamentally follows a conceptual model that was established in the mid 1950's by Ludlum (1955) and others. The concept is based on the fact that the development of snow is hindered or delayed, under certain cloud conditions but over extended periods of time, by the lack of natural ice nuclei (IN). IN are those atmospheric particles onto which water vapor condenses and subsequently freezes to start the growth into ice particles and snow. Natural IN that activate or start the freezing process in layer clouds at temperatures warmer than about $-15\text{ }^{\circ}\text{C}$ ($+5^{\circ}\text{F}$) are sparse. Introducing large numbers of artificial IN that activate at warmer temperatures can “jump start” the snow growth process and presumably make it more efficient.

The conceptual model of seeding winter orographic clouds has been refined over several decades as our understanding of the complexities of mountain flows and precipitation processes advanced. In simplified terms, the following chain of events is hypothesized for seeding from the ground. Artificial IN in the form of silver iodide (AgI) particles are released from a ground-based generator and carried by the wind toward the target area. The plume of AgI rises and disperses such that it can effectively reach a relatively large volume of cloudy air. The AgI particles nucleate ice in cloudy conditions at temperatures colder than about $-5\text{ }^{\circ}\text{C}$ ($+23^{\circ}\text{F}$) but with a nucleation efficiency increasing by orders of magnitude as temperatures cool to $-8\text{ }^{\circ}\text{C}$ ($+18^{\circ}\text{F}$). The ice crystals then grow by vapor deposition, riming, and/or aggregation in cloudy regions where supercooled water droplets exist, forming precipitation-sized particles. These larger particles fall to the ground as snow, enhanced in number, size, and/or density from what would have fallen naturally. This process is shown schematically in Figure 1.1.

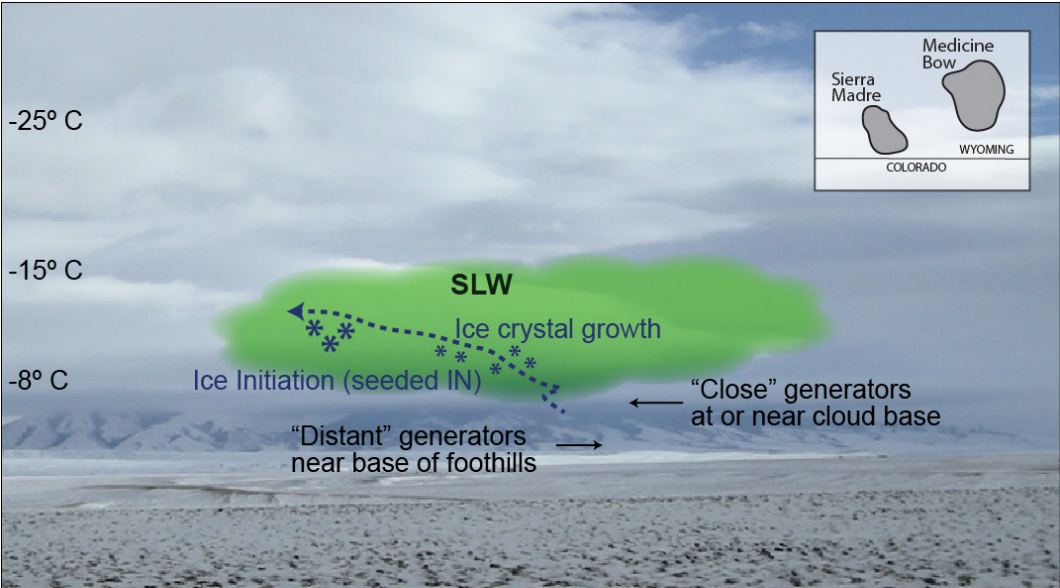


Figure 1.1 Relevant seeding processes labelled on a photograph of a precipitating orographic storm over the Medicine Bow Range in Wyoming – see inset in the upper right. Conceptual location of supercooled liquid water (SLW) is shaded in green. Temperature levels are approximate and applicable over the central part of the figure. The dashed line schematically represents the seeding plume, which would end with precipitation (snow over the higher terrain into the page and not visible in the photograph). “Close” generators are those closest to the target area and on higher terrain; “distant” generators are farther from the target area and at lower elevations.

One of the critical steps necessary for cloud seeding to be effective, and one of the more difficult to assess, is the transport of seeding material into cloud conditions susceptible to seeding. These conditions are the regions in clouds where liquid cloud droplets exist at sub-freezing temperatures - supercooled liquid water (SLW) – warmer than about -15 °C. Seeding plumes can be generated by ground-based generators or through airborne seeding, although all of the Colorado programs utilize ground-based generators. Therefore, the first step in evaluating the effectiveness of an operational cloud seeding program is to create a climatology of “seedable” conditions and then to assess the dispersion of seeding plumes from the ground-based generators during the subsequent snowfall events. Such an analysis is needed to determine: 1) the frequency and duration of seedable conditions; 2) the percentage of time such conditions exist in relation to all snowfall events; 3) if seeding plumes are consistently affecting the target areas; 4) the potential effects of seeding on other areas such as downwind of the target areas; 5) if there are ineffective ground-based generators; and 6) if it makes sense economically and logistically to move generators or deploy additional generators.

There are currently seven wintertime cloud seeding programs in Colorado spanning the state from the San Juan’s in the southwest to the Winter Park area of the central Rockies. These programs involve more than 100 ground-based generators. The focus of this study was limited to Target Area 2, shown in Figure 1.2, of the Central Colorado Mountains River Basins program (CCMRB), which include 27 ground-based generators. Two major tasks were proposed and completed as a proof-of-concept in evaluating the effectiveness of the CCMRB program:

Task 1. Develop a climatology of conditions relevant to seeding, using criteria such as temperature, cloud water content, and winds at various levels, liquid water path, stability, and snow water equivalent or snowfall, for precipitation events across Target Area 2. The climatology utilized output from eight winter seasons (2000-2008) of Weather Research and Forecast (WRF) model runs at 4-km resolution.

Task 2. Simulate a seeding case to assess the utility and improvement of using a higher resolution model (≤ 1 -km grid spacing) to simulate seeding events compared to the 4-km WRF runs. The high-resolution model run was then used to assess seeding plumes using the HYSPLIT transport and diffusion modeling tool.

This report includes background on the conceptual seeding model, extra-area effects, and operational seeding criteria to provide context for the CCMRB programs. A detailed climatology of winter conditions in Target Area 2 is presented and combined with seeding criteria to highlight areas of seedable conditions, specific during northwesterly flow. A high-resolution model simulated a seeded storm, targeting the Winter Park area, and was compared to the coarser 4-km WRF model simulation. HYSPLIT was used to investigate plume behavior for ten seeding generators close to Winter Park, not all of which were used in this seeding event. Results from past studies outlined in the background and the results of this study led to preliminary recommendations on generalized seeding generator locations and operations, and outlined the next steps in better assessing the seeding assumptions and operations in the CCMRB program.

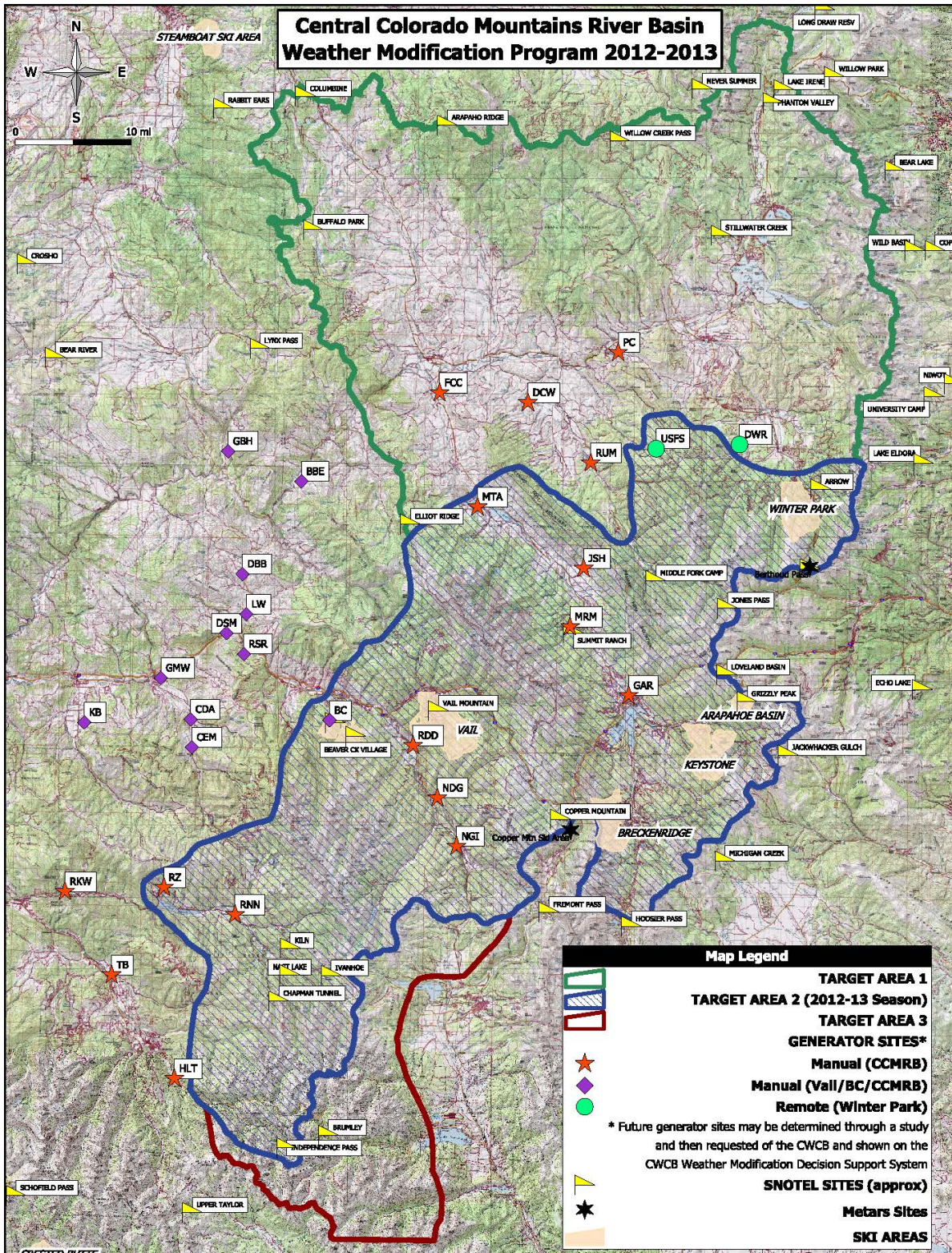


Figure 1.2 Map of the Central Colorado Mountains River Basins Weather Modification area and various facilities (generators, SNOTELs, Metars sites). See legend for details. Blue-hatched area – Target Area 2 – is the focus of this study. (Map generated by CWCB, 2012.)

2 Background

2.1 Conceptual model

Since the seminal work on glaciogenic seeding in the late 1940's (Schaefer 1946; Vonnegut 1947; Kraus and Squires 1947; Langmuir 1948; Coons et al. 1948; Bergeron 1949), a number of programs have investigated precipitation processes and seeding effects to determine if AgI seeding could produce additional snow from winter orographic clouds. Evaluation of this hypothesis has been attempted over the last half century using randomized statistical experiments, observational studies, and numerical modeling of both natural and seeded clouds. Huggins (2009) summarized physical studies and some randomized experiments that included strong physical evidence that verified aspects of the conceptual model. Recently, winter orographic seeding experiments in Australia (Manton et al. 2011) and Wyoming (Breed et al 2014) have contributed to the body of work documenting evidence that wintertime cloud seeding is effective when cloud conditions specified in the conceptual model exist.

2.1.1 Randomized experiments

Noteworthy randomized studies include the Climax experiments in the central Colorado mountains (Mielke et al. 1981; Grant 1986), the Bridger Range Experiment (BRE) in southwestern Montana (Super and Heimbach 1983), the Snowy Precipitation Enhancement Research Program (SPERP) in the Snowy Mountains of Australia (Manton et al. 2011), and the recently completed Wyoming Weather Modification Pilot Project (WWMPP) in southern Wyoming (Breed et al. 2014).

The Climax Experiments (Climax I, 1960-1965, and Climax II, 1965-1970) were exploratory and confirmatory randomized seeding experiments that used existing instruments and observations as covariates and for ancillary (ex post facto) studies. Both Climax I and Climax II reported precipitation increases with high statistical confidence (Mielke et al. 1981). A reanalysis of the complete Climax data set (I and II) showed that for warm 500 hPa temperatures, precipitation increases of 25% were realized. However, the validity of the experiments was questioned on the basis of the experimental execution and evaluation methodology (Rangno and Hobbs 1987, 1993), and the continuing debate left the results unresolved.

The BRE was conducted in the Bridger Mountains of southwest Montana from 1969 to 1972 (Super 1974; Super and Heimbach 1983). Randomized experiments were conducted during the winters of 1970-1971 and 1971-1972, and follow-on physical measurements were later made (Super and Heimbach 1988). This project produced statistical evidence of seeding effects and considerable documentation of the physical "chain-of-events" that began with seeding and led to the observed precipitation changes. An estimate of ~15% more seasonal target-area precipitation than predicted on nonseeded days resulted, while a target-control analysis of independent snow-course data showed that seeding enhanced the seasonal snowpack more than 15%. A strong recommendation was made for placing ground-based generators more than midway up the western or upwind side of the barrier. This was supported, for example, by airborne plume-tracing observations which provided evidence of effective targeting of the AgI seeding.

The Australian experiment, SPERP, has provided recent evidence of an increase in precipitation due to AgI seeding of winter orographic clouds based on a 5-year statistical program (Manton and

Warren 2011). Precipitation increases of 14% were established, at a 3% significance level, after thresholding the cases according to generator hours – indicating sufficient AgI coverage of the target area. Physical studies included silver-in-snow measurements, which showed effective targeting of the AgI seeding agent.

The results of the Wyoming project, WWMPP, have recently been summarized in an executive report (WWDC 2014) and included statistical, physical, and modeling analyses. The accumulation of evidence from these analyses suggests that “*cloud seeding is a viable technology to augment existing water supplies, for the Medicine Bow and Sierra Madre Ranges*”. The primary statistical analysis implied a 3% increase in precipitation with a 28% probability that the result occurred by chance, which does not meet the acceptable level of significance. While this primary statistical analysis did not show a significant impact of seeding, statistical analysis stratified by generator hours, similar to the SPERP analyses, showed increases of 3-17% for seeded storms. Furthermore, high-resolution modeling studies that simulated three of the experimental seasons, or about half of the total number of seeding cases, showed positive seeding effects of 10-15%.

The physical evidence from radiometer measurements taken during the WWMPP showed that ample SLW existed at temperatures conducive to generating additional snow by AgI seeding over the ranges studied. High-resolution and quality-controlled snow gauges were critical in evaluating the effectiveness of cloud seeding and validating the performance of the numerical model used during the WWMPP. A climatology study based on high-resolution model data showed that ~30% of the wintertime precipitation over the Medicine Bow and Sierra Madre Ranges fell from storms that met the WWMPP seeding criteria. Ground-based silver iodide measurements indicated that ground-based seeding reached the intended target, and in some cases, well downwind of the target.

So, in spite of the result of no seeding effect from the primary randomized statistical experiment, ancillary studies, using physical considerations to stratify the WWMPP precipitation data, and modeling studies over three full winter seasons, led to an accumulation of evidence from the statistical, modeling, and physical analysis which suggest “*a positive seeding effect on the order of 5 to 15%*”. Based on the results of the WWMPP, the recommendation was made to consider implementing the cloud-seeding technology in Wyoming by carefully addressing each of five components: 1) Barrier identification, 2) Program design, 3) Operational criteria, 4) Program evaluation, and 5) Program management. These were further detailed in the executive report.

2.1.2 Physical studies

Although several of the randomized seeding experiments included physical studies aimed at verifying the seeding conceptual model, other cloud seeding research programs that did not include randomized seeding have also attempted to clarify the seeding conceptual model. The Colorado Orographic Seeding Experiment in the northern Colorado mountains (Rauber and Grant 1986) employed airborne and ground-based observations to elucidate the characteristics and evolution of SLW in orographic storms, focusing on how the distribution of SLW impacts precipitation development and the implications for cloud seeding.

Through detailed case studies using observations and modeling, the Sierra Cooperative Pilot Project showed that dry ice and AgI seeding likely caused additional precipitation over the Sierra

Nevada Range of California (Deshler et al. 1990; Reynolds 1988). This well-controlled field experiment suggested that orographic seeding has the potential to enhance precipitation under certain conditions.

The Colorado River Augmentation Demonstration Program (CRADP) was conducted over the Grand Mesa of Western Colorado from 1983-1988 (Holroyd et al. 1988; Super and Boe 1988). The CRADP conducted a series of physical experiments that included airborne plume mapping over the mesa top, and extended the chain-of-events from seeding from precipitation development aloft to increased precipitation at the surface.

The Utah Atmospheric Modification Program was composed of a series of physical experiments conducted from 1984 through 1998, initially over the Tushar Mountains of southwestern Utah, and later (beginning in early 1990) over the Wasatch Plateau of northeastern Utah. For the Wasatch experiment, instrumented mobile platforms collected observations in canyons and along the winter-maintained highway atop the plateau. The program included both ground-based measurements with remote-sensing equipment and aircraft observations (e.g. Long et al. 1990; Sassen et al. 1990; Campistron et al. 1991; Huggins 1995; Heimbach et al. 1997, 1998; Huggins 2007). Super (1999) summarizes the efforts of the Utah studies, which collectively substantiated many of the processes in the orographic seeding concept, and recommended ways to improve Utah's operational seeding program at that time.

These studies and evidence from randomized seeding experiments provide a detailed physical picture of AgI plume transport, ice nucleation, and snow development. More sophisticated measurements and improved numerical models over the last decade continue to refine and validate the seeding conceptual model. For example, recent fine-scale radar measurements from an aircraft documented differences between seeded and unseeded clouds, verifying steps in the conceptual model that describe increased snowfall rate due to seeding (Geerts et al, 2010). Likewise, recent modeling studies incorporating AgI seeding into the processes that lead to precipitation have shown promise in simulating seeding effects (Xue et al, 2013a, b).

2.1.3 Numerical modeling - targeting

The transport and diffusion of AgI material from ground-based generators is critical to assessing whether cloud seeding impacts the desired target areas. Many observational and modeling studies have documented seeding plume behavior as well as the uncertainty of plume dispersion in complex terrain (e.g., Hill 1980, Super and Heimbach 1988, Holroyd et al. 1988, Griffith et al. 1992, Heimbach et al. 1998). Although a number of observational techniques, such as silver-in-snow detection, tracer experiments, and ice nuclei measurements, can provide important details on plume dispersion and seeding effectiveness, they are generally cost prohibitive and limited to a few cases or specific sites. Thus, using numerical models provides a more economical and comprehensive analysis as long as there is confidence in the model through validation with observations. Several types of weather numerical models can be used for plume tracking and general evaluation of winter cloud seeding programs. Two discussed here are plume models and mesoscale models.

Plume models are single-purpose and hence relatively simple models that calculate the transport and spread of airborne material, such as might arise from accidental spills, pollution sources, dust

events, volcanic eruptions, intentional chemical/biological releases, and others. Various plume modeling approaches have been successfully applied to winter orographic cloud seeding conditions, based on spot observations for model verification. Plume models depend on input from observations or more often a three-dimensional weather model to “drive” the plume model with winds, temperature, pressure, underlying topography and land-use.

The advantage of using plume models is the ability to include many simulations with these relatively simple models (e.g., SCIPUFF – Sykes and Gabruk 1997, HYSPLIT¹, Lagrangian particle models). However, the simplifying assumptions in such models as well as their coarse resolution when driven by typical forecast models – of order 20-km grid – are disadvantages, and the results should reference some type of benchmark. A high-resolution model or detailed observations could be used to provide such a benchmark to assess their applicability. Therefore, careful analysis and validation is required to gain confidence that such models faithfully portray seeding plumes.

Mesoscale models are complex three-dimensional models that can be used to forecast fine details of the weather (*prognostic*) or reproduce weather events in greater detail than observations alone (*diagnostic*). These models generally cover spatial scales of several states down to the scale of a single watershed or basin. In order to efficiently use computer resources, a mesoscale model is often “nested” from coarser resolution (order of 20-km grids) to finer resolution (1- to 4-km grids) to capture the areas of interest in sufficient detail.

An early attempt to apply a mesoscale model, the CSU Regional Atmospheric Modeling System or RAMS model, during seeding operations in the central Colorado Rockies demonstrated the evolving capabilities of detailed numerical models to assess cloud seeding effectiveness (CWCB 2005). More recently, the Weather Research and Forecast (WRF) model (Skamarock et al. 2008) has been used in a number of studies on winter snowpack and cloud seeding evaluation that have verified the model’s ability to accurately simulate plume transport and snowfall over a variety of time and space scales. For example, the WRF model was used to simulate eight seasons of snowfall in the Rocky Mountains, covering all of Colorado and parts of adjacent states (Ikeda et al. 2010). The model runs at various resolutions were compared to SNOTEL data, and grid resolutions of 6 km at a minimum were needed for reasonable agreement. Although 6-km resolution was adequate, the model run at 2-km grid resolution was best at capturing local topographic forcing on regional snowfall.

On a smaller scale, the WRF model can be configured at very high resolution, called a large eddy simulation or LES. The LES model was run on a case in the Medicine Bow Range of southern Wyoming at 100-m resolution and proved to be successful in simulating details of the airflow and plume dispersion for that case, validated by results of airborne mapping of the seeding plumes (Xue et al. 2014).

Model resolution is clearly a major factor in accurately simulating seeding plumes, as demonstrated in the studies mentioned above and others. A very high-resolution model such as

¹ HYbrid Single-Particle Lagrangian Integrated Trajectory
(http://www.arl.noaa.gov/documents/Summaries/Dispersion_HYSPLIT.pdf)

the LES would be useful in mapping the seeding plumes of ground-based AgI generators such as those deployed in the CCMRB program. Unfortunately, an LES simulation requires vast computer resources and is impractical for a long-term or large-scale study. However, running WRF at high-resolution (~1-km) – but coarser than the LES – can provide a detailed mapping of variables that drive a plume model. The WRF model alone may also generate good simulations of plume transport and diffusion and consequently effects on precipitation. There is evidence that this might be practical, based on an LES model comparison in the Medicine Bow Range of Wyoming. A part of this study would be to determine the effect of “nesting” down to a relatively high resolution, from 4-km to ~1-km for example, over the CCMRB seeding areas to assess the simulation of the seeding plumes as well as variations in snowfall over the complex terrain.

2.2 Extra-area seeding effects

A potential change in precipitation due to seeding in regions outside of primary target areas or during periods beyond what might be expected from seeding operations is an issue frequently raised by water users, stakeholders, and the general public. These potential extra-area effects are also important scientifically in evaluating seeding projects. The background on this issue is focused on two areas: 1) water balance estimates in the hydrologic cycle, which is a large-scale approach; and 2) a review of past studies concentrating on winter orographic storm projects.

2.2.1 Atmospheric water balance in the hydrologic cycle

In the hydrologic cycle, atmospheric water is generally in balance, at least over time periods or at scales sufficiently large to neglect short-term variations. This means that under such conditions the total column moisture flux is balanced by evapotranspiration and evaporation, precipitation, and atmospheric moisture storage. Large amounts of atmospheric water in the form of water vapor pass over a region every day. Some of it condenses forming clouds, and a portion of the condensed or frozen cloud water forms precipitation.

As the moist flow encounters orography, it is forced upward. As it rises, it cools, and clouds and precipitation form over the mountains. Typically just over 20% of the total water vapor in a column of air condenses into cloud water, although the exact amount depends on a number of variables often revealed in thermodynamic profiles (e.g., Braham 1952; Gao and Li 2008; Trenberth et al. 2007; Li et al. 2011). The other 80% of the total moisture remains uncondensed in vapor form, because the air containing it never gets cold enough to condense it all. The efficiency of orographic clouds at converting cloud water into precipitation – the precipitation efficiency – is highly variable and depends on stability profiles, mountain characteristics, microphysical conditions, and other factors (e.g., Colle 2004; Jiang 2003; Houze and Medina 2005; Smith and Barstad 2004). If we use a 30% estimate of storm precipitation efficiency and the 20% estimate of atmospheric water vapor to cloud water, then about 6% of the total atmospheric moisture falls out naturally as precipitation. If cloud seeding is successful in increasing the natural precipitation by 15%, then 15% of the 6% is 0.9% more of the total atmospheric water vapor that might fall as precipitation when seeding is conducted. A pie chart of these estimates is provided in Figure 2.1 (WMI 2005).

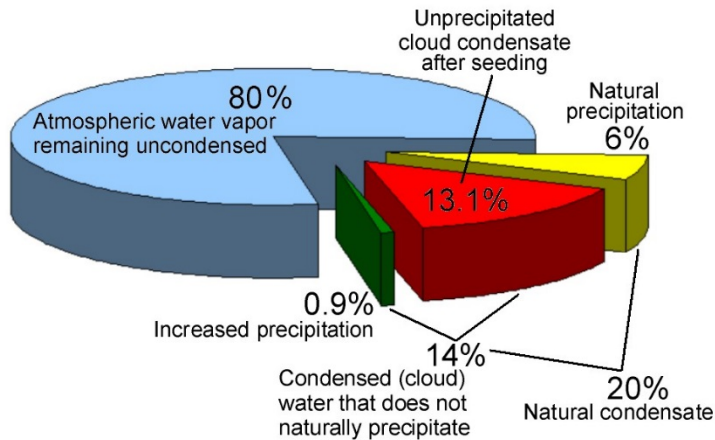


Figure 2.1 Pie-chart of the distribution of atmospheric water vapor assuming a cloud seeding impact of a 15% increase in precipitation from a storm (from WMI 2005).

In terms of extra-area effects, the approximate 1% change in atmospheric water components (vapor to condensate to precipitation) due to precipitation increases from seeding is negligible and nearly impossible to

measure at the time scales and areal scales covered by standard rawinsonde and satellite observations. Hence, in this context the argument that increased precipitation due to seeding measurably decreases precipitation downwind is weak. However, at shorter temporal and spatial scales, precipitations changes or re-distribution due to seeding may have enhanced effects that reach measurable amounts.

2.2.2 Past studies of AgI persistence and extra-area effects

Typical cloud-seeding efforts focus on increasing the precipitation efficiency in seeded clouds such that their precipitation falls within a target area. A seeded cloud or cloud system often moves with the wind, implying its precipitation may fall over an extended ground area. Even for orographically-induced clouds, which dissipate downwind of the barrier, the plume of seeding material will advect some distance beyond the target area. Therefore, seeded precipitation could conceivably fall beyond the boundaries of the target area, and the AgI could also advect beyond the target – so-called “extra-area” effects.

Reinking (1972), Boucher (1956), and Grant (1963) suggest that a fraction of the released nuclei do not immediately reach the cloud and are not used. These nuclei are available to be transported out of the seeded area or to remain trapped in the target area. Reinking’s (1972) study in the Colorado mountains suggested that IN concentrations were approximately five times above background for two days after seeding. Rottner et al. (1975) summarized a study of persistence from two projects, the Colorado River Basin Pilot Project and the Jemez Atmospheric Water Resources Research Project. Using the NCAR acoustic ice nucleus counter, they found concentrations of AgI IN on the order of 100 to 1000 times higher for several hours after seeding.

According to Super et al. (1975), AgI can remain active as an ice nucleant for a considerable time (> 5 hr) and distance (> 100 km). Therefore, it is reasonable to expect seeding effects beyond the primary target. The estimation of extra-area effects due to cloud seeding depends on how well dynamical and ensuing microphysical effects are characterized during the extra-area transport of the seeding material. Thus, representative cloud-scale measurements are needed to quantify effects due to cloud seeding and the weaker extra-area effects. These effects are functions of a complex set of processes and their interactions: a) persistence and effectiveness of seeding material; b) dispersion (transport and diffusion); c) seeding agent concentration; d) background cloud microstructure (hydrometeors and natural IN); and e) the air-mass characteristics, including

state parameters and aerosols, in which the cloud was formed. Observations relevant to some of these processes have been reported (Deshler and Reynolds 1990; Hill 1980; Holroyd et al. 1988; Orr and Klimowski 1996; Rosenfeld and Woodley 2003; Rosenfeld et al. 2005; Warburton et al. 1995), but none have comprehensively covered all the processes.

Transport and diffusion of seeding material has also been verified using tracer measurements of SF₆, IN and ice crystal concentrations, trace chemical analyses of silver and background or tracer elements in snow samples, and trajectory models. In the case of winter orographic clouds, analyses suggest that seeding effects are detectable in the target area and as far as a few hundred kilometers beyond the target area, with nearly all such studies indicating an increase in precipitation (Long 2001; Silverman 2001; Solak et al. 2003; Griffith et al. 2005; Wise 2005). However, the database is still small and equivocal, such that doubt remains about the validity of such positive extra-area seeding effects as well as the precipitation increase in the target areas.

The climatological distribution of precipitation indicates that any extra-area effects will be quite variable, and are likely to be quite small for more isolated mountain ranges. Precipitation downwind of a mountain barrier is often a factor of ten less than that on the upwind side. Huggins (1995) described the rapid decrease in SLW in the region downwind of the primary upslope region of a mountain barrier. Warburton and Wetzel (1992) documented similar liquid water patterns over the SPERP target area in Australia in 1989. Therefore, the detection of seeding effects in downwind regions will be much less likely than in the main upwind target area.

Overall, the comprehensive summaries by Long (2001) and more recently by DeFelice et al. (2014) showed fairly consistent evidence of downwind effects of precipitation *enhancement* by cloud seeding. The spatial extent of the positive extra-area seeding effects may extend to a couple hundred kilometers. The extra-area effects did not appear to produce regional impacts on the water balance, nor on the natural precipitation on a regional scale. However, the results require more verification. The NRC (2003) report supports these conclusions, suggesting that extended-area effects will become better defined as seeding impacts in target areas are more carefully quantified and new tools enable better understanding of clouds and their response to seeding.

2.3 Operational seeding criteria

The conceptual model for seeding wintertime orographic clouds requires just three criteria: super-cooled liquid water, effective cloud temperatures for the seeding material used, and a form of delivery that puts sufficient seeding material into the “seedable” cloud. Corollary conditions are that the cloud is not naturally efficient, which is akin to requiring seedable conditions, and that precipitation trajectories impact the desired target, which is an extension of the delivery requirement. Super and Heimbach (2005) provides a thorough and still relevant summary of studies that have identified or listed seeding criteria, which address the following basic steps:

1. Seeding material must be successfully and reliably produced.
2. Seeding material must be transported into a region of cloud that has SLW.
3. Seeding material must be dispersed sufficiently in the SLW cloud, so that a significant volume is affected by the desired concentration of IN and a significant number of ice crystals (IC) are formed.

4. The temperature must be low enough, depending on the seeding material used, for substantial IC formation.
5. ICs formed by seeding must remain in an environment suitable for growth long enough to enable them to fall into the target area.

The first three steps are related to the type of generator used, its location, and the spacing of multiple generators. In terms of seeding material release rate, 20-30 g h⁻¹ has been shown to be effective, depending on generator spacing, and is commonly used (ASCE 2004). Remotely-operated Agl generators are typically designed to release ~25 g h⁻¹ of seeding material. Manually-operated Agl generators are capable of releasing 5-25 g h⁻¹ of seeding material, although many operational programs use an average release rate of about 10 g h⁻¹, which is likely to be inadequate alone. Under most operational scenarios, operating manual generators at the higher release rates or, if mechanically limited (e.g., nozzles, flow rates), co-locating two generators may be more effective depending on their elevation. As mentioned earlier, the transport and diffusion characteristics of the seeding plumes are difficult to assess. However, many observational studies have found that high elevation releases are regularly effective in transporting seeding material into orographic clouds (e.g., Super and Heimbach 2005). High-elevation generator sites are usually much closer to the target area, which feeds back into step 5 above, depending on the mountain and orographic cloud configuration.

The seeding criteria are best determined from direct observations of SLW, temperature, winds, IN concentrations, and possibly precipitation. Recent programs in Australia, Idaho, and Wyoming have demonstrated the utility of radiosondes, microwave radiometers, icing meters, and numerical models in directly determining seeding conditions. Advances in remote sensing technology, such as wind profilers, acoustic sounders, cloud-sensing radars, as well as microwave radiometers, allow for better determination of seeding criteria than in past programs. Making direct measurements is highly recommended for operational programs, but some of these instruments are economically or logistically impractical for some operations. Hence, proxies for many of these observations/criteria are generally used in decision-making – when to seed. One of the challenges for both direct observations and particularly for proxy variables is determining a value or a threshold for a seeding criterion.

Many proxy variables have been identified, used, and refined by cloud seeding operators over many decades. Those proxies determined to be most useful or threshold values that best characterize seedable conditions are geographically dependent and often based on experience. Some of the more common proxy variables used are: cloud-top temperatures, cloud cover, temperatures at standard levels such as 850 mb, 700 mb, and 500 mb, cloud-base height referenced to a mountain crest or a particular mountain feature, maximum wind speeds, lack of inversions which in turn are determined a number of ways, humidity or precipitable water, and the start or existence of precipitation.

The seeding criteria used by operators in the CCMRB program are heavily weighted toward the use of proxy variables. For this study, numerical model output is formulated or “translated” into proxy variables that mimic the criteria for seeding decisions. This was done to provide continuity in the climatology compared to seeding criteria used in practice. Although verification of the numerical model output is not extensive, demonstrating the utility of using high-resolution

numerical models for refining seeding criteria and making seeding decisions is an auxiliary goal of this study, bolstered by the results of the Idaho and Wyoming programs.

3 Climatology of seeding conditions in CCMRB target area

3.1 Objective

The objective of this task was to develop a climatology of conditions relevant to established seeding or “seed” criteria for precipitation events across Target Area 2 of the CCMRB region. The climatology utilizes output from the 2000-2008 winter seasons of WRF model runs at 4-km resolution. A cursory model validation has been done using data from one SNOTEL site.

3.2 Methodology

3.2.1 Colorado Headwaters WRF data set

The model data used in this study were output from WRF model runs at 4-km grid spacing. These output data were generated as part of another NCAR project called the Colorado Headwaters Program. The simulation start date was 1 October 2000 and end date 30 September 2008. The model was configured for a single domain of 1200×1000 km² with 45 vertical levels. The details of the simulations are given in Ikeda et al. (2010) and a description of the model configuration and data set is given in Appendix A.

The data cover a longitude range of -99.14 to -114.86 degrees and a latitude range of 34.05 to 43.73 degrees. Figure 3.1 shows a terrain height plot of this domain. The Colorado Headwaters domain created a data set too large to analyze using a desktop computer. So each file was re-sampled into a smaller domain, centered geographically over the CCMRB Target Area 2, with a longitude range of -104.46 to -108.01 degrees and a latitude range of 38.00 to 41.06 degrees. This re-sampled domain is shown in Figure 3.2. The pressure levels were also reduced from 15 to 4 – 750, 700, 650 and 600 mb.

The re-sampled WRF data, hereafter ‘data’, consists of 24 meteorological variables deemed necessary for calculating parameters used as seed criteria in the CCMRB programs. A list of the variables is given in Appendix A. Since the cloud seeding operations are conducted using ground generators, it was important to analyze the data at the pressure levels closest to the ground. The 750, 700, 650 and 600 mb isobaric levels were analyzed. Figure 3.3 shows an example of temperature field plots at each of these isobaric levels for 1 November 2000 at 0000 UTC. The colored contours show where data are present while the white patches represent missing data. When the geopotential height is below the terrain height, the data are missing. In Figure 3.3, (a) 57% of the data within the domain are missing at 750 mb, (b) 20% missing at 700 mb, (c) 2% missing at 650 mb, and (d) 0% missing at 600 mb. Due to the variation in geopotential height across the domain, the total number of missing data points varies. The fraction of missing data inside just Target Area 2 is approximately 97%, 66%, 7% and 0% at 750, 700, 650 and 600 mb. These missing data imposed constraints on formulating seed criteria for the target area.

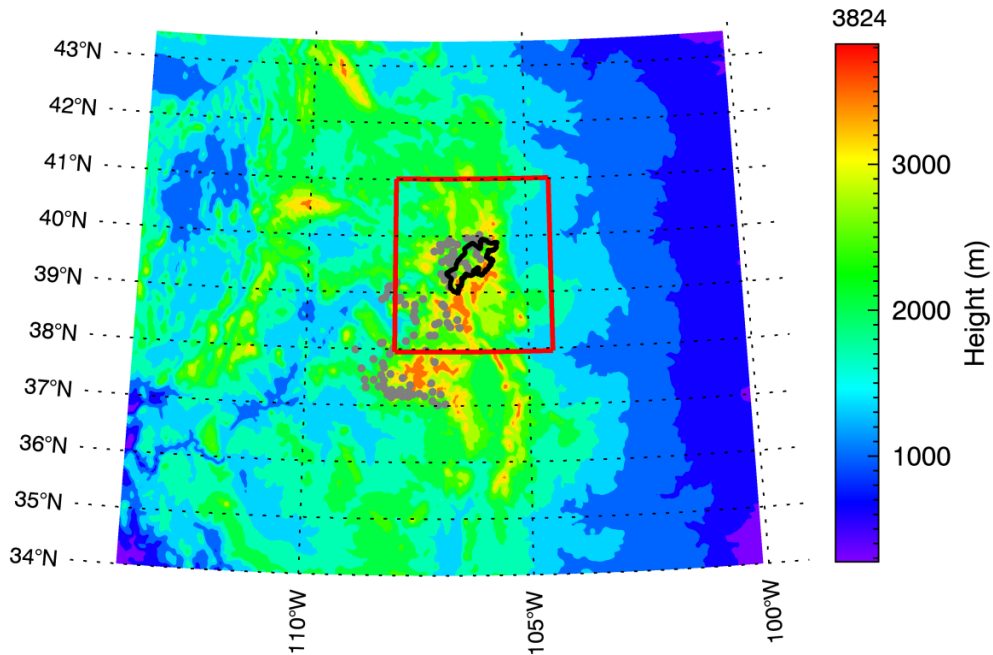


Figure 3.1 Plot of terrain height covering the full WRF domain. All cloud seeding generator locations identified by the CWCB are indicated by the gray dots, but not all of them are part of the CCRMB program. Target Area 2 is identified by the black trace, and the re-sampling domain is denoted by the red polygon.

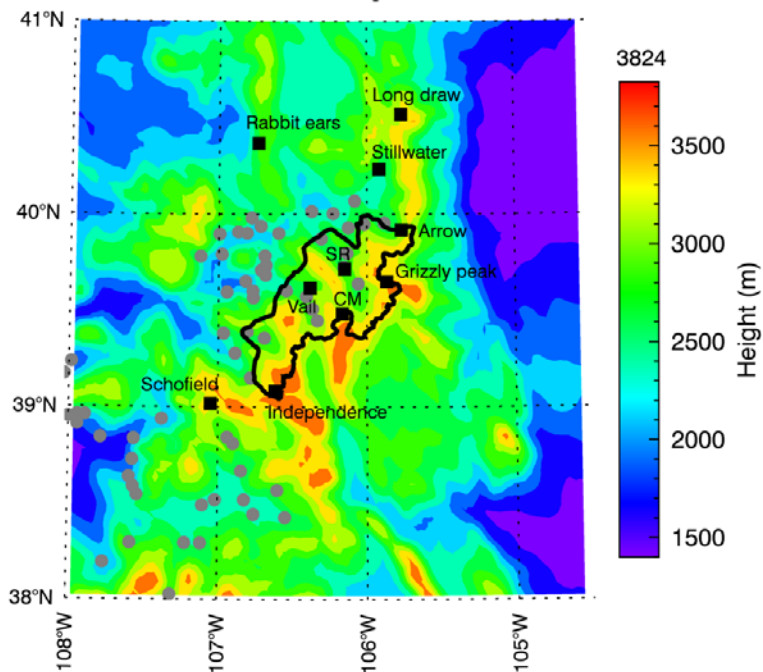


Figure 3.2 Plot of terrain height over the re-sampled WRF domain, similar to Figure 3.1. A selection of SNOTEL sites are identified by black square symbols (abbreviations: SR - Summit Ranch, CM - Copper Mountain).

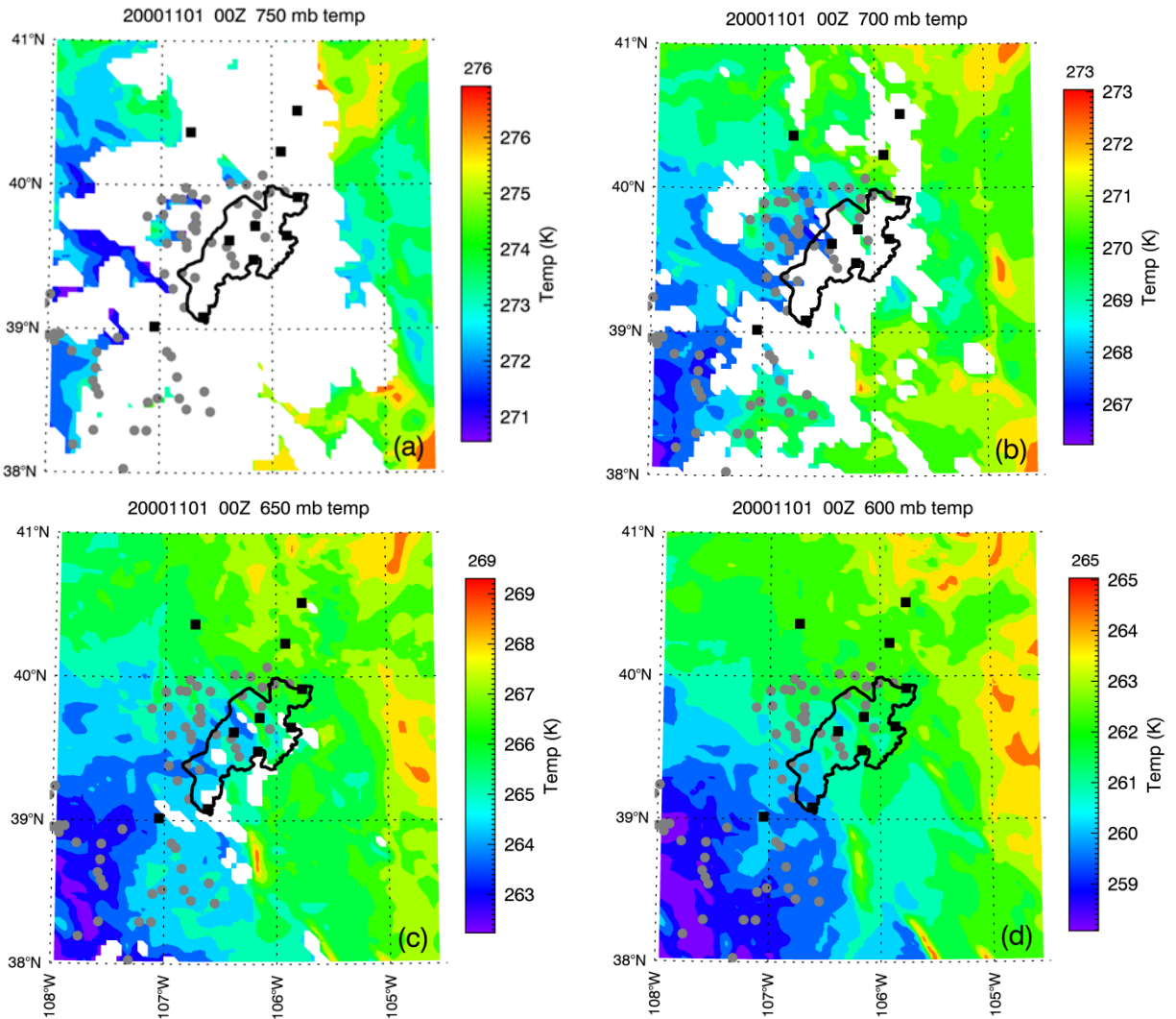


Figure 3.3 WRF temperature field at: (a) 750 mb, (b) 700 mb, (c) 650 mb, and (d) 600 mb, on 1 November 2000 at 0000 UTC. Temperature color scale (deg K) on right of each panel.

3.2.2 Formulating seed criteria

In order to establish seed criteria for Target Area 2, the operational criteria for seeding were considered. These criteria vary slightly from one operator to another. The two operators for Target Area 2 are Western Weather Consultants (WWC) and Desert Research Institute (DRI), and the various criteria are summarized in Table 3.2.

Table 3.2 Summary of seeding criteria utilized in Target Area 2 by each operator

Operational Criteria	WWC	DRI
1a. Cloud base heights are below the mountain barrier crest	✓	
1b. Cloud cover 50% to 100% over the target		✓
1c. Temperatures at 10,000 ft are ≤ -5 °C		✓
1d. Temperatures below mountain crest are ≤ -5 °C	✓	
1e. Winds from the surface to cloud base favor movement toward target	✓	
1f. Wind direction 280° through 341° and speed ≤ 40 mph (17.9 m/s)		✓
1g. No stable layers or inversions between the surface and -5 °C level	✓	
1h. Temperature at 10,000 ft (700 mb level) > -15 °C	✓	
1i. The occurrence of precipitation	✓	✓

Two approaches were taken in formulating seed criteria for the re-sampled WRF domain.

(i) Target area analysis (criteria 2a-2c)

The first approach taken in establishing periods when seed criteria are met was to treat the target area separately. The WRF data were reduced by drawing a polygon around Target Area 2 and data points within the polygon were treated as the dataset. Statistics for WRF variables at points inside the target area were produced. These statistics include minima, maxima, mean and standard deviation values for variables in the re-sampled data set (Appendix A, Table A1). Using the criteria in Table 3.2, the following conditions were imposed on the resulting statistics to define a seedable event:

2a) mean temperature at 700 mb between 268 K (-5 °C) and 258 K (-15 °C)

2b) maximum cloud water mixing ratio at 650 and 600 mb > 0.05 g kg⁻¹

2c) environmental lapse rate $<$ moist adiabatic lapse rate

These criteria are suitable if the target area is treated as its own dataset. If an attempt is made to analyze seed criteria spatially, the above criteria would have to be modified due to a possible bias that would result from missing data at 750, 700 and 650 mb. Therefore the criteria were changed so that a spatial analysis of seeding opportunity could also be performed.

(ii) Re-sampled domain spatial analysis (criteria 3a-3e)

The second approach taken was to run the seed criteria for every point within the domain to identify spatial variability in seeding opportunity inside and outside the target area. For the spatial analysis, the WRF criteria for seedable events were:

3a) temperature at 600 mb between 256.3 K (-16.6 °C) and 246.3 K (-26.7 °C)

3b) cloud water mixing ratio at 650 or 600 mb > 0.05 g kg⁻¹

3c) environmental lapse rate < moist adiabatic lapse rate

3d) horizontal wind direction at 10 m between 280 and 341 degrees

3e) horizontal wind speed at 10 m < 17.9 m/s (40 mph)

The spatial analysis complements the target area analysis in various ways. The target area approach is an area analysis where a single statistic (e.g., mean, maximum, minimum) is calculated on the value of each grid point and integrated within the target area polygon. The result is a single value that describes the entire target area. The spatial analysis produces statistics at each grid point that are presented spatially allowing for the comparison of sub-areas within the target area.

3.2.3 Implementing the seed criteria

The operational seed criteria (criteria 1a-1i) were formulated for the WRF target area (criteria 2a-2c) and the spatial analysis approach (criteria 3a-3e). Criterion 1a was represented by implementing criteria 2b and 3b in WRF. The difference between 2b and 3b is that in 2b, the 'and' condition requires that cloud be present at both 650 and 600mb while in 3b, the 'or' criteria is satisfied if cloud is present at either 650 or 600 mb. Criterion 3b is formulated using the 'or' condition due to missing data at 650 mb. In addition, the maximum cloud water mixing ratio within the target area is used in 2b. Criteria 1a and 1b could be more accurately represented in WRF by ensuring that cloud at 650 mb, which is below some of the mountain crests, is present and covers at least 50% of the points within the target area. This is a suggestion for future implementation and has not been done in this work.

Criteria 1c and 1h were represented in WRF by criteria 2a and 3a. In 2a, the minimum temperature within the target area is used, while in 3a, the temperature at each time step is used. In 3a, the temperature at 600 mb is used because of missing data at 700 mb. In this case a dry adiabatic lapse rate (DALR) was used to formulate the temperature criteria of 3a. For example, based on the DALR of 9.8°C per km, -5°C at 700 mb (~3000 m) would correspond to -16.6°C at 600 mb (~4200 m).

Consistent with criteria 1e and 1f, a wind condition was added as an example of favorable seeding conditions occurring in northwesterly flow. The DRI criteria for wind speed and direction (criteria 1f) in the DW-WP target area were used and adopted across Target Area 2 (criteria 3d and 3e). In future implementations, the wind criteria could be represented more accurately by considering mean wind direction at each generator site in relation to the target area. This is also a suggestion for improvement in the technique, but could prove to be quite complicated to implement.

Criterion 1g was represented in WRF by ensuring that the environmental lapse rate (ELR) was smaller than the moist adiabatic lapse rate (MALR) at each pressure level. This is called the condition of absolute stability where the DALR > MALR > ELR. In criterion 3c, the MALR is calculated at each pressure level by using the WRF temperature and water vapor mixing ratio. The ELR is calculated by subtracting the temperature at a higher pressure level from that of a lower pressure level. In criterion 2c, the mean temperature and maximum water vapor mixing ratio in the target area at each time step are used. In criterion 3c, the WRF temperature and water

vapor mixing ratio at each time step are used. If $MALR < ELR$ at any level, then the stability criteria are not met at that time step. Figure 3.4 shows plots of mean temperature for the month of January 2001 in the target area at each pressure level for out of cloud and in-cloud data points where condition 2a is satisfied. In this case, 510 hours – data points – out of 744 hours satisfied condition 2a. Out of these 510 hours, 277 hours were out of cloud and 233 hours were in-cloud at 650 mb. Of the in-cloud fraction, 17 hours (data points) did not satisfy criteria 2c at 650 mb. If the stability criterion was not met at any level, then that time-step failed the stability criterion. In this case the 17 time-steps that fail the criteria at 650 mb would cause those same time-steps to fail the stability criterion at each level. This ensures that no stable layers are present at any particular time as identified in criteria 1g. This measure of stability or more specifically inversions is admittedly coarse and probably unrepresentative of stability closer to the altitudes of the generators. Further work is needed to establish a reasonable stability parameter from model data that addresses the trapping potential of inversions on seeding material.

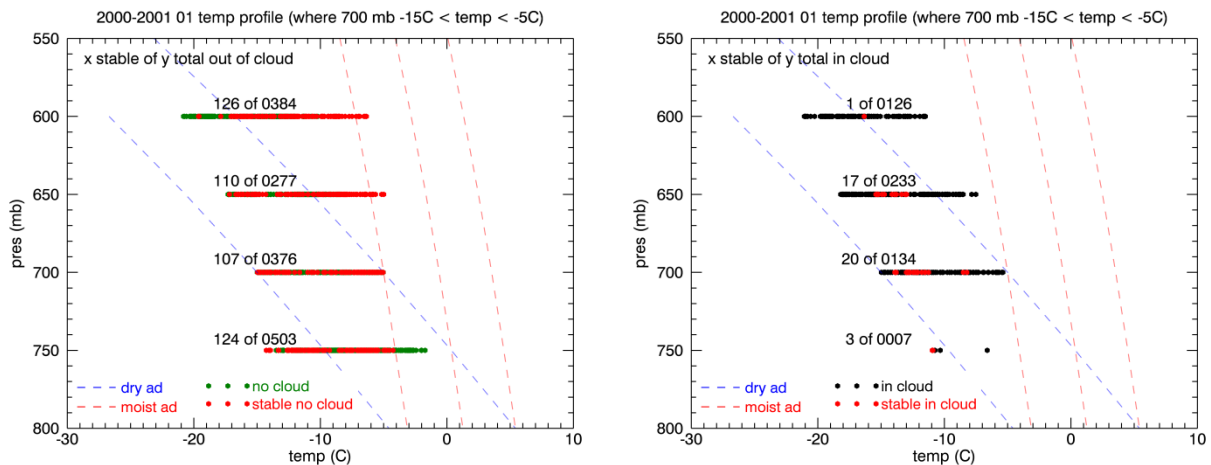


Figure 3.4 January 2001 mean temperature in the target area at each pressure level for out of cloud (left) and in-cloud (right) data points where the 700 mb temperature is between -5 °C and -15 °C. To compare temperature ranges between pressure levels, adiabatic lapse rates are indicated.

Once each of the conditions 2a-2c and 3a-3e are formulated, the seed criteria are then calculated at each time-step by calculating the logical ‘and’ operation between each of the conditions. This implies that for the seed criteria to be met, each of the conditions would need to be met. Describing this formulation in logical terms, for the seed criteria to equal ‘seed’, each of 2a, 2b and 2c would have to be equal ‘seed’. The same applies for criteria 3a-3e.

There is some variability in the number of seed time-steps or hours that satisfy the criteria as formulated from the model. In order to explore the variability in the number of seed hours that satisfy each condition, slight variations in condition 2b were tested while 2a and 2c were kept constant. The variations tested for 2b are shown in Table 3.3. As expected, the number of ‘seed’ hours decreased as the criteria became more stringent. The most stringent condition (4d) was adopted and implemented as the cloud criterion

Time periods when seed criteria were met resulted in a text file that was used to generate the statistics for the monthly, seasonal, and eight-year periods. An example is given in Appendix B.

Table 3.3 Variations in cloud conditions (2b) and percentage of the time condition was 'seed'

Variation in criterion 2b	% time seed
4a) cloud water mixing ratio at 650 mb > 0.01 g kg ⁻¹	28
4b) cloud water mixing ratio at 650 mb > 0.05 g kg ⁻¹	27
4c) cloud water mixing ratio at 650 and 600 mb > 0.01 g kg ⁻¹	21
4d) cloud water mixing ratio at 650 and 600 mb > 0.05 g kg ⁻¹	18

3.3 Example model comparison with one SNOTEL site

Model validation was performed using one month of SNOTEL data from one site as an example. Data from the Summit Ranch SNOTEL (39.72°N, 106.15°W) was used for this analysis. The Summit Ranch (SR) SNOTEL is located in the north central section of Target Area 2 at an altitude of 2865 m (9400 ft). Three WRF data points closest to SR were used for the comparison. These points were all located within 10 m elevation and 4.7 km distance from SR. The mean values of these three points were then compared with SR SNOTEL. There was an insignificant difference between the mean value of the three points and the value at the point closest to SR (39.72°N, 106.13°W).

Comparing means and trends in the data provides an indication of how well the model performed. A common measure of the difference between values predicted by a model and the values actually observed is the root mean square error (RMSE). The bias between modeled and measured data is also used as a measure of model prediction error. Figure 3.5 shows plots of WRF and SR SNOTEL data for November 2004. As might be expected given the model resolution, the temperature trace is dampened for the model values, leading to an elevated RMSE of 3.06°C for the whole month. But the observed temperature bias over the whole month is only -0.05°C. The traces of bias and RMSE are shown in the second panel of Figure 3.5. The bias and RMSE are printed on the subsequent traces for snow depth and snow water equivalent. The SR SNOTEL data were not quality controlled and there are some obvious spikes and inconsistencies in the snow measurements. Although the model generally underestimates snowfall, the comparisons are reasonable once the data problems with the SNOTEL observations are taken into account.

A potential problem with this comparison is evident in the location of SR. It is located in close proximity to the base of a valley that is only about 15 km wide. Since the WRF model resolution is 4-km, simulating the strong gradients likely to be present between the valley and local mountain tops would tax the resolution of the model. Diurnal temperatures and precipitation amounts in particular would be damped.

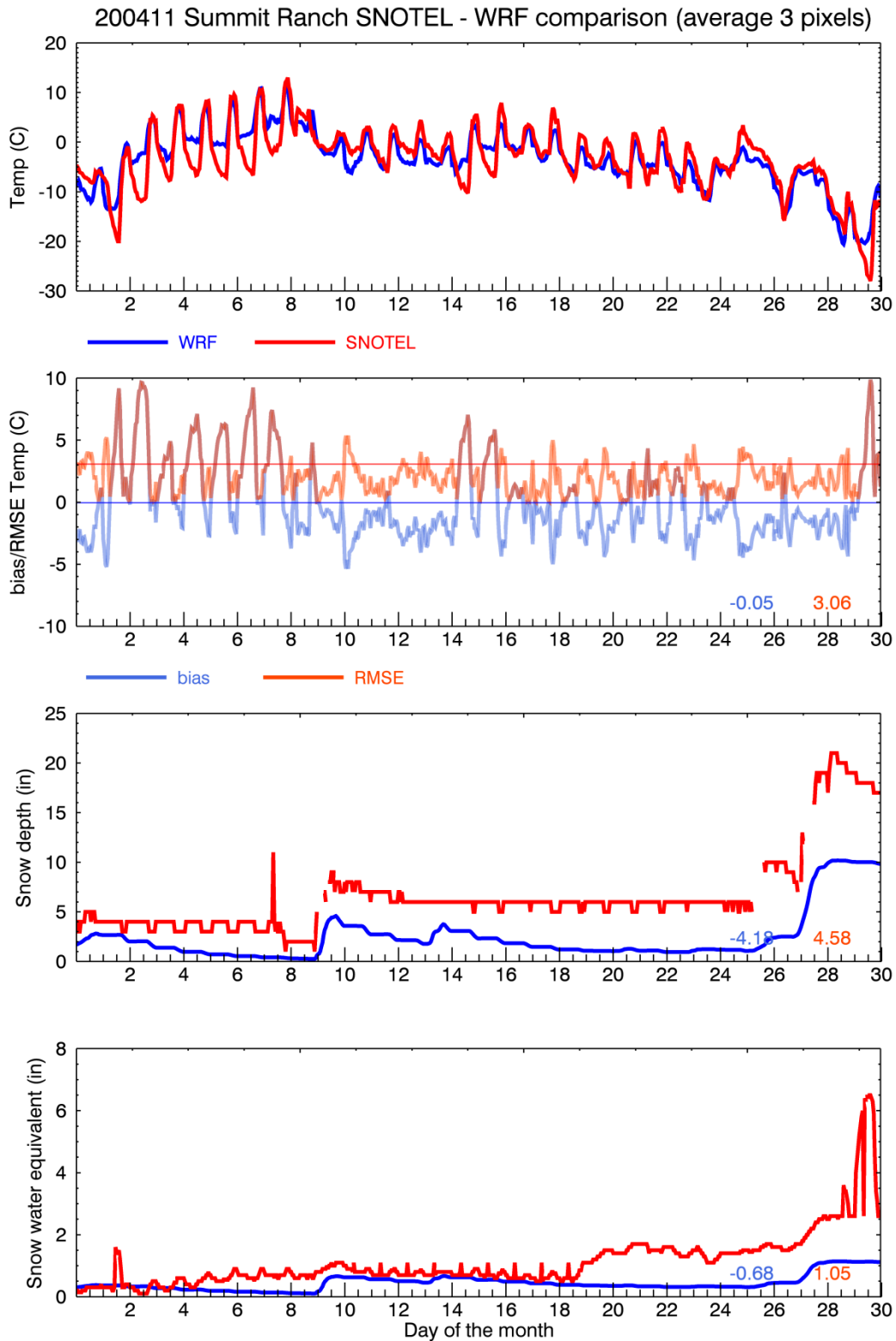


Figure 3.5 Summit Ranch SNOTEL-WRF comparison for November 2004. The bias (blue) and RSME (red) values are listed in the bottom three plots.

A thorough WRF-SNOTEL evaluation of this dataset has already been done by Ikeda et al. (2010) showing that for a wide range of monthly precipitation totals the model agrees within ~15-20% from November through March. The largest contribution to the differences tend to be due to an outlier storm that the model grossly under- or over-predicted. The large-scale agreement between the model and the SNOTEL precipitation provides confidence that the high-resolution WRF model can properly simulate snowfall over the domain. Other detailed comparisons, such as with radiometer-derived liquid water path, have shown very good agreement between the WRF model and observations (e.g. results of the Wyoming Weather Modification Pilot Program, final report in preparation).

3.4 Climatology of seedable and non-seedable *periods*

The first step in compiling a climatology of seed and non-seed periods across Target Area 2 entailed running each time-step of the WRF data through the 2a-2c seed criteria as described in Section 3.2.2 (i). This process identified the time-steps when the seed criteria were met. The time-series plots in Figure 3.6 show traces of mean temperature, maximum cloud water mixing ratio, maximum snow mixing ratio, maximum ice mixing ratio, 1-hour precipitation and mean wind direction for Target Area 2 during the 2000-2001 season as an example. Other examples are shown in Appendix C. The red portion of each trace indicates time segments when the seed criteria were met. For example, in the 2000-2001 season, 1039 hours satisfied the seed criteria, 23% of the time, while 3305 hours did not. Another way to compare no-seed and seed conditions is to use histogram plots. For example, histogram data are shown for mean temperature within Target Area 2 at each pressure level for non-seed segments (Figure 3.7) and seed segments (Figure 3.8). The minimum, mean and maximum temperatures at each level are displayed in the upper right corner of each panel. These statistics were produced for each month and each season starting November 2000 and ending April 2008. A table of statistics for several variables during the 2000-2001 and 2007-2008 seasons and example plots for the 2007-2008 season are given in Appendix C.

Clearly the results of the climatology are dependent on the formulation of the seed criteria. For example, the effect of the temperature criteria is apparent in the 2000-2001 WRF data plotted in Figures 3.7 and 3.8. Seed cases are colder at 700 mb with a mean temperature of -8.5 °C. Non-seed cases had a mean temperature of -6.1 °C. The same is true for all seasons (shown in Appendix C) with an overall mean of -6.1 °C, a mean for seed cases of -9.0 °C, and a mean for non-seed cases of -5.3 °C. Due to the temperature criterion 2a and the stability criterion 2c, the mean temperature for seed cases has a narrow distribution around the mean. Examination of the stability criterion 2c shows that it does not affect a large number of cases. For example, Figure 3.9 shows that out of a total of 3881 data points in-cloud, only 258 cases or 6.6% were stable during the 2007-2008 season.

The implementation of seed criteria 2a-2c for the entire Target Area 2 has been demonstrated through frequency distributions and time-series plots. The frequency distributions show how the seed criteria variables fluctuated at each pressure level and between seed and non-seed cases. The time-series presentations provide information on the intermittent duration of seed events and describes how specific variables, such as temperature, impact the duration of each event.

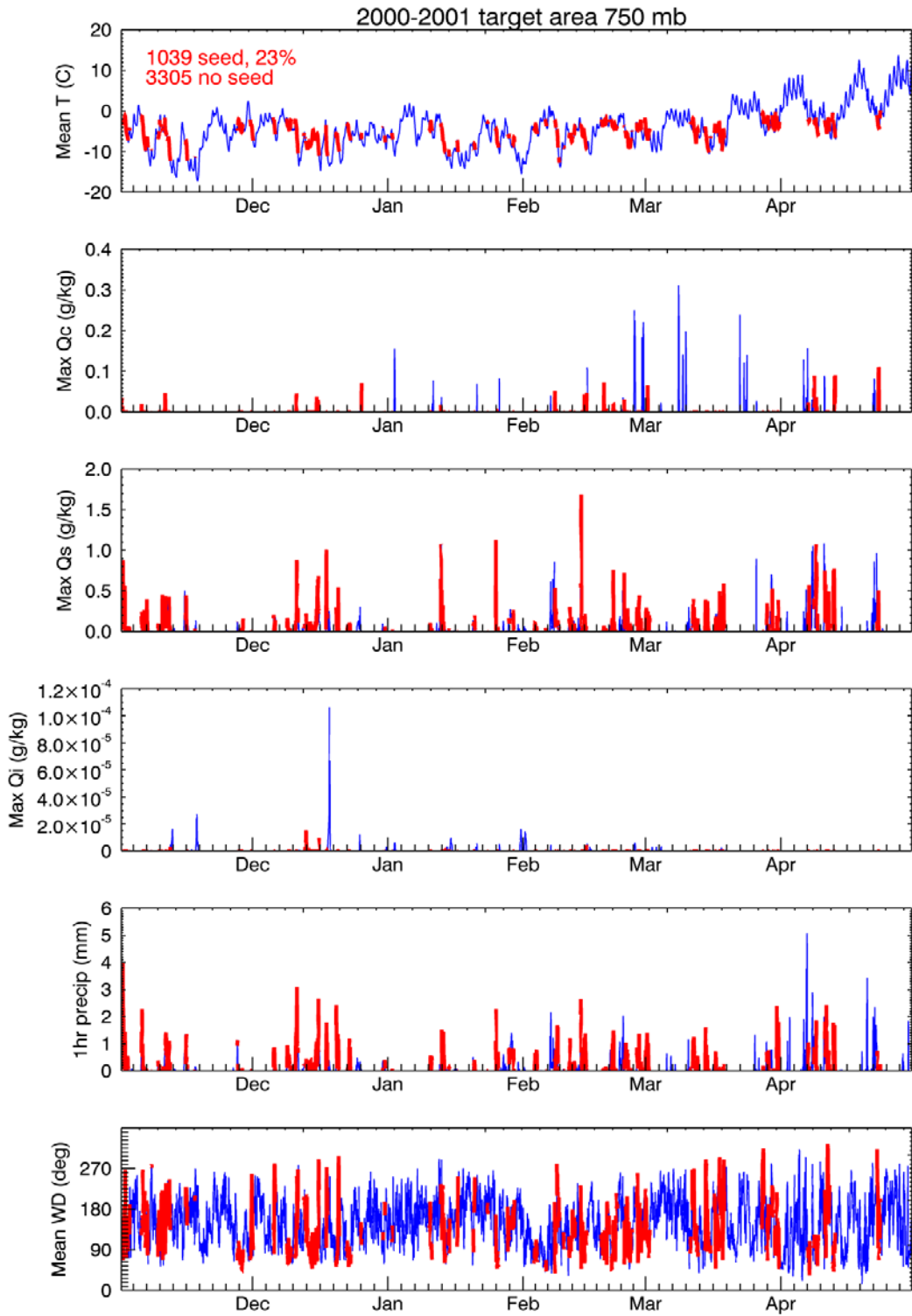


Figure 3.6 Mean temperature, maximum cloud water mixing ratio, maximum snow mixing ratio, maximum ice mixing ratio, 1-hour precipitation and mean wind direction for Target Area 2 during the 2000-2001 season. The red trace indicates that the seeding criteria 2a-2c were met.

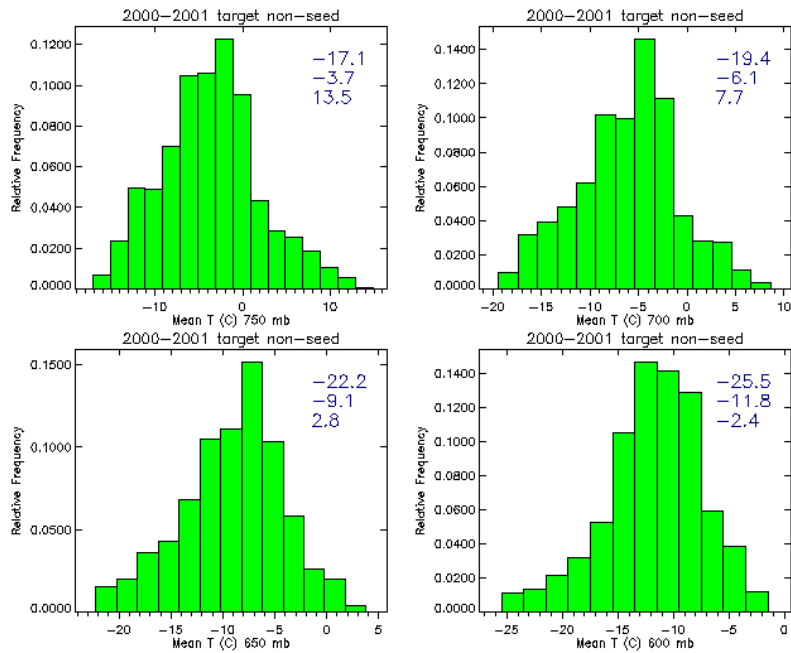


Figure 3.7 Mean temperature at 750, 700, 650 and 600 mb for no-seed cases during the 2000-2001 season. The minimum, mean and maximum temperatures of the distribution are printed in the upper right corner.

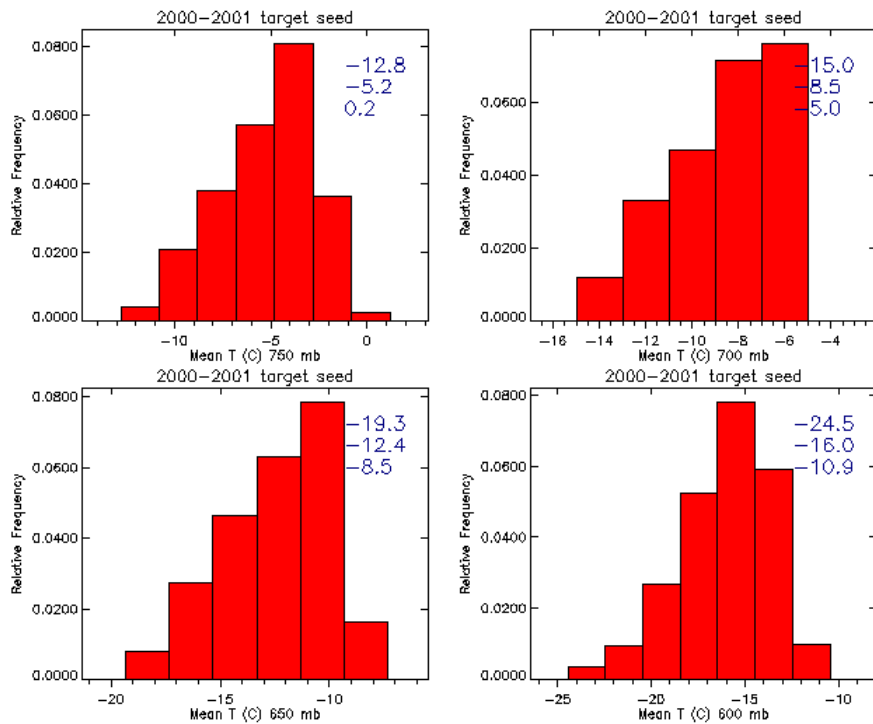


Figure 3.8 Mean temperature at 750, 700, 650 and 600 mb for seed cases during the 2000-2001 season. The minimum, mean and maximum temperatures of the distribution are printed in the upper right corner.

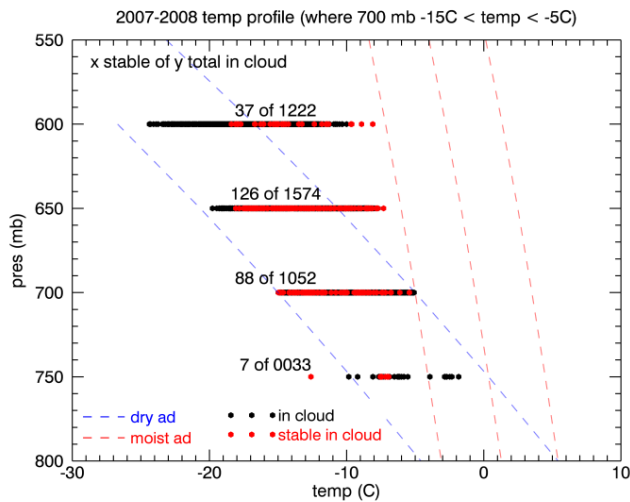


Figure 3.9 2007-2008 season mean temperature in the target area at each pressure level for in-cloud data points where the 700 mb temperature is between -5 °C and -15 °C.

3.5 Climatology of seedable and non-seedable areas

A spatial analysis of seeding criteria was done by applying seed criteria 3a-3e at each grid point allowing for the comparison of sub-areas within the target area. The first step was to grid the WRF variables spatially within the re-sampled domain. An example is given in Figure 3.10 where (a) shows the cloud water mixing ratio at 600 mb, (b) cloud water mixing ratio at 650 mb, (c) 10-m mean wind direction, (d) 10 m-mean wind speed, and (e) 600 mb mean temperature. The next step was to populate a gridded data set of binary values for each time step to indicate which grid points satisfied criteria 3a-3e. Since the binary value assigned to a grid point for each 1-hour time-step that satisfied the criteria was 1 (0 was assigned if criteria not satisfied), the addition of the binary values for each grid point over a period of a month amounted to the time in hours when seeding criteria were met. Figure 3.11 shows an example of this step where each criteria or a set of criteria are used to produce the frequency of hours that satisfies the condition. Figure 3.11 (e) is a composite of Figures 3.11 (a-d) where all the criteria are used to produce final seed criteria. Figure 3.11 (e) shows that for the month of January 2008 there was a maximum of 150 hours (20%) out of 744 hours when seeding criteria 3a-3e were met. This maximum was in the northern part of Target Area 2.

The spatial analysis produces statistics at each grid point. These statistics were produced for each month and each season starting November 2000 and ending April 2008. Appendix C elaborates on these statistics and shows plot examples.

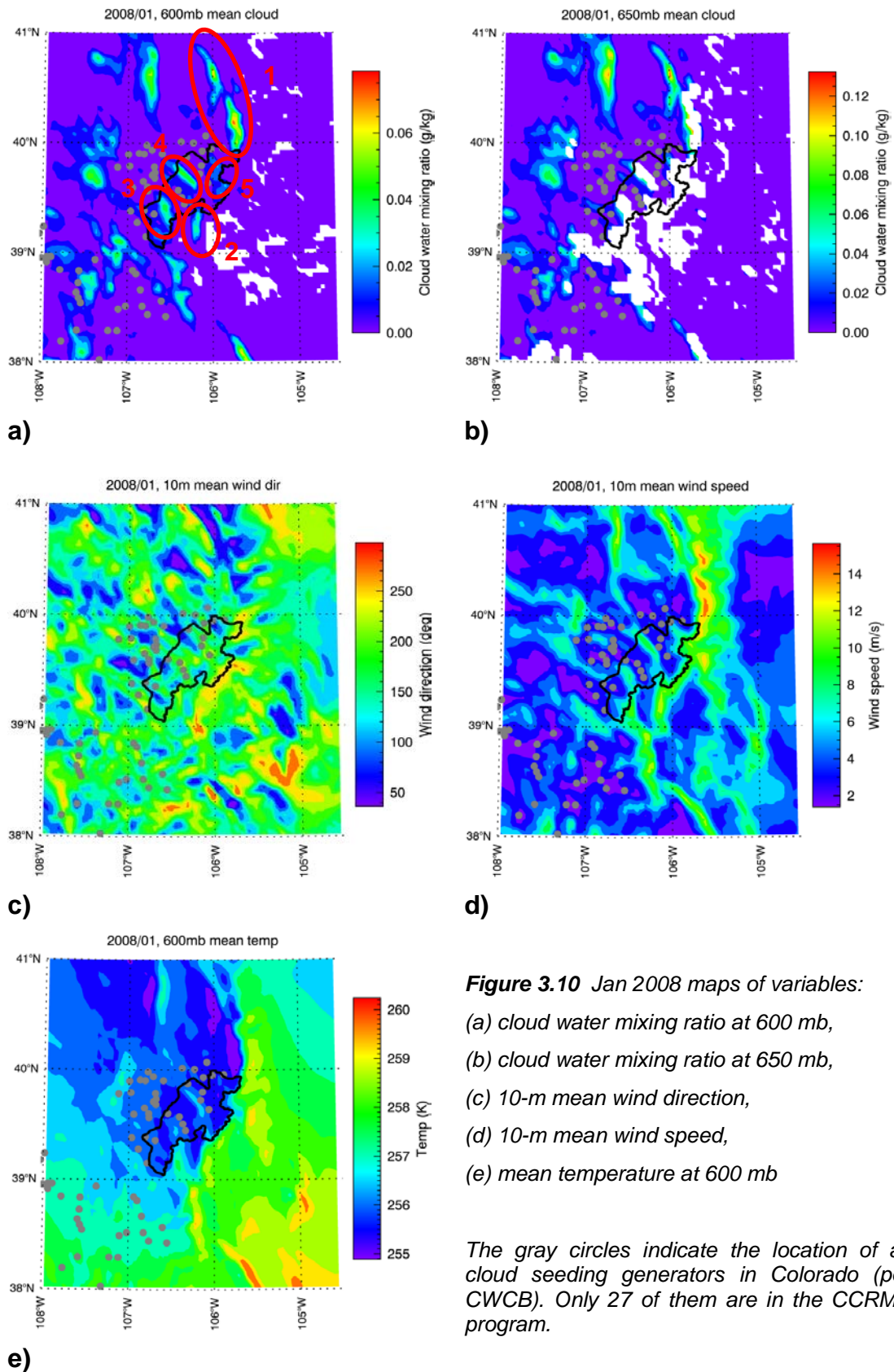


Figure 3.10 Jan 2008 maps of variables:

- (a) cloud water mixing ratio at 600 mb,
- (b) cloud water mixing ratio at 650 mb,
- (c) 10-m mean wind direction,
- (d) 10-m mean wind speed,
- (e) mean temperature at 600 mb

The gray circles indicate the location of all cloud seeding generators in Colorado (per CWCB). Only 27 of them are in the CCRMB program.

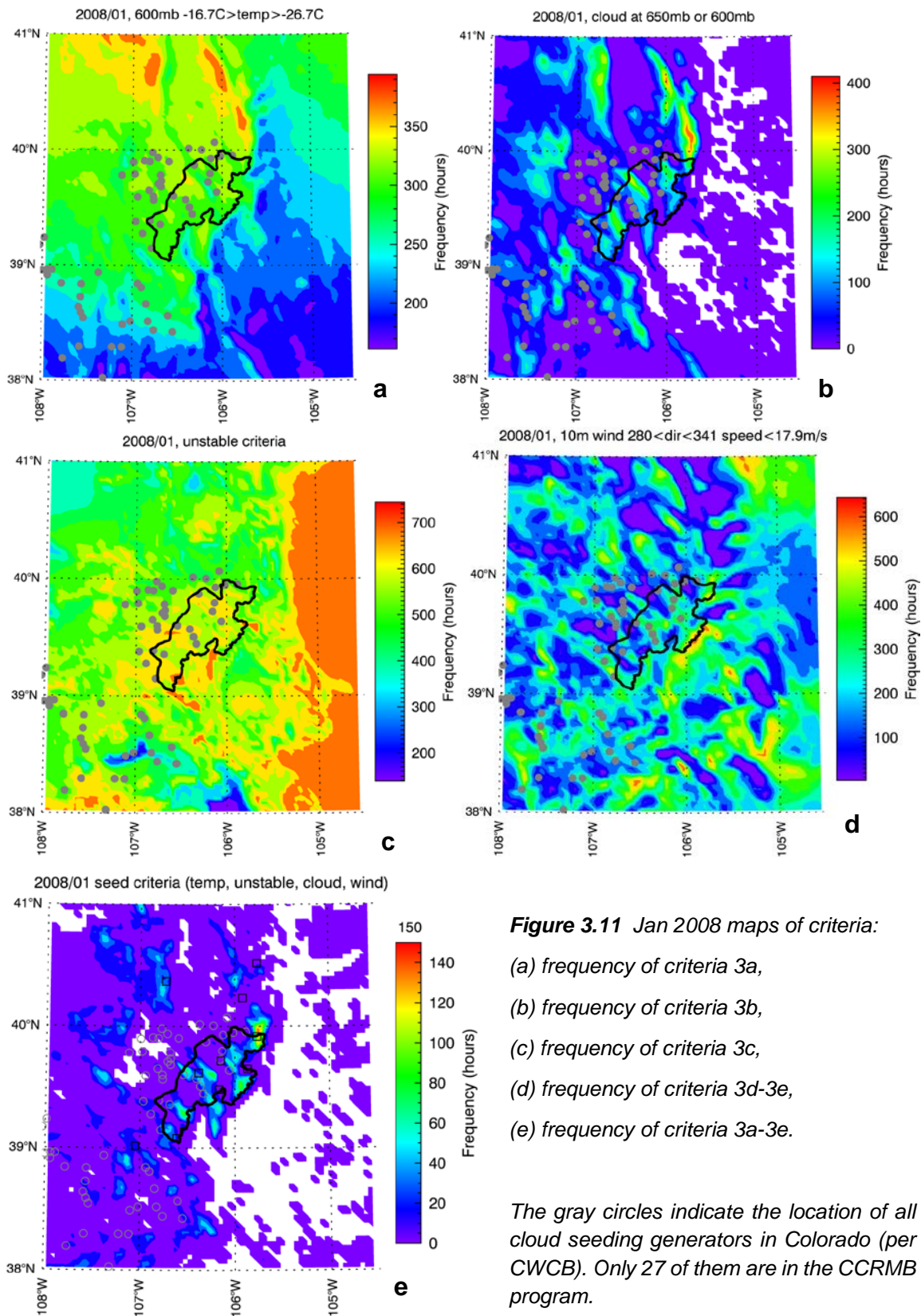


Figure 3.11 Jan 2008 maps of criteria:

- (a) frequency of criteria 3a,
- (b) frequency of criteria 3b,
- (c) frequency of criteria 3c,
- (d) frequency of criteria 3d-3e,
- (e) frequency of criteria 3a-3e.

The gray circles indicate the location of all cloud seeding generators in Colorado (per CWCB). Only 27 of them are in the CCRMB program.

The spatial analysis allows for the observation of meteorological features relevant to the seed criteria within the target area as well as outside the target area. Figure 3.10 shows mean values for each variable for January 2008. Figure 3.10 a) and 3.10 b) show the mean spatial distribution of cloud water at 600 and 650 mb respectively. The cloud water mixing ratio shows a maximum along the Front Range and north of Winter Park, just north of the target area. This area is identified as sub-area 1 in Figure 3.10 a). Wind speeds along this area and to the east along the Divide are a maximum reaching 14 m s^{-1} . Temperatures along this section of the Divide are also the coldest during January 2008.

Another area that shows similar meteorological features extends from Copper Mountain to the south along the Mosquito Range. This area, identified as sub-area 2, falls on higher terrain reaching heights greater than 3.5 km MSL. Cloud water mixing ratio is high and temperatures low compared to surrounding areas.

Sub-areas 3 and 4 also have the same meteorological features. Area 3 in the Vail/Battle Mountain area and area 4 in the Eagles Nest Wilderness area are at the same elevation range, with equally high mean cloud water mixing ratio, similar wind direction and speed, and a similar temperature range.

Figure 3.11 shows the frequency in hours that seed criteria are met for temperature at 600 mb (a), cloud at 650 or 600 mb (b), instability (c), and wind direction and speed (d). Figure 3.11 e) shows the frequency when all the seed criteria (3a-3e) are met. The higher frequency contours coincide with the sub-areas defined in Figure 3.10 a), within and outside the target area where seed criteria are satisfied more frequently. Temperature criteria are met more frequently along the Front Range in sub-area 1. This is also where the frequency of clouds at 650 or 600 mb is the highest, making this area favorable for seeding. The instability is highest along the Plains, but some areas (e.g. sub-area 2) show pockets of high instability. Wind criteria 3d and 3e are satisfied at high frequency in sub-area 2 and along the eastern edge of the target area in sub-area 5. In this case, the seeding conditions during January 2008 were most favorable in the southern portion of area 1 and in each of areas 2-5. All these sub-areas are within Target Area 2 except for the southern tip of area 1.

The spatial mean values for cloud water, wind and temperature for all seasons (2002-2008) are shown in Appendix C, and have similar contour patterns to the January 2008 example in Figure 3.10. This suggests that the meteorological fields are strongly correlated with terrain features. Although this is not investigated further, future work could focus on studying this observation and its relevance to seedability.

3.6 Seedability and seeding potential

In Section 3.5, the seedability using criteria 2a-2c was discussed. This analysis identified time segments when seeding criteria were met for the target area. Table 3.4 summarizes these monthly results. The seedability varies from 2% of the time in April 2002 to 44% of the time in February 2008. The month with the lowest mean seedability is April and the highest is February. The mean seedability for all seasons was 20%. These results are shown graphically in Figure 3.12.

Table 3.4 Percentage of time 2a-2c seed criteria are met

Season	Mean %	Nov %	Dec %	Jan %	Feb %	Mar %	Apr %
2000-2001	23	25	27	14	38	25	12
2001-2002	16	13	24	21	17	18	2
2002-2003	21	18	23	16	33	26	13
2003-2004	18	22	21	20	22	19	6
2004-2005	23	15	24	23	25	39	10
2005-2006	22	16	22	29	25	28	11
2006-2007	15	13	19	13	30	8	8
2007-2008	25	5	17	31	44	26	26
Mean %	20	16	22	21	29	24	11

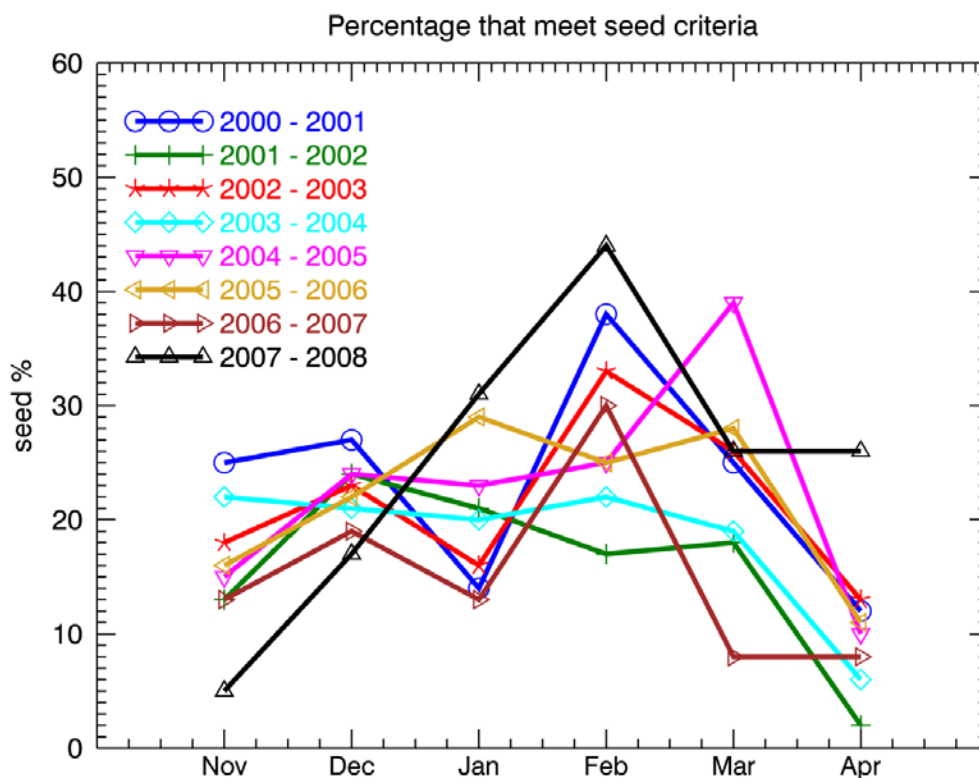


Figure 3.12 Percentage of time during each season that 2a-2c seed criteria are met

The climatology analysis also uses a spatial analysis of seeding criteria by applying criteria 3a-3e to each grid point. Figures 3.13 - 3.16 show the results of the spatial distribution of each of these criteria and Figure 3.17 shows the aggregation of each of these into a composite seed criterion. Figure 3.17 highlights the variation in frequency of seedability. The target area encompasses sub-regions where the frequency of seedability exceeds 5% while surrounding areas have a very low seedability.

Regions of high seedability present true potential for seeding if the snowfall is sufficient to warrant seeding activity. In order to investigate this more thoroughly, a variable called "seed potential" was formulated. Seed potential is the normalized product of seed frequency and snow gain. Snow gain is the snow water equivalent at the beginning of the day subtracted from that at the end of the day, which is essentially the daily snow water equivalent. By relating the snowfall to the seedability, it is possible to determine the best opportunity for seeding.

Figure 3.18 shows the spatial distribution of snow water gain accumulated through all eight seasons. Snow gain is the highest in the Park Range near Steamboat Springs and is quite high in other regions along the Front Range. The frequency distribution of seed potential for 2000-2008 is shown in Figure 3.19. The plot shows that the distribution of seed potential follows the snow gain but not precisely. Eight regions have been identified where the seed potential exceeds 50%. These areas are identified as sub-areas 1-8 and are located along the Front Range, Bull Mountain, Burro Mountain, Flattop Mountain on the Continental Divide and the Elk Mountains. Four of these areas lie within the target area. The highest potential lies just outside and to the north of the target area in the Indian Peaks Wilderness.

The seed potential spatial distribution provides a climatologically-based analysis of the true seeding potential derived from operational seed criteria and snow water equivalent. The formulation of the seed criteria and seed potential provide an opportunity to either identify new target areas or to confirm that existing target areas have good seeding opportunities.

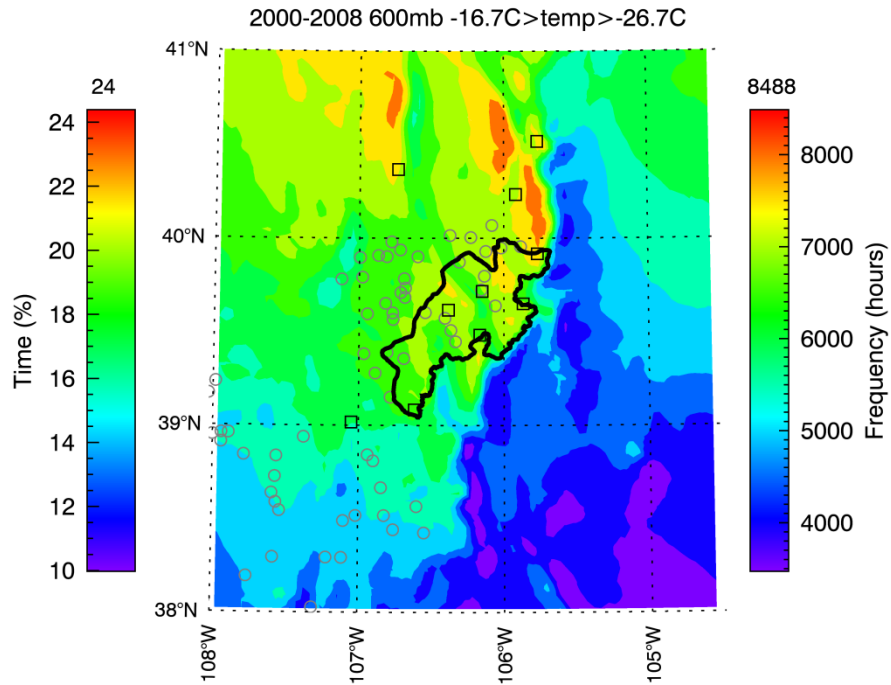


Figure 3.13 2000-2008 frequency of criteria 3a (-16.7°C > temperature > -26.7°C)

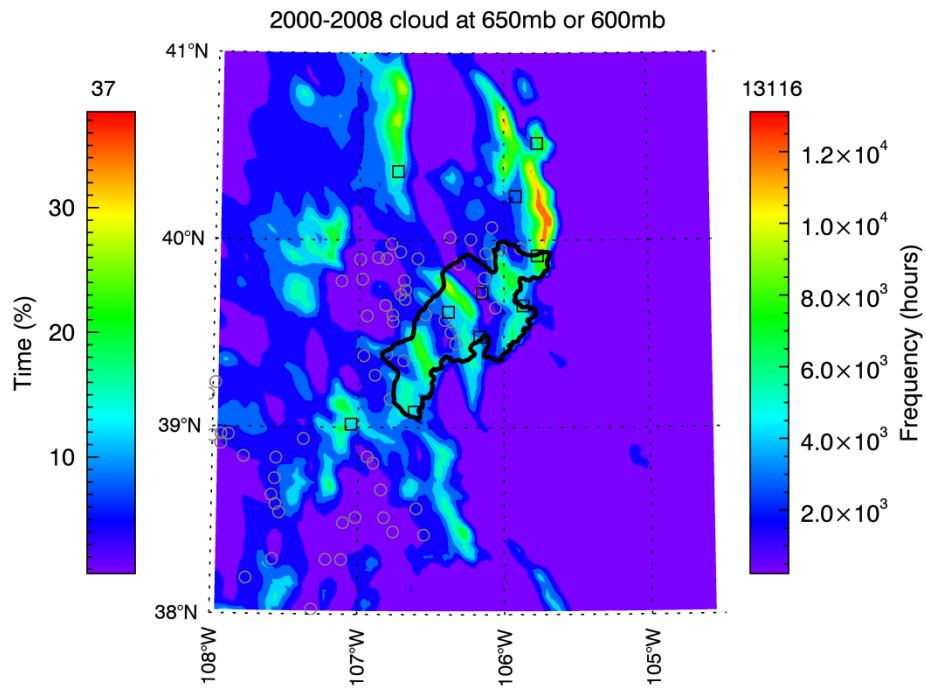


Figure 3.14 2000-2008 frequency of criteria 3b (cloud at 650 or 600 mb)

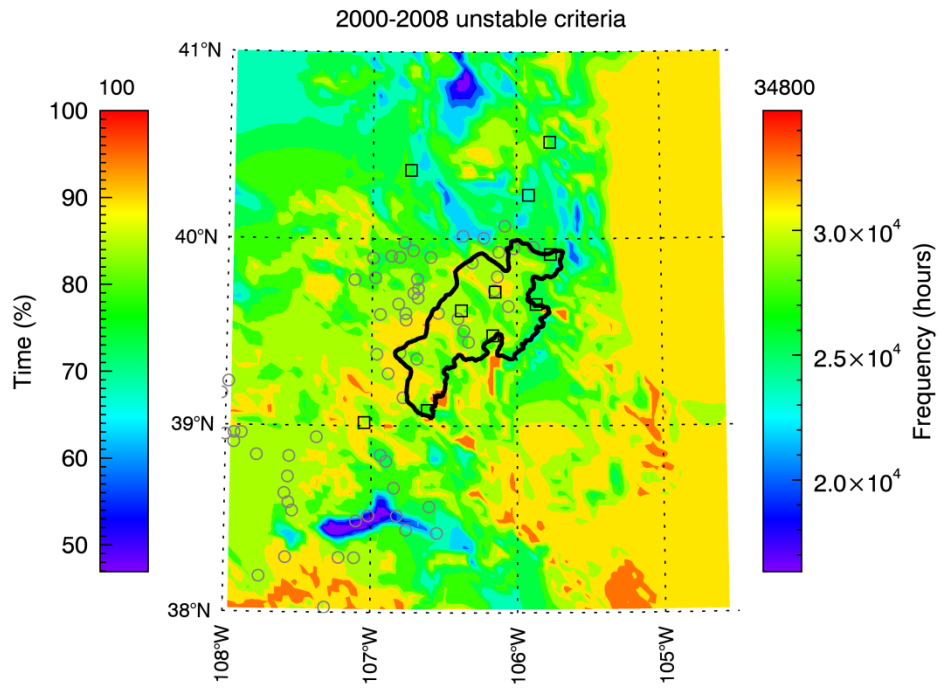


Figure 3.15 2000-2008 frequency of criteria 3c (instability)

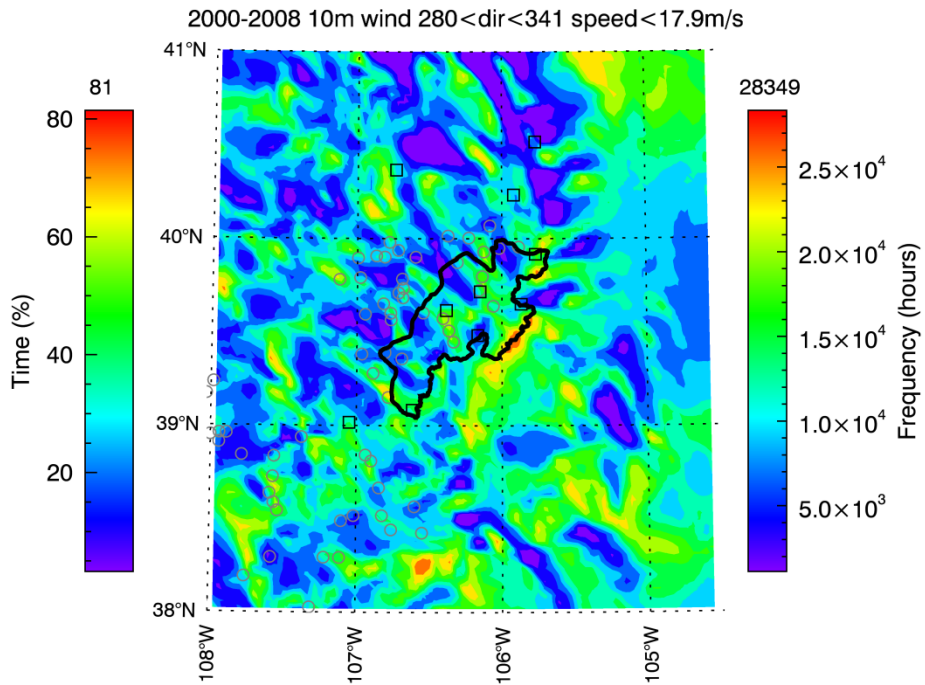


Figure 3.16 2000-2008 frequency of criteria 3d-3e (wind speed and direction)

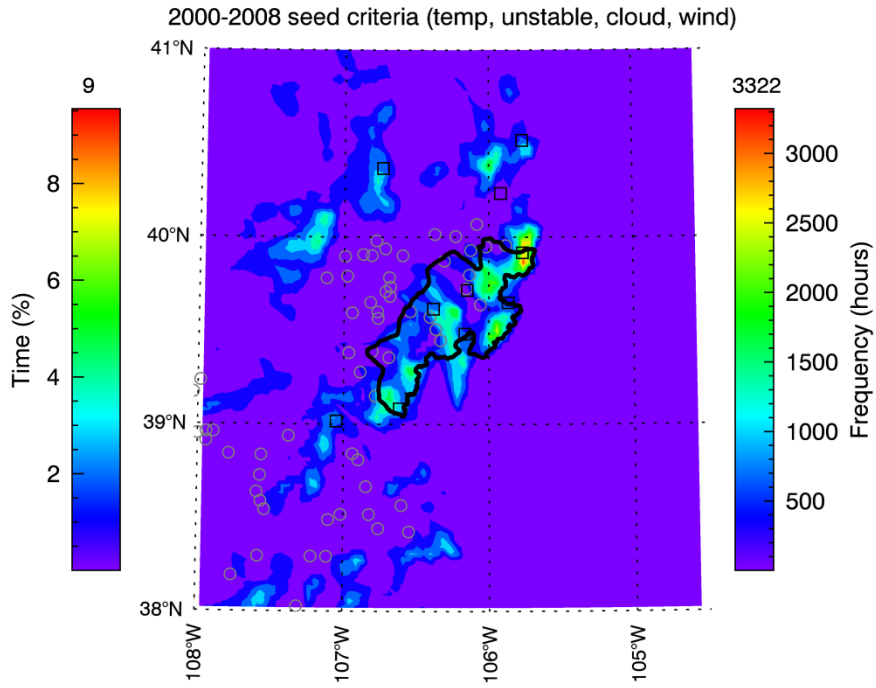


Figure 3.17 2000-2008 frequency of criteria 3a-3e (all criteria)

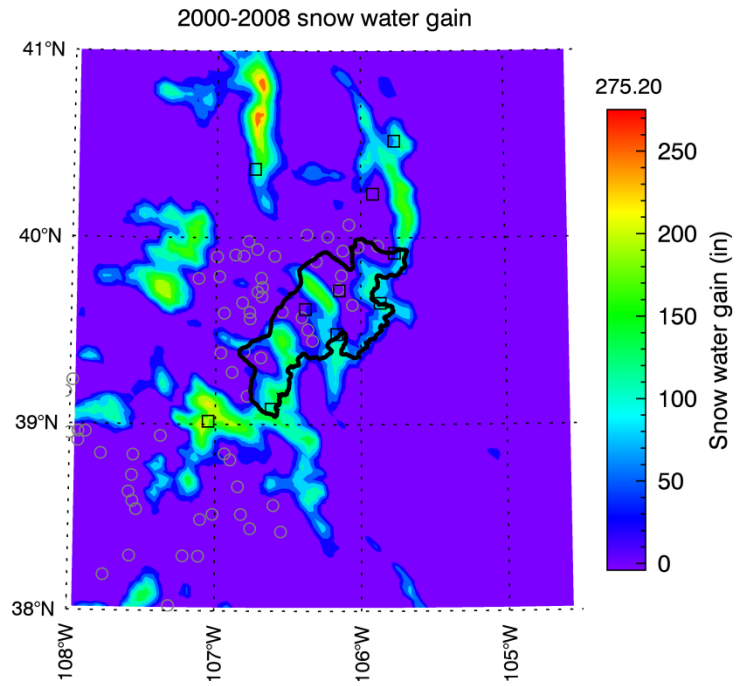


Figure 3.18 2000-2008 snow gain

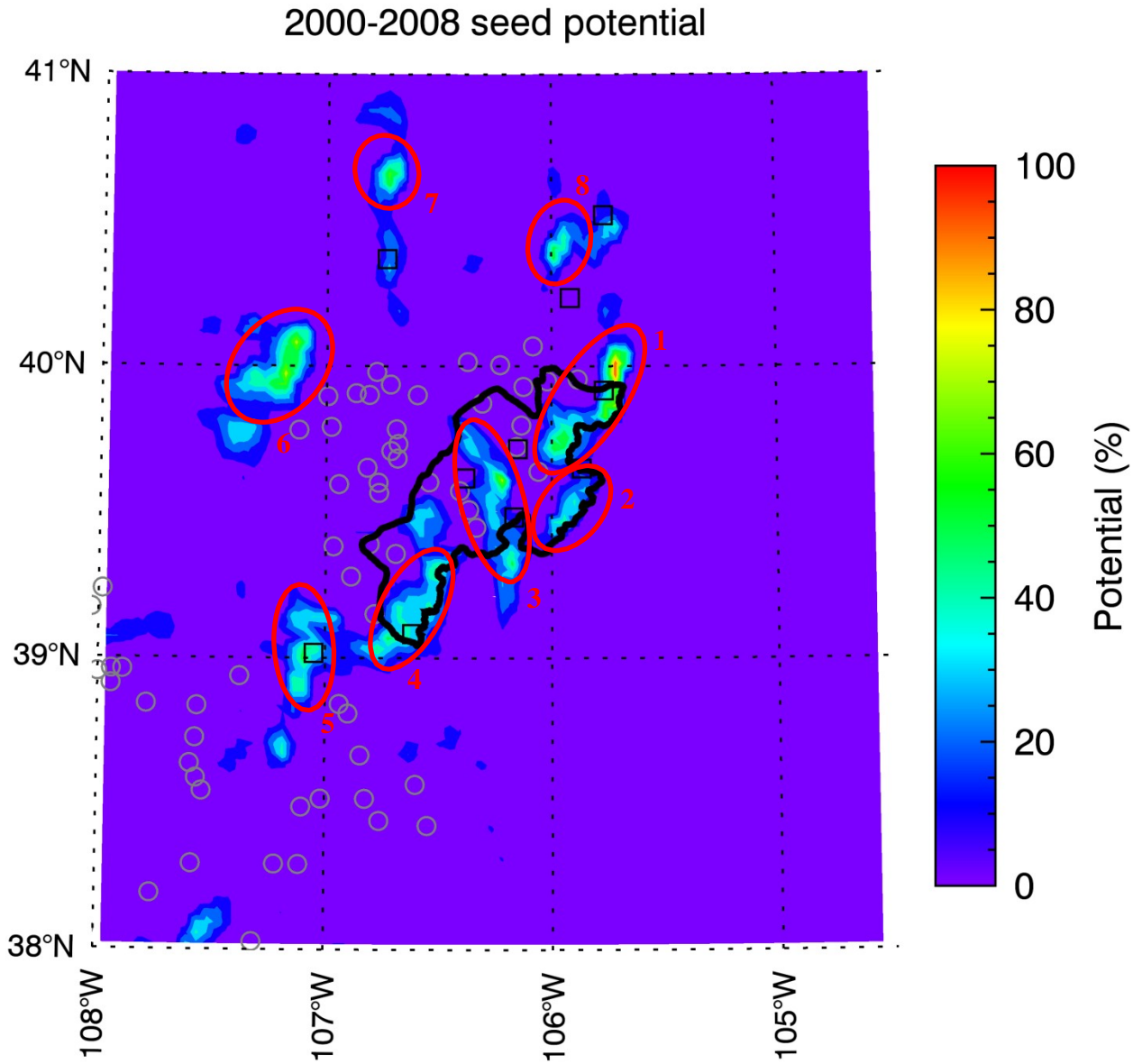


Figure 3.19 2000-2008 normalized distribution of 'seed potential'

4 WRF model simulation at 800-m resolution – one example

4.1 Choice of storm event

For the initial high-resolution WRF model simulation in the CCMRB area, a seeding case with supporting observations was desirable. Ideally, a case from a day(s) used in the climatology analyses would allow for some direct comparisons. However, the observational data set did not include days from the 2000-2008 period, so a recent seeding event was chosen.

Seeding events when the DRI remote-controlled generators operated were examined because of the additional observations at Winter Park. The 28-29 January 2013 period was chosen for the model simulation since it included a major snow event and two closely spaced seeding periods. A figure from the DRI 2013 report to CWCB (Figure 4.1) shows seeding periods at the end of January, along with observations. The 28-29 January seeding periods are marked as grey bars straddling 1/29/13 in the figure.

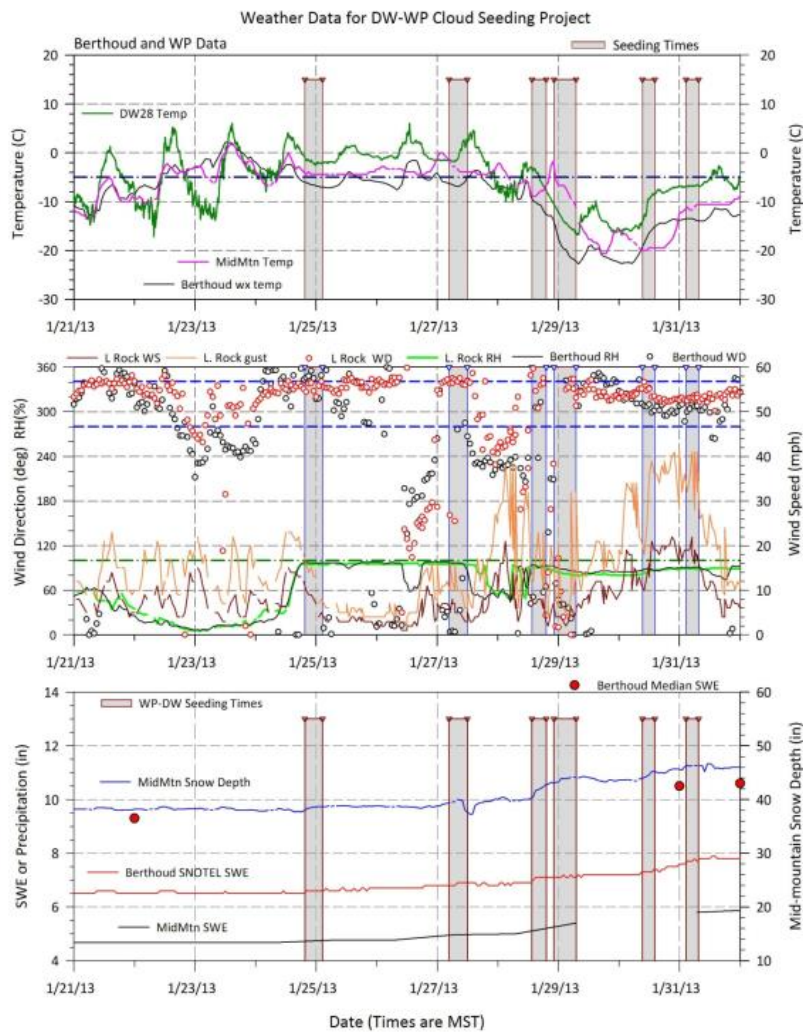


Figure 4.1 Observational data and seeding events (grey bars) for 21Jan – 1 Feb 2013 at the Winter Park target area. Model simulation included the two seeding events on 28-29 January. (From DRI 2013 report.)

4.2 Model setup and simulations

The WRF model was nested from the 32-km grid spacing of the NARR data set to a 4-km grid, and then nested again to an 800-m grid. A map of the topography on the 4-km and nested 800-m domains (Figure 4.2) shows the region covered by the smaller grid spacing and the change in resolution of the topography. The model was initialized at 0000 UTC on 28 January 2013. The 800-m grid model was also initialized at 0600 UTC for a comparison test run, but the results presented here are for the 0000 UTC run. Details of the model setup are listed in Appendix D. Other than the nested grid spacing, the other general point to be made is that the model ran for 36 hours, beginning 20-21 hours before seeding started. The first 6 hours or so of such simulations usually involve “spin-up” errors, as the model comes into balance, so sufficient time for model stability was planned.

Domain configuration

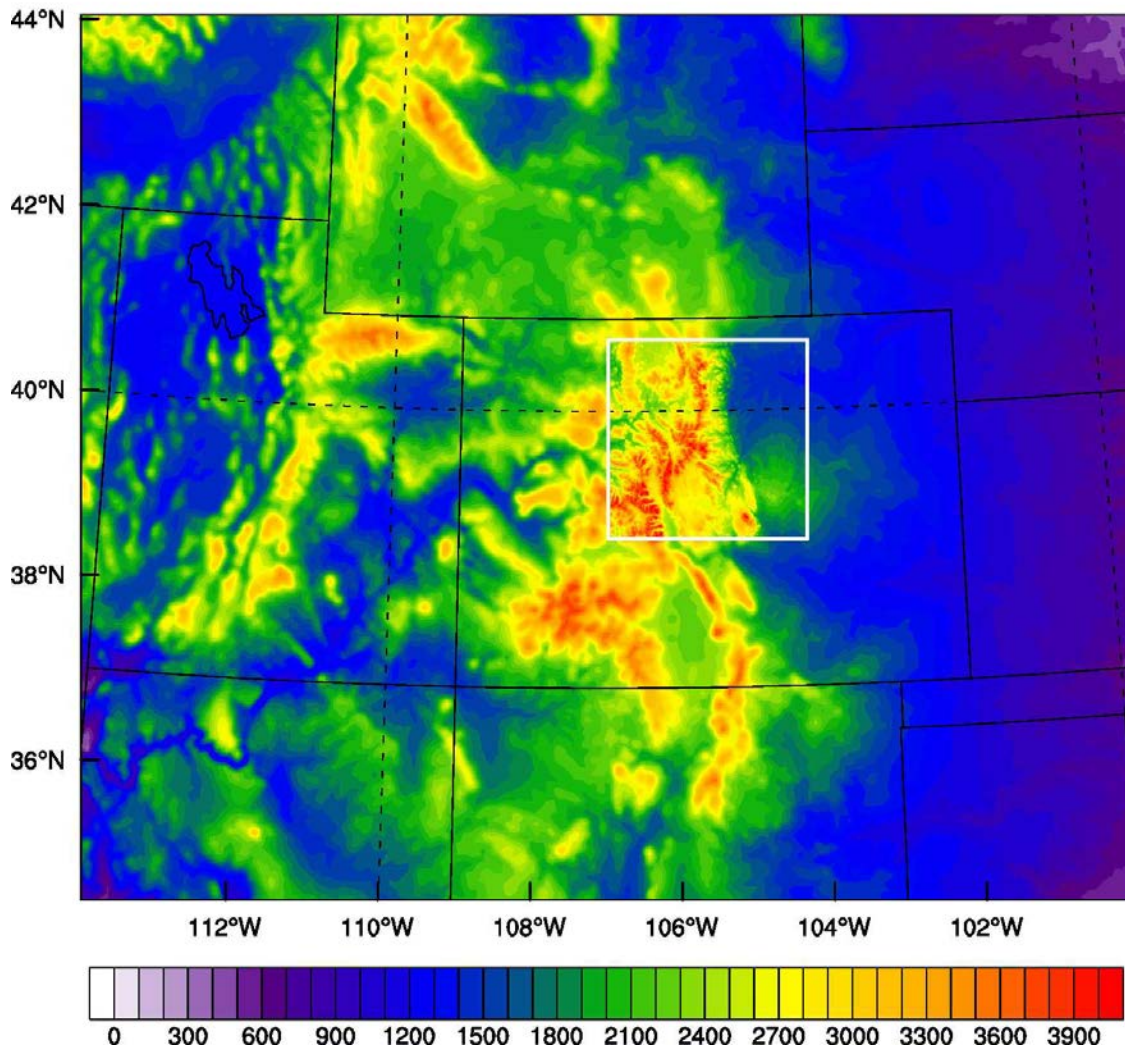


Figure 4.2 Topographical map of the 4-km grid domain and nested 800-m grid domain (white rectangle). Elevation color code is in meters above mean sea level.

4.3 Comparisons of model output with observations

Hourly data from three sites at Winter Park were made available (Lochridge 2014, personal communication) and compared to model output data. Data from the closest model grid point to each data site were plotted along with available parameters from each data site. Unfortunately, because of the staggered WRF grid for other than the temperature parameter, the same grid point was used for the “Rock” and “Cone” observation sites, resulting in only one modeled data point for the comparison.

Figure 4.3 shows a 36-hr time series of hourly data from the observations and the modeled data. The parameters of most interest are the wind direction, wind speed, and temperature. The WRF model simulates the wind direction fairly well until about 1500 UTC when it fails to capture the variability in the observations. Outside of about one hour with higher wind speeds, the directional variability coincides with light winds, less than about 5 m s^{-1} (~10 mph). From 2100 UTC (28 Jan) to 0200 UTC (29 Jan), which is during the first seeding period, the modeled wind direction is consistently southwesterly versus the observed flow which is mostly northwesterly but variable between northerly and westerly. Therefore, the model does not adequately represent the wind criteria for seeding with the DRI remotely-operated generators.

Temperature comparisons show that the modeled temperatures are biased cold by about 2° C , except for the period between 1800 UTC (28 Jan) and 0100 UTC (29 Jan). During this period, it appears that the model does not capture or adjust quickly to the momentarily strong westerly flow that warms and dries the Winter Park area. Web cameras and nearby precipitation sites indicate that snow falls shortly after that event and is well captured in the model, but without quantitative observations for comparison.

The focus of the comparisons has been on the first seeding period (~2100-0200 UTC), because both DRI remotely-operated generators ran during that period and the snow rate was greatest during that period, as opposed to the later 0500-1400 UTC (29 Jan) seeding period. In general, the model simulated the trends and changes reasonably well for such a small time period and small area. However, it demonstrated a cold bias that has been found in other WRF simulations (e.g., Ritzman et al 2015). More importantly, for simulating seeding trajectories, the wind direction had a more southerly component than the actual case. This suggests that seeding trajectories modeled from the WRF output would not accurately reflect the actual trajectories for this event. But, the seeding trajectories would be applicable to a southwesterly flow event, with the variations in speed and direction that were modeled during this period. This flow regime is fairly typical for the Winter Park target area, although the speeds are slightly weaker than average.

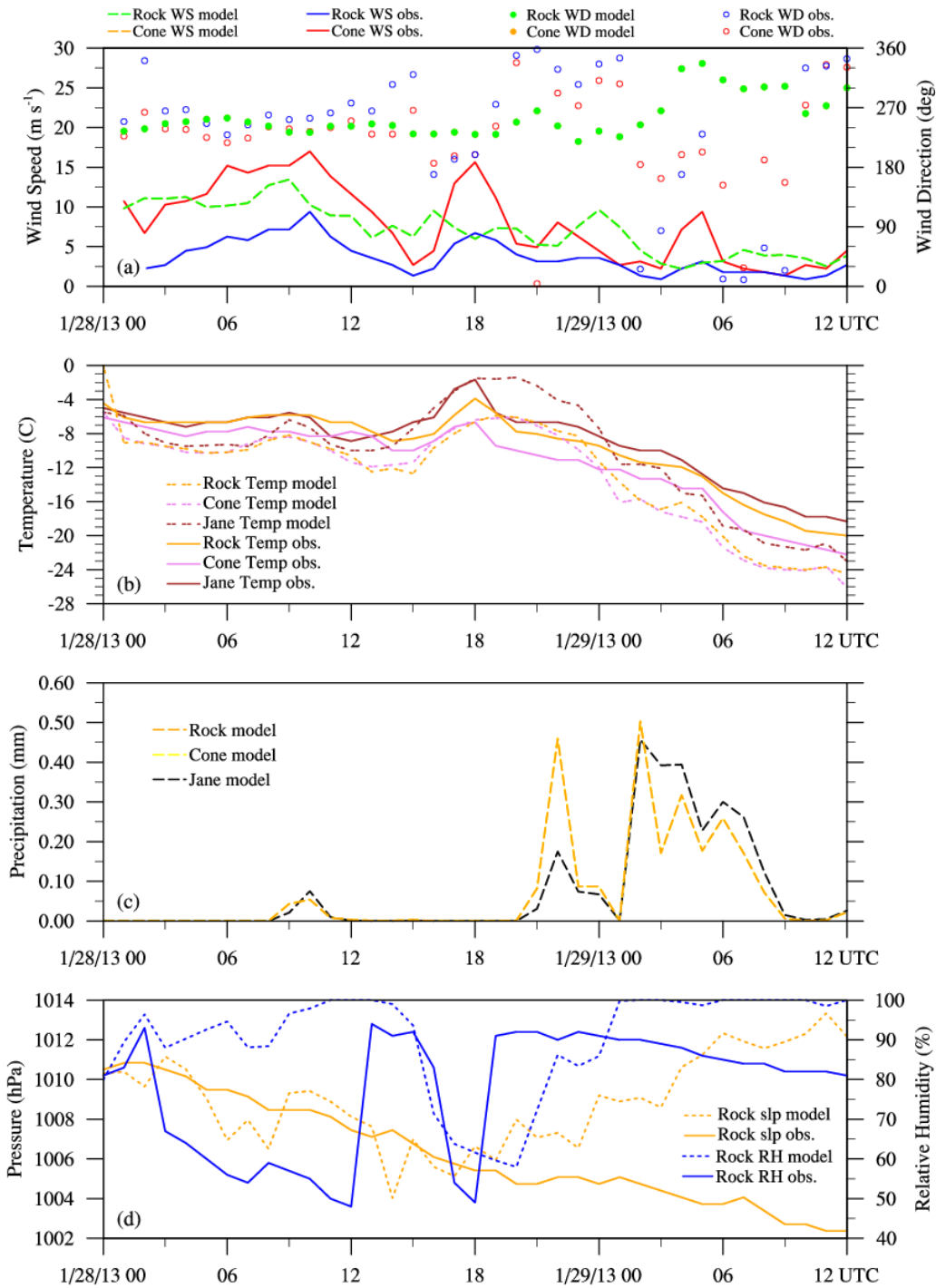


Figure 4.3 Time-series plots of observational data from the Winter Park sites: Jane, Rock and Cone, and WRF model data from the nearest gridpoints to these sites. Each panel has a legend for observations and model data. Rock and Cone model data are often from the same gridpoint and hence not distinguishable from each other. Not all parameters were observed at the three sites.

4.4 HYSPLIT model results

4.4.1 Trajectories from all generators near Winter Park target

HYSPLIT is a transport and diffusion model developed and distributed by NOAA's Air Resources Laboratory. HYSPLIT uses gridded data (i.e., model output) to derive dispersion parameters, leading to hourly trajectories and concentrations in the online version of the model. The advantage of using HYSPLIT in general is its availability and ease of use. Options in choosing the gridded data on which HYSPLIT operates are also readily available. Limitations in using HYSPLIT include its reliance on gridded data that is often too coarse to adequately simulate dispersion in a regional setting and in complex terrain, the underestimation of dispersion in the initial grid box, especially vertical dispersion, and the coarse time resolution in the online version. These limitations can be overcome with high-resolution gridded output, such as the WRF run in this study, and by applying more specialized parameterizations and time resolution than the HYSPLIT version available online. In this application, the online version was used to depict trajectories and concentration plots derived for ground-based generators near the Winter Park target area.

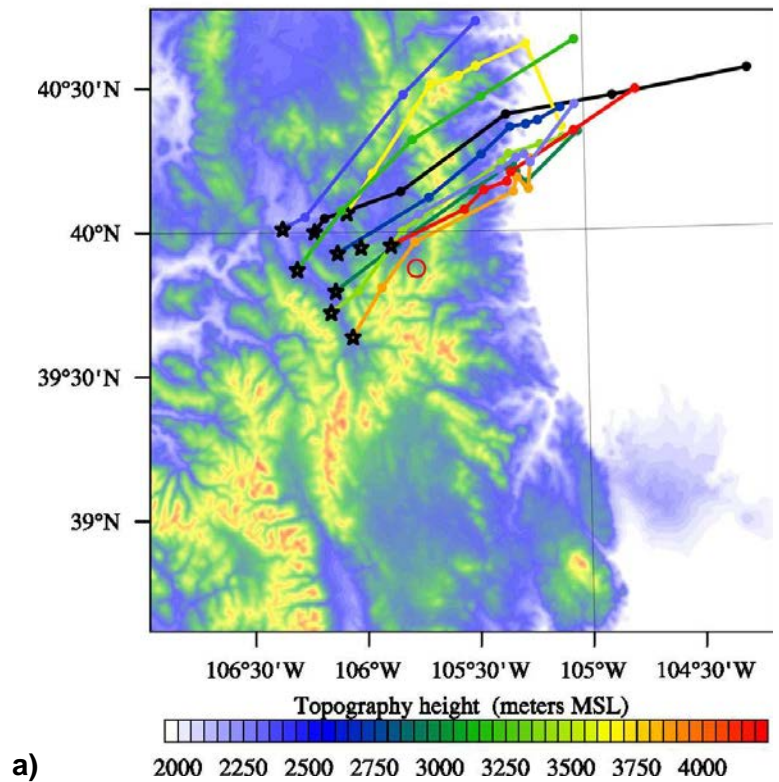
Locations of ten ground-based generators, two of which were the remotely-controlled generators operated by DRI and closest to the target area, were input into the HYSPLIT model. Six-hour trajectories were calculated from each generator for three different start times covering the 2100-0200 UTC seeded period. The first 2-3 hours of the trajectories are the most applicable for interpreting the potential path of the seeding plume. Figures 4.4 – 4.6 show the resulting HYSPLIT trajectories for 2100, 2300, and 0100 UTC start times. The general path of the trajectories show the predominance of southwesterly flow (contrary to the NW flow that actually occurred during this period), although there is a more westerly component for the 0100 UTC start time. The trajectories beginning at 2100 UTC (Figure 4.4) appear to be influenced by slightly stronger wind speeds, carrying them farther downwind than the other start-time trajectories. An accelerated vertical dispersion, shown in the time-height plot of Figure 4.4, may have exposed the simulated plumes to higher above-ground speeds. Also four of the trajectories show air parcels lofting quite high, probably due the influence of a gravity wave in the lee of the Indian Peaks. But, in general, the trajectories do not show rapid plume transport during the first hour or so.

The 2300 UTC start-time trajectories (Figure 4.5) reflect weaker, variable winds as observed at the Winter Park meteorological sites. There is slightly less vertical dispersion and only the two southern trajectories encounter gravity waves in the lee of the mountains. Three of the generator trajectories are clearly impacted by valley flows, with one or two others stagnant during the first hour. The 0100 UTC trajectories (Figure 4.6), as well as their vertical dispersion, are similar to the 2300 UTC trajectories except more are subject to valley flows and stagnant conditions over the first 1-2 hours. No trajectories are lofted sufficiently in the lee of the mountains to encounter gravity waves.

The overall conclusion from the trajectory results indicate that southwesterly flow does not target the Winter Park area very well (with the ten chosen generators), nor was it expected to. The coverage improves as the winds/trajectories shift more westerly. In spite of the crosswind component to the mountain ridges, valley flow dominates some of the generator locations, creating uncertain trajectories and targeting. Re-running HYSPLIT at higher time resolution than

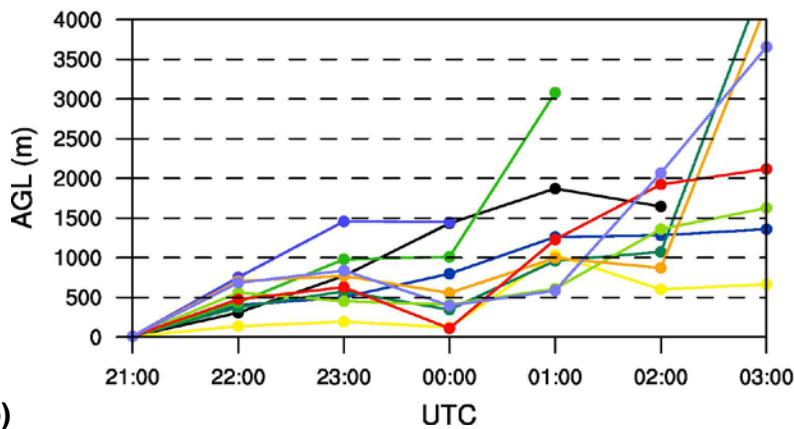
1-hr would help verify these general results and specify potential problem locations under southwesterly flow.

Forward trajectories starting at 2100 UTC 28 Jan 13



a)

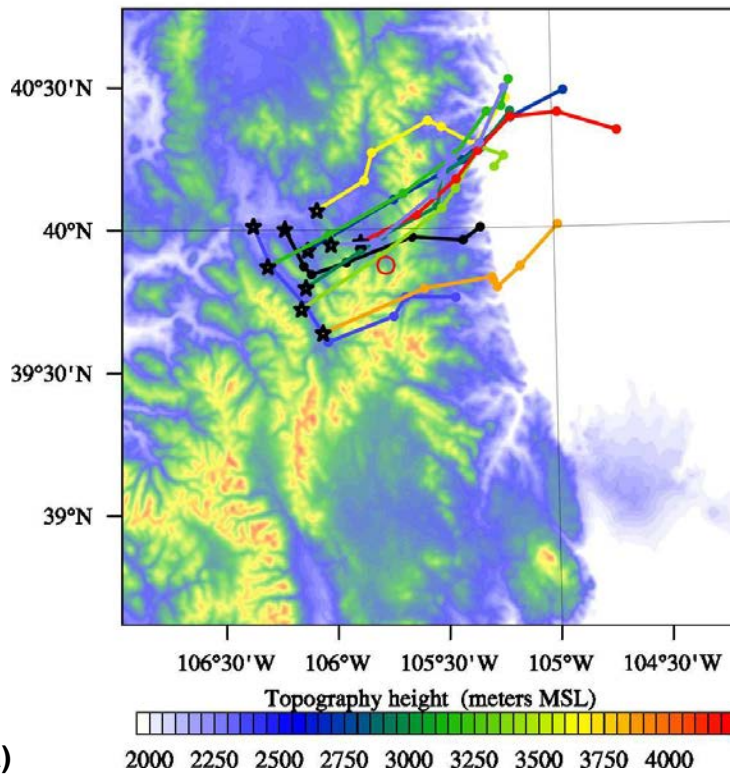
Forward trajectories starting at 2100 UTC 28 Jan



b)

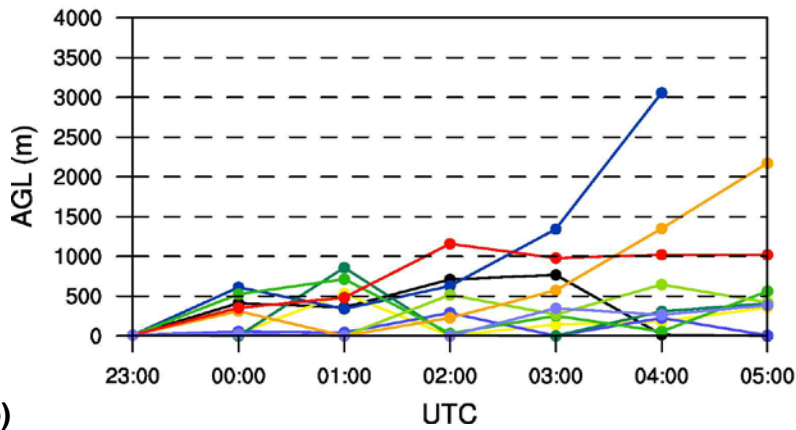
Figure 4.4 HYSPLIT trajectories from the WRF model output, starting at 2100 UTC, 28 January 2013. a) Plan view showing 6-hr trajectories (dot at each hour) from 10 nearby generators to Winter Park – marked as a red circle. Background shows the topography with color code at the bottom. b) Time-height plot of each generator trajectory – same color as in a). Elevation is AGL (above ground level).

Forward trajectories starting at 2300 UTC 28 Jan 13



a)

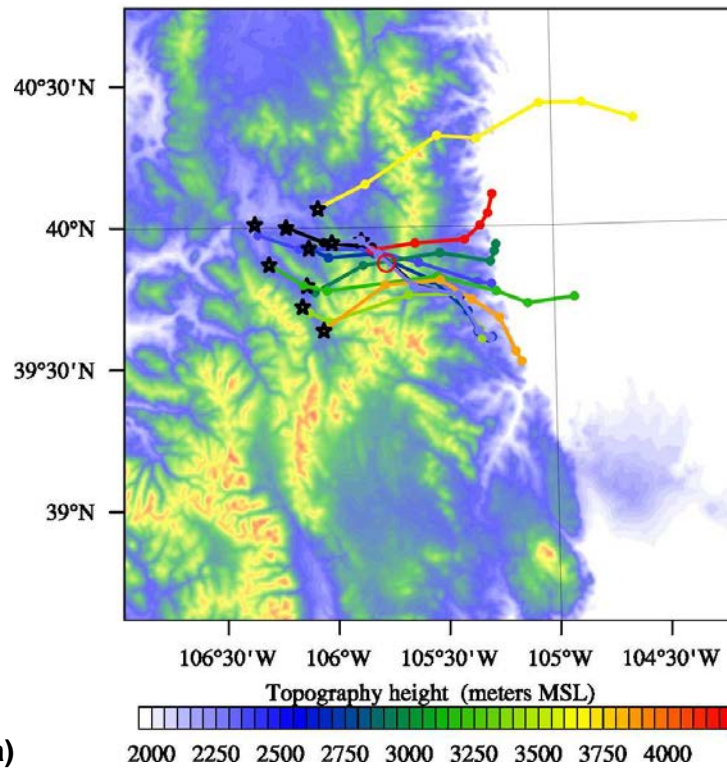
Forward trajectories starting at 2300 UTC 28 Jan



b)

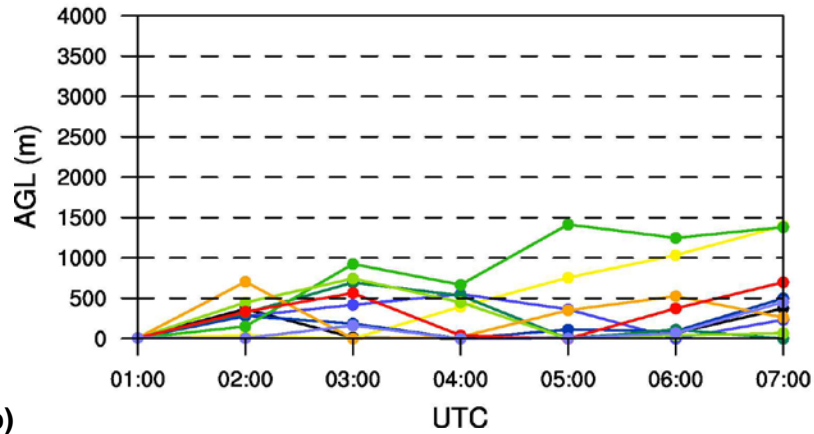
Figure 4.5 HYSPLIT trajectories from the WRF model output, starting at 2300 UTC, 28 January 2013. All else is the same as Figure 4.4.

Forward trajectories starting at 0100 UTC 29 Jan 13



a)

Forward trajectories starting at 0100 UTC 29 Jan



b)

Figure 4.6 HYSPLIT trajectories from the WRF model output, starting at 0100 UTC, 29 January 2013. All else is the same as Figure 4.4.

4.4.2 Relative concentrations from the DRI remotely-operated generators

The online version of the HYSPLIT model includes an option to calculate concentrations and ground deposition from mass releases at single locations. The model was run, driven by the 800-m WRF run, for the DRI generators with a start time appropriate for each generator – 2032 UTC for the eastern generator (“DW”) and 2142 UTC for the western generator (“USFS”). The domain of the HYSPLIT plots is replicated in the WRF model domain shown in Figure 4.7. This can be used for reference when interpreting the HYSPLIT plots.

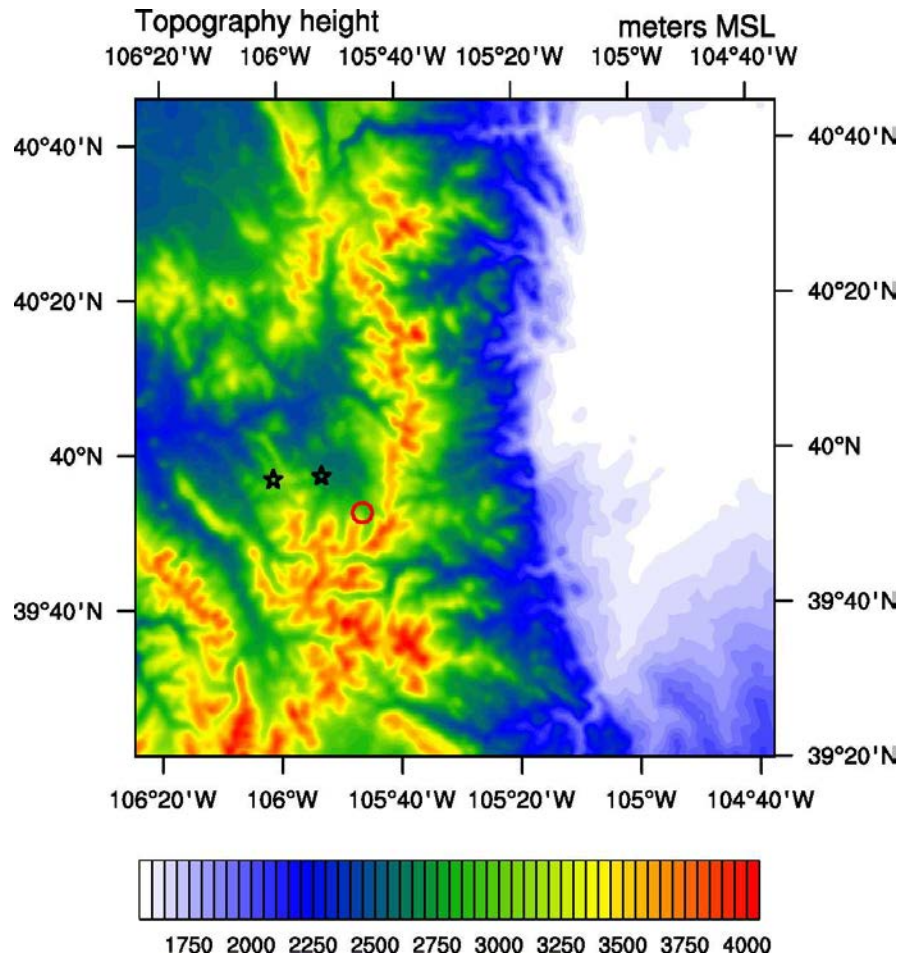


Figure 4.7 Topographical map of the 800-m grid WRF model domain with the DRI generators denoted by black stars and the Winter Park area denoted with the red circle. For scale, the distance from the generators to the eastern edge of the Rocky Mountain Foothills (dark blue shading) is about 60 km. Elevation color code is in meters MSL.

Plots of ground deposition and integrated concentration between 100m and 1000m AGL for the 6-hr run of the HYSPLIT model are given in Figure 4.8 for the eastern DRI generator (Denver Water site). The plume reflects the southwesterly flow and stays fairly narrow. There is some horizontal dispersion to the southeast but not sufficient to impact the target area in this run. The

ground deposition plot (Figure 4.8 a) also shows the narrow plume and the impact of the plume on the high mountains (e.g. Indian Peaks) NNE of Winter Park.

Although the concentration plot is a different color scale, the HYSPLIT run for the western – USFS – generator shows a significant southeasterly spread of the plume, just impacting the Winter Park area (Figure 4.9 b). The ground deposition plot also shows the greater plume spread for this generator and this time period (Figure 4.9 a), and the displaced deposition locations along the higher elevations E to NNE of Winter Park.

The two concentration/deposition plots from the online interface of the HYSPLIT model run show the general plume patterns under southwesterly flow. There is significant variability between the two locations and the one-hour difference in time period, and it is not clear which is the most important. Running HYSPLIT with a higher time resolution (needing interpolation of WRF model output) or trying another transport and diffusion model are the next steps in resolving the uncertainties. The plots also highlight the fact that the online version of HYSPLIT, while useful, needs “customizing” to adequately assess plumes from individual generator locations. Also, the relative mass concentrations need to be put into context with IN concentrations appropriate to seeding plumes.

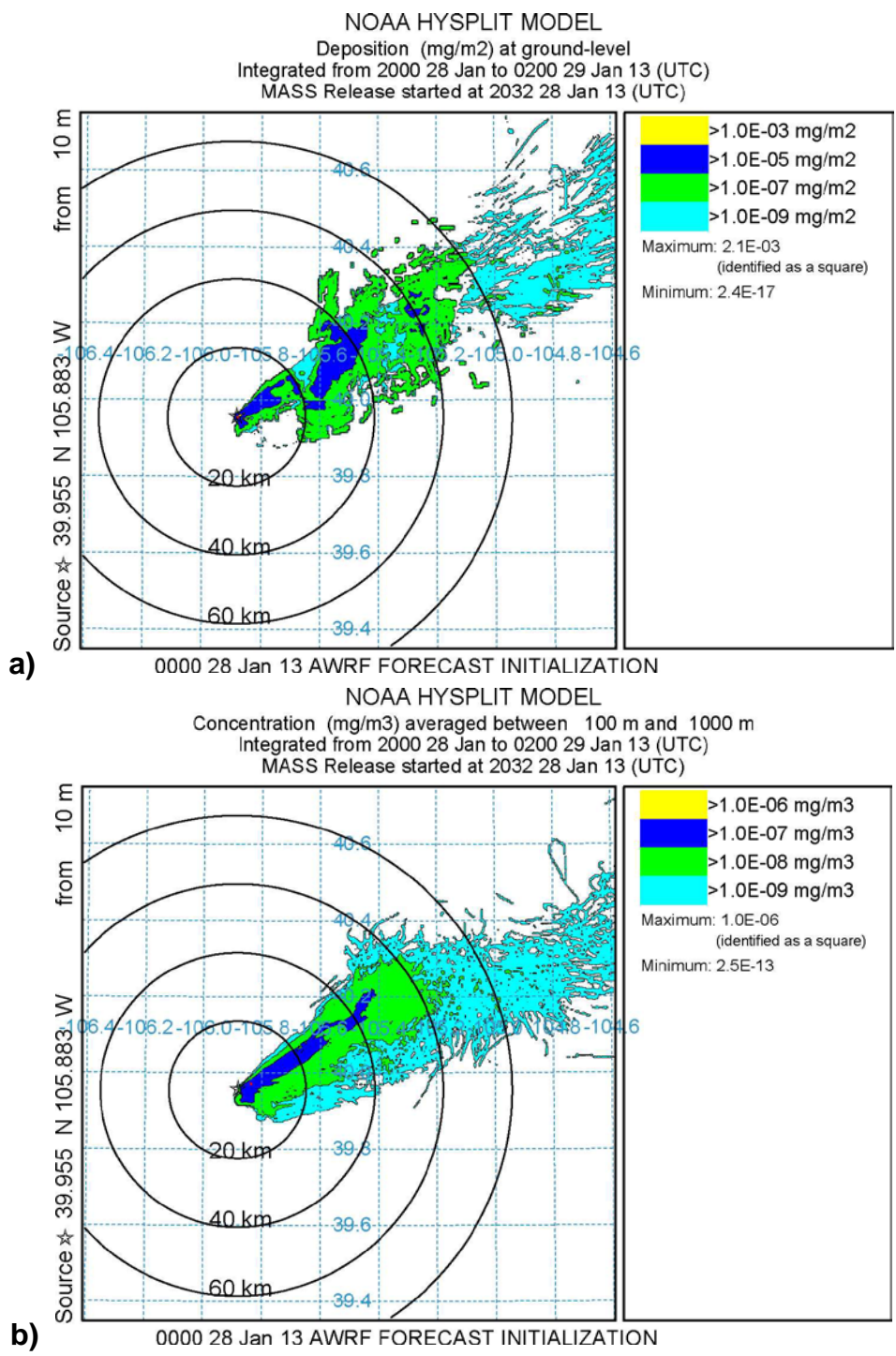


Figure 4.8 HYSPLIT model results for 6-hr run beginning at 2000 UTC 28 January 2013 with mass release (seeding) starting at 2032 UTC. Source is the DRI generator at the DW site. a) Ground deposition of mass (mg m⁻²). Color changes every two orders of magnitude. b) Concentration of mass (mg m⁻³) integrated over 100-1000 m AGL. Color changes every one order of magnitude.

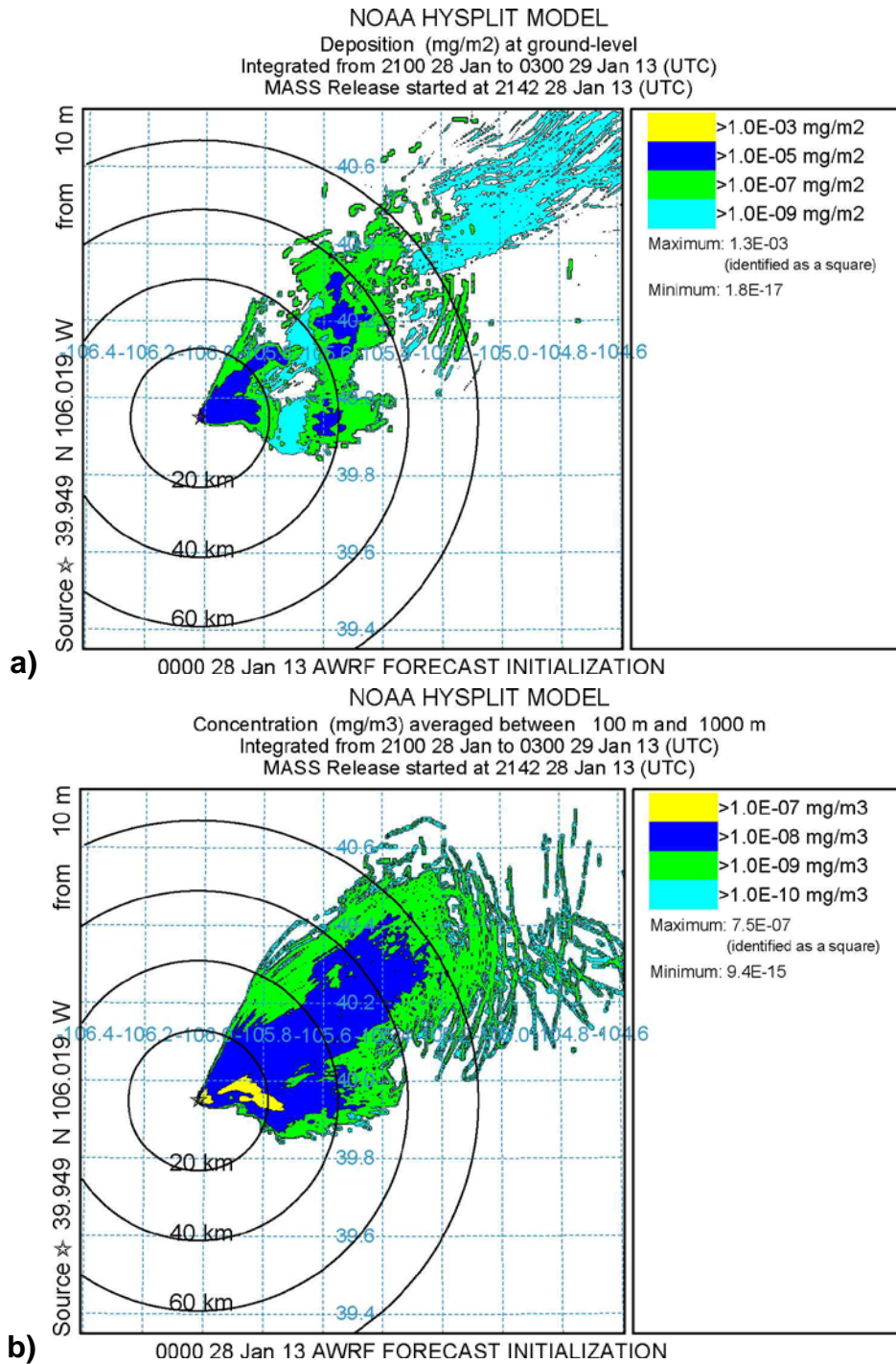


Figure 4.9 HYSPLIT model results for 6-hr run beginning at 2100 UTC 28 January 2013 with mass release (seeding) starting at 2142 UTC. Source is the DRI generator at the USFS site. a) Ground deposition of mass (mg m⁻²). Color changes every two orders of magnitude. b) Concentration of mass (mg m⁻³) integrated over 100-1000 m AGL. Color changes every one order of magnitude (different than Figure 4.8 b).

5 Conclusions and Recommendations

5.1 Climatology results

An eight-year climatology of winter weather conditions over the Central Colorado Mountain River Basins (CCMRB) program area was performed using 4-km WRF numerical model output. This model has been well-verified for seasonal studies, and in many cases, for daily values and trends. A numerical model is needed to capture all the variables used in deciding whether to seed winter storms or not – the seeding criteria. The seeding criteria of the two operators were used to assess seeding conditions over the entire Target Area 2 of the CCMRB program. This approach provided an estimate of the time seeding conditions occurred over Target Area 2, being about 20% of the total winter season period (Figure C1). The next logical step is to relate this frequency to the frequency of snow occurring in Target Area 2. While the time-series plots indicate that about 50% of the total snowfall fell during seedable conditions, further analysis is required to specifically quantify this percentage and also to reveal monthly trends, identifying which month is likely to be higher or lower than the seasonal average.

Analyses of the model output was further refined to allow gridpoint estimates of the seeding conditions, using the additional constraint of wind direction (280°-341°) and speed (<18 m s⁻¹ or 40 mph). Spatial patterns over the modeled domain were revealed with this approach. When combined with snowfall patterns, a plot of “seeding potential” resulted. Maximum frequencies ranged from 4-7%, but this is in relation to total hours in a season. Local maxima of seeding potential could be used to refine targets or define new target areas. This preliminary look at seeding potential needs further refinement though. For example, only one wind quadrant was attempted in this “proof of concept” approach, and the seeding potential was weighted by snowfall amount rather than just the occurrence of snowfall, which may be more appropriate or useful.

5.2 WRF (800-m) model results

One storm case (28-29 January 2013) was simulated using a 4-km resolution model nested down to 800-m resolution. The 800-m model was run with two different start times, both prior to the storm event. These model runs showed a small sensitivity of the output to initial conditions and we concentrated on the 0000 UTC 28 January 2013 initialization time for further analyses. The output of the 800-m model run was used to “drive” the community dispersion/trajectory model called HYSPLIT. Three time periods, concentrated on the 2100 – 0200 UTC seeding event in the two-day storm period, were run to assess targeting and plume extent from 10 nearby generators.

The resulting modeled trajectories suffered from coarse time resolution (1-hr time-steps) and modeled winds that were more southwesterly than the W-NW winds observed. However, the overall conclusion from the trajectory results indicate that southwesterly flow does not target the Winter Park area very well, but the coverage improves as the winds/trajectories shift more westerly. This is consistent with the wind criterion established for operating the DRI remote generators. In spite of the crosswind component to the mountain ridges, valley flow dominates some of the manual generator locations, creating uncertain trajectories and targeting. A more sophisticated use of the HYSPLIT model or a better-resolved trajectory model would help verify these general results and specify potential problem locations under southwesterly flow.

The results of the modeling portion of the study show its utility in assessing seeding trajectories from generator sites. For example, several of the lower elevation generators clearly showed funneling in valley flows. There is also a high sensitivity to the elevation or location of the various generators. Past studies have criticized the use of valley-placed generators, and emphasized the need for remote-controlled generators for effective operations. The trajectory model results, while still uncertain, tend to support these past studies.

5.3 Recommendations

Operational seeding criteria are heavily reliant on proxy variables, those not directly measuring the relevant seeding conditions according to the seeding conceptual model. Using observations if at all possible, such as from rawinsonde releases, microwave radiometric sensing, and strategically-placed surface observations (including high-resolution precipitation gauges), is highly recommended. Formulating seeding criteria from model output could be improved to generate a more consistent climatology of seeding conditions. These include specifying cloud coverage at appropriate pressure levels, partitioning data using the modeled wind at specific generator locations, and refining the stability parameter to identify potential inversions.

While the climatological analyses demonstrated the utility and potential of using areal and time-resolved approaches, recommendations for completing a seeding climatology include: 1) specifying the percentage of total winter snowpack associated with seedable conditions; 2) examining the spatial distributions and changes associated with varying wind directions and speeds; and 3) facilitating this additional work through the use of GIS tools. The third point is necessary to provide the flexibility in specifying seeding criteria for investigating the additional scenarios, and to allow third parties to investigate their own scenarios.

The 800-m resolution WRF model simulation needs some obvious extensions that would address more specifics, particularly when focused by a clearer climatology of seeding conditions and times. These include running several more cases over a range of storm directions and possibly stability criteria. These would drive a more customized application of the HYSPLIT model, aimed at addressing plume behavior and targeting, the effectiveness of current generators, and potential changes in or additions to generator locations. These recommendations would constitute a second phase of the current work, which established the analysis concept and provided the framework for further study.

REFERENCES

- American Society of Civil Engineers, 2004: Standard practice for the design and operation of precipitation enhancement projects. ASCE/EWRI 42-04, ASCE, Reston, Virginia, 63 pp.
- Bergeron, T., 1949: The problem of artificial control of rainfall on the globe. I. General effects of ice-nuclei in clouds. *Tellus*, **1**, 32-43.
- Boucher, R.J., 1956: Operation Overseed. Final Report to the Advisory Committee on Weather Control, December 1955-January 1956, Mount Washington Observatory, 88 pp.
- Braham, R.R., 1952: The water and energy budgets of the thunderstorm and their relation to thunderstorm development. *J. Meteor.*, **9(4)**, 227-242.
- Breed, D., R. Rasmussen, C. Weeks, B. Boe, and T. Deshler, 2014: Evaluating winter orographic cloud seeding: Design of the Wyoming Weather Modification Pilot Project (WWMPP), *J. Appl. Meteor. Climatol.*, **53**, 282-299.
- Campistron, B.A., A.W. Huggins, A.B. Long, 1991: Investigations of a winter mountain storm in Utah. Part III: Single-Doppler radar measurements of turbulence. *J. Atmos. Sci.*, **48**, 1306-1318.
- Colle, B.A., 2004: Sensitivity of orographic precipitation to changing ambient conditions and terrain geometries: An idealized modeling perspective. *J. Atmos. Sci.*, **61**, 588–606.
- Coons, R.D., R.C. Gentry, and R. Gunn, 1948: First partial report on the artificial production of precipitation: Stratiform clouds, Ohio. *Bull. Amer. Met. Soc.*, **29**, 266-269.
- CWCB, Colorado Department of Natural Resources, 2005: Numerical Simulations of Snowpack Augmentation for Drought Mitigation Studies in the Colorado Rocky Mountains, Final Report to the USBR Weather Damage Modification Program, 186 pp. (available at <http://cwcb.state.co.us/>)
- DeFelice, T.P., J. Golden, D. Griffith, W. Woodley, D. Rosenfeld, D. Breed, M. Solak, and B. Boe, 2014: Extra area effects of cloud seeding — An updated assessment, *Atmos. Res.*, **135**, 193–203.
- Deshler, T., and D.W. Reynolds, 1990: The persistence of seeding effects in a winter orographic cloud seeded with silver iodide burned in acetone, *J. Appl. Meteor.*, **29**, 477-488.
- Deshler, T., D.W. Reynolds, and A.W. Huggins, 1990: Physical response of winter orographic clouds over the Sierra Nevada to airborne seeding using dry ice or silver iodide, *J. Appl. Meteor.*, **29**, 288-330.
- Gao, S., and X. Li, 2008: *Cloud-Resolving Modeling of Convective Processes*. Springer, New York, 210 pp.
- Geerts, B., Q. Miao, Y. Yang, R. Rasmussen, and D. Breed, 2010: An airborne profiling radar study of the impact of glaciogenic cloud seeding on snowfall from winter orographic clouds. *J. Atmos. Sci.*, **67**, 3286-3302.
- Grant, L.O., 1963: Indication of residual effects from silver iodide released into the atmosphere. *Proceedings of the Western Snow Conference 1963*, 109-115.

- Grant, L.O., 1986: Hypotheses for the Climax wintertime orographic cloud seeding experiments. *Precipitation Enhancement – A Scientific Challenge, Meteor. Monogr.*, No. 43, R. Braham, Jr., Ed., Amer. Meteor. Soc., 105-108.
- Griffith, D.A., G.W. Wilkerson, W.J. Hauze, and D.A. Risch, 1992: Observations of ground released sulfur hexafluoride tracer gas plumes in two Utah winter storms. *J. Wea. Modif.*, **24**, 49-65.
- Griffith, D.A., M.E. Solak, R.D. Almy, and D. Gibbs, 2005: The Santa Barbara cloud seeding project in Southern California, Summary of results and their implications. *J. Wea. Modif.*, **37**, 21-27.
- Heimbach, J.A., W.D. Hall, and A.B. Super, 1997: Modeling and observations of valley-released silver iodide during a stable winter storm over the Wasatch Plateau of Utah. *J. Wea. Modif.*, **29**, 33-41.
- Heimbach, J.A., A.B. Super, and W.D. Hall, 1998: Modeling AgI targeting effectiveness for five generalized weather classes in Utah. *J. Wea. Modif.*, **30**, 35-50.
- Hill, G.E., 1980: Dispersion of airborne-released silver iodide in winter orographic clouds. *J. Appl. Meteor.*, **19**, 978-985.
- Holroyd, E.W., J.T. McPartland, and A.B. Super, 1988: Observations of silver iodide plumes over the Grand Mesa of Colorado. *J. Appl. Meteor.*, **27**, 1125-1144.
- Houze, R.A., Jr. and S. Medina, 2005: Turbulence as a mechanism for orographic precipitation enhancement. *J. Atmos. Sci.*, **62**, 3599–3623.
- Huggins, A.W., 1995: Mobile microwave radiometer observations: Spatial characteristics of supercooled cloud water and cloud seeding implications. *J. Appl. Meteor.*, **34**, 432-446.
- Huggins, A.W. 2007: Another wintertime cloud seeding case study with strong evidence of seeding effects. *J. Wea. Modif.*, **39**, 9-36.
- Huggins, A.W. 2009: Summary of studies that document the effectiveness of cloud seeding for snowfall augmentation. *J. Wea. Modif.*, **41**, 119-126.
- Ikeda, K., R. Rasmussen, C. Liu, D. Gochis, D. Yates, F. Chen, M. Tewari, M. Barlage, J. Dudhia, W. Yu, K. Miller, K. Arsenault, V. Grubisic, G. Thompson, and E. Guttman, 2010: Simulation of seasonal snowfall over Colorado. *Atmos. Res.*, **97**, 462-477.
- Jiang, Q., 2003: Moist dynamics and orographic precipitation. *Tellus*, **55**, 301–316.
- Kraus, E.B., and P. Squires, 1947: Experiments on the simulation of clouds to produce rain. *Nature*, **159**, 489-491.
- Langmuir, I., 1948: The growth of particles in smokes and clouds and the production of snow from supercooled clouds. *Proc. Am. Philos. Soc.*, **92**, 167.
- Li, X., X. Shen, and J. Liu, 2011: A partitioning analysis of tropical rainfall based on cloud budget. *Atmos. Res.*, **102**, 444-451.
- Long, A.B., B.A. Campistrone, and A.W. Huggins, 1990: Investigations of a winter mountain storm in Utah. Part I: Synoptic analyses, mesoscale dynamics, and water release rates. *J. Atmos. Sci.*, **47**, 1302-1322.

- Long, A.B., 2001. Review of downwind extra-area effects of precipitation enhancement, *J. Wea. Modif.*, **33**, 24-45.
- Ludlum, F.H., 1955: Artificial snowfall from mountain clouds. *Tellus*, **7**, 277-290.
- Manton, M.J., L. Warren, S. L. Kenyon, A.D. Peace, S.P. Bilish, and K. Kemsley, 2011: A confirmatory snowfall enhancement project in the Snowy Mountains of Australia. Part I: Project design and response variables. *J. Appl. Meteor. Climatol.*, **50**, 1432-1447.
- Manton, M.J., and L. Warren, 2011: A confirmatory snowfall enhancement project in the Snowy Mountains of Australia. Part II: Primary and associated analyses. *J. Appl. Meteor. Climatol.*, **50**, 1448-1458.
- Mielke, P.W. Jr., G.W. Brier, L.O. Grant, G.J. Mulvey, and P.N. Rosenweig, 1981: A statistical reanalysis of the replicated Climax I and II wintertime orographic cloud seeding experiments. *J. Appl. Meteor.*, **20**, 643-659.
- National Research Council, 2003: *Critical Issues in Weather Modification Research*. National Academies Press, Washington, D.C., 123 pp.
- Orr, B.W., and B.A. Klimowski, 1996: Dispersion characteristics of ground-based cloud seeding in mountainous terrain. *Preprints 13th AMS Conf. on Planned and Inadvertent Weather Modification*. Atlanta, Amer. Meteorol. Soc., Boston, 184-189.
- Rangno, A.R., and P.V. Hobbs, 1987: A reevaluation of the Climax cloud seeding experiments using NOAA published data. *J. Appl. Meteor. and Climatol.*, **26**, 757-762.
- Rangno, A.R., and P.V. Hobbs, 1993: Further analysis of the Climax cloud seeding experiments. *J. Appl. Meteor.*, **32**, 1837-1847.
- Rauber, R.M., and L.O. Grant, 1986: The characteristics of cloud water over the mountains of northern Colorado during wintertime storms. Part II: Spatial distribution and microphysical characteristics. *J. Climate Appl. Meteor.*, **25**, 489-504.
- Reinking, R.P., 1972: Target area persistence of cloud seeding material. *Preprints 3rd AMS Conf. on Weather Modification*. Rapid City, S.D., Amer. Meteorol. Soc., Boston, 109-112.
- Reynolds, D.W., 1988: A report on winter snowpack augmentation. *Bull Amer. Meteor. Soc.*, **69**, 1290-1300.
- Ritzman, J., T. Deshler, K. Ikeda, and R. Rasmussen, 2015: Estimating the fraction of winter orographic precipitation that is produced under conditions meeting the seeding criteria from the Wyoming weather modification pilot project. *J. Appl. Meteor. Climatol.*, Accepted January 2015.
- Rosenfeld, D., and W. L. Woodley, 2003: Closing the 50-year circle: From cloud seeding to space and back to climate change through precipitation physics. *Cloud Systems, Hurricanes, and the Tropical Rainfall Measuring Mission, Meteor. Monogr.*, No. 51, Amer. Meteor. Soc., 59–80.
- Rosenfeld, D., Y. Xing, and J. Dai, 2005: Satellite retrieved microstructure of Agl seeding tracks in supercooled layer clouds. *J. Appl. Meteor.*, **44**, 760-767.
- Rottner, D., S.R. Brown, and O.H. Foehner, 1975: The effect of persistence of Agl on randomized

- weather modification experiments. *J. Appl. Meteor.*, **14**, 939–945
- Sassen, K., A.W. Huggins, A.B. Long, J.B. Snider, and R.J. Meitin, 1990: Investigations of a winter mountain storm in Utah. Part II: Mesoscale structure, supercooled water development, and precipitation processes. *J. Atmos. Sci.*, **47**, 1323-1350.
- Schaefer, V.J., 1946: The production of ice crystals in a cloud of supercooled water droplets. *Science*, **104**, 457-459.
- Silverman, B.A., 2001: A critical assessment of glaciogenic seeding of convective clouds for rainfall enhancement, *Bull. Amer. Meteor. Soc.*, **82**, 903-923.
- Skamarock, W. C., Klemp, J. B., Dudhia, J., Gill, D. O., Barker, D. M., 2008: A description of the Advanced Research WRF version 3. NCAR Tech. Note NCAR/TN-475+STR
- Smith, R.B., and I. Barstad, 2004: A linear theory of orographic precipitation. *J. Atmos. Sci.*, **61**, 1377–1391.
- Solak, M.E., D.P. Yorty, D.A. Griffith, 2003: Estimations of downwind cloud seeding effects in Utah. *J. Wea. Modif.*, **35**, 52-58.
- Super, A.B., 1974: Silver iodide plume characteristics over the Bridger Mountain Range, Montana. *J. Appl. Meteor.*, **13**, 62-70.
- Super, A.B., J.T McPartland, and J.A. Heimbach, Jr., 1975: Field observations of the persistence of AgI-NH₄I-acetone ice nuclei in daylight. *J. Appl. Meteor.*, **14**, 1572-1577.
- Super, A.B., and J.A. Heimbach, Jr., 1983: Evaluation of the Bridger Range winter cloud seeding experiment using control gauges. *J. Appl. Meteor.*, **22**, 1989-2011.
- Super, A.B., and J.A. Heimbach, Jr., 1988: Microphysical effects of wintertime cloud seeding with silver iodide over the Bridger Range, Montana. *J. Appl. Meteor.*, **27**, 1152-1165.
- Super, A.B., and J. A. Heimbach, Jr., 2005: Feasibility of snowpack enhancement from Colorado winter mountain storms: Emphasis on supercooled liquid water and seeding with silver iodide and propane. Final Report to Technical Services Center, Bureau of Reclamation, Denver, CO, 13 November 2005, 73 pp. (available at <http://cwcb.state.co.us/>)
- Super, A.B., and B.A. Boe, 1988: Microphysical effects of wintertime cloud seeding with silver iodide over the Rocky Mountains, Part III: Observations over the Grand Mesa, Colorado. *J. Appl. Meteor.*, **27**, 1166-1182.
- Super, A.B., 1999: Summary of the NOAA/Utah Atmospheric Modification Program: 1990-1998. *J. Wea. Modif.*, **31**, 51-75.
- Sykes, R. I., and R. S. Gabruk, 1997: A second-order closure model for the effect of averaging time on turbulent plume dispersion. *J. Appl. Meteor.*, **36**, 1038-1045.
- Trenberth, K.E., L. Smith, T. Qian, A. Dai, and J. Fasullo, 2007: Estimates of the global water budget and its annual cycle using observational and model data. *J. Hydrometeorology—Special Section*, **8**, 758-769.
- Vonnegut, B., 1947: The nucleation of ice formation by silver iodide. *J. Appl. Phys.*, **18**, 593-595.
- Warburton, J.A., R.H. Stone, and B.L. Marler, 1995: How the transport and dispersion of AgI

aerosols may affect detectability of seeding effects by statistical methods. *J. Appl. Meteor.*, **34**, 1929-1941.

Warburton, J.A., and M.A. Wetzel, 1992: Field study of the potential for winter precipitation enhancement in the Australian Snowy Mountains. *Atmos. Res.*, **28**, 327–363.

WWDC, 2014: The Wyoming Weather Modification Pilot Program – Level II Study, Draft Executive Summary, 15 pp. (available at <http://wwdc.state.wy.us/>)

WMI, 2005: *Level II Weather Modification Feasibility Study*, Report to the Wyoming Water Development Commission by Weather Modification, Inc., Fargo, ND, March 2005. 151 pp.

Wise, E.A., 2005: Precipitation Evaluation of the North Dakota Cloud Modification Project (NDCMP). MS Thesis, University North Dakota, Grand Forks, ND, 63pp.

Xue, L., and Coauthors, 2013a: Agl cloud seeding effects as seen in WRF simulations. Part I: Model description and idealized 2D sensitivity tests. *J. Appl., Meteor. Climatol.*, **52**, 1433-1457.

Xue, L., S. Tessendorf, E. Nelson, R. Rasmussen, D. Breed, S. Parkinson, P. Holbrook, and D. Blestrud, 2013b: Agl cloud seeding effects as seen in WRF simulations. Part II: 3D real case simulations and sensitivity tests. *J. Appl. Meteor. Climatol.*, **52**, 1458-1476.

Xue, L., X. Chu, R. Rasmussen, D. Breed, B. Boe, and B. Geerts, 2014: The dispersion of silver iodide particles from ground-based generators over complex terrain, Part 2: WRF large-eddy simulations vs. observations. *J. Appl. Meteor. Climatol.*, **53**, 1342-1361.

Appendix A: WRF model configuration and data set

The model data used in this study was output from WRF version 3.1.1 model runs at 4-km grid spacing. The model configuration, from the Colorado Headwaters study, includes the following parameterizations:

- The Mellor–Yamada–Janjic (MYJ) Planetary Boundary Layer scheme
- Noah land-surface model with new enhanced snow albedo
- The NCAR Community Atmosphere Model (CAM) longwave and shortwave schemes
- Thompson cloud microphysics scheme

The WRF data was stored in Network Common Data Form (netCDF) format. Each file of 1.4 Gigabytes contained WRF output data for one day (24 hours). Each of these files had maximum dimensions [317, 263, 15, 24], which are 317 data points in the west-east direction, 263 data points in the south-north direction, 15 pressure levels and 24 time steps, for a total of 30,013,560 data points in one day. The Colorado Headwaters domain was too large to operate on using a desktop computer so each file was re-sampled to trim the maximum dimensions to [75, 85, 4, 24], which reduced the file size to 35.1 Megabytes (612,000 data points). The trimmed netCDF files, with 75 data points in the west-east direction, 85 data points in the south-north direction, 4 pressure levels and 24 time steps, were centered geographically over Target Area 2 of the CCMRB with a longitude range of -104.46 to -108.01 degrees and a latitude range of 38.00 to 41.06 degrees. The pressure levels were also reduced from 15 to 4 and include 750, 700, 650 and 600 mb.

The re-sampled WRF data, hereafter 'data', consists of 24 meteorological variables. These variables exist at each data coordinate for each time step. A summary of all the variables is shown in Table A1. These data consist of temperature, humidity, geopotential height, water vapor mixing ratio, condensed water (cloud, rain, snow, graupel and ice) mixing ratio and 3-D winds at each pressure level. Surface variables such as snow water equivalent, snow depth and accumulated precipitation were also sampled.

Table A1. Description of WRF output data variables

Name	Description	Units	Dimensions
Qv	water vapor mixing ratio at constant pressure levels	kg kg ⁻¹	[75, 85, 4, 24]
Qc	cloud water mixing ratio at constant pressure levels	kg kg ⁻¹	[75, 85, 4, 24]
Qr	rain water mixing ratio at constant pressure levels	kg kg ⁻¹	[75, 85, 4, 24]
Qs	snow mixing ratio at constant pressure levels	kg kg ⁻¹	[75, 85, 4, 24]
Qg	graupel mixing ratio at constant pressure levels	kg kg ⁻¹	[75, 85, 4, 24]
Qi	ice mixing ratio at constant pressure levels	kg kg ⁻¹	[75, 85, 4, 24]
TK_p	temperature at constant pressure levels	K	[75, 85, 4, 24]
RH_p	RH at constant pressure levels	%	[75, 85, 4, 24]
U_p	x-component wind at constant pressure levels	m s ⁻¹	[75, 85, 4, 24]
V_p	y-component wind at constant pressure levels	m s ⁻¹	[75, 85, 4, 24]
W_p	z-component wind at constant pressure levels	m s ⁻¹	[75, 85, 4, 24]
GHT	geopotential heights at constant pressure levels	gpm	[75, 85, 4, 24]
SLP	sea level pressure	mb	[75, 85, 24]
Q2	QV at 2 m	kg kg ⁻¹	[75, 85, 24]
T2	temperature at 2 m	K	[75, 85, 24]
U10	U at 10 m	m s ⁻¹	[75, 85, 24]
V10	V at 10 m	m s ⁻¹	[75, 85, 24]
SNOW	snow water equivalent	kg m ⁻²	[75, 85, 24]
SNOWH	physical snow depth	m	[75, 85, 24]
RAINNC	accumulated total grid scale precipitation	mm	[75, 85, 24]
SNOWNC	accumulated total grid scale snow and ice	mm	[75, 85, 24]
GRAUPELNC	accumulated total grid scale graupel	mm	[75, 85, 24]
ACSNOW	accumulated snow	kg m ⁻²	[75, 85, 24]
ACSNOM	accumulated melted snow	kg m ⁻²	[75, 85, 24]

Appendix B: Text output data of seed times.

Example of text output for time steps when seed criteria 2a-2c are met. The first column is the date in format YYYYMMDD and the second column is the hour (GMT). The example shown below is for November 2007. Seeding criteria were satisfied for 40 hours on 6 days, 5.6 % of the time, and on 14 November and 24 November, only one hour met the seed criteria. The data files have the filename format *YYYY-YYYY_MM_seedcases.txt* where YYYY-YYYY is the season (in this case 2007-2008).

20071114	14.0000
20071121	7.00000
20071121	8.00000
20071121	9.00000
20071121	10.0000
20071121	11.0000
20071121	12.0000
20071121	13.0000
20071121	14.0000
20071121	15.0000
20071121	16.0000
20071121	17.0000
20071121	18.0000
20071121	19.0000
20071121	20.0000
20071121	21.0000
20071121	22.0000
20071121	23.0000
20071123	23.0000
20071123	24.0000
20071124	4.00000
20071126	19.0000
20071126	20.0000
20071126	21.0000
20071128	6.00000
20071128	7.00000

20071128	8.00000
20071128	9.00000
20071128	10.0000
20071128	11.0000
20071128	12.0000
20071128	13.0000
20071128	14.0000
20071128	15.0000
20071128	18.0000
20071128	19.0000
20071128	20.0000
20071128	21.0000
20071128	22.0000
20071128	23.0000

Appendix C: Climatology plots and statistics

Climatology of seedable and non-seedable periods

Table C1 shows a list of plots produced by this analysis. Twenty-four plots were produced for each month, totaling 192 plots for eight seasons and 1152 plots for 48 months. Tables C2 and C3 lists the statistics for seasons 2000-2001 and 2007-2008 as examples. The values in each of the columns represent the overall mean, the non-seed mean, and the seed mean. The seeding criteria are used to separate the 'non-seed' from 'seed' variables. Figure C1 shows the seed and non-seed cases for all eight seasons. The numbers on the right side of the figure panels show the mean, non-seed mean, and the seed mean values for each variable. Between November 2000 and April 2008, the seedable time segments amounted to 21% of the time. Figures C2-C5 show the frequency distribution of temperature, wind direction, wind speed and snow mixing ratio within the target area for 2007-2008 during non-seed, seed and all time segments.

Focusing on the 2000-2001 season, shown in Section 3.4, and the 2007-2008 season, shown here, the 700 mb mean temperatures were colder during these seasons than the 8-yr seasonal mean. Seasonal differences in seed and non-seed cases show that the seed mean temperature values are 2.5° to 4.5° C cooler than non-seed values. In general, mean temperatures seem to be normally distributed at all pressure levels (see Figure C2). The differences between seed and non-seed mean temperature tends to become colder at lower pressure. From month to month, this temperature structure becomes more complex. In the warm season of months November, March and April, the seed cases are much colder than the mean with the coldest being in November at 600 mb. Seed cases in November 2007 had the lowest temperatures at 600 and 650 mb. This does not come as a surprise as it is often too warm during these months for seed temperature criteria to be met. However, these November seed events are colder than the seasonal average seed case at lower pressure, meaning that cold air aloft is an important property that is characteristic of seedable conditions in warmer months. In the colder months of December, January and February, the seed cases are nearly the same or warmer at 750 and 700 mb but colder at 600 mb. In almost all months, the non-seed cases are warmer than the mean temperature of all cases.

Very little structure is observed in wind speeds (Figure C4 for example). The seed cases tend to have slightly higher wind speeds at 750 and 700 mb. Wind direction is mostly southeasterly at 750 and 700 mb and westerly at 650 and 600 mb. Figure C3 shows a high frequency of northwesterly cases at 700 mb compared to non-seed cases. The high frequency of easterlies in seed cases is not present at 650 mb, indicating that westerly storm tracks are most seedable. Seed cases tend to have westerly winds during the warm months of November, March and April. In the cold months of December, January, and February, seed cases are more southeasterly at 750 and 700 mb becoming northwesterly at 650 and 600 mb.

Snow mixing ratio is maximum at 650 mb with the highest mixing ratio observed in April followed by March. February is often the month with the least snow mixing ratio. In most cases, seed cases produce higher snow mixing ratios than non-seed cases. Figure C5 shows a trace of snow mixing ratios for the month of January 2008. The highest snow mixing ratio values occur at 600 mb. These snow events are not seedable during the whole duration of the event. Figure C7 is a time

series of temperature at 700, 650 and 600 mb. Figure C6 shows ~12 snow events with snow mixing ratio greater than 0.1 g/kg. It is apparent that in the big events, such as event 1 and 11, the start of the event is not seedable due to warm temperatures. In some cases, such as events 2, 6 and 7), snow events are not seedable as temperatures are too cold. As shown in Figure C8 for January 2008, the narrow distribution of temperature in seed cases imposes an intermittent duration in the seedability of snow events identified in Figure C6.

Table C1. Plots produced by analysis of 2a-2c criteria for Target Area 2

Plot type for target area	month	season	units
750 mb – mean T, mac Qc, max Qs, max Qi, 1 hr precip, mean WD	✓	✓	as in Fig. 6
700 mb – mean T, mac Qc, max Qs, max Qi, 1 hr precip, mean WD	✓	✓	
650 mb – mean T, mac Qc, max Qs, max Qi, 1 hr precip, mean WD	✓	✓	
600 mb – mean T, mac Qc, max Qs, max Qi, 1 hr precip, mean WD	✓	✓	
Temperature stability profile – out of cloud	✓	✓	°C
Temperature stability profile – in-cloud	✓	✓	°C
Mean wind speed histogram – seed	✓	✓	ms ⁻¹
Mean wind speed histogram – non-seed	✓	✓	ms ⁻¹
Mean wind speed histogram – all	✓	✓	ms ⁻¹
Mean wind direction histogram – seed	✓	✓	deg
Mean wind direction histogram – non-seed	✓	✓	deg
Mean wind direction histogram – all	✓	✓	deg
Mean temperature histogram – seed	✓	✓	°C
Mean temperature histogram – non-seed	✓	✓	°C
Mean temperature histogram – all	✓	✓	°C
Maximum snow mixing ratio histogram – seed	✓	✓	g kg ⁻¹
Maximum snow mixing ratio histogram – non-seed	✓	✓	g kg ⁻¹
Maximum snow mixing ratio histogram – all	✓	✓	g kg ⁻¹
Maximum ice mixing ratio histogram – seed	✓	✓	g kg ⁻¹
Maximum ice mixing ratio histogram – non-seed	✓	✓	g kg ⁻¹
Maximum ice mixing ratio histogram – all	✓	✓	g kg ⁻¹
Maximum cloud water mixing ratio histogram – seed	✓	✓	g kg ⁻¹
Maximum cloud water mixing ratio histogram – non-seed	✓	✓	g kg ⁻¹
Maximum cloud water mixing ratio histogram – all	✓	✓	g kg ⁻¹

Table C2. Mean values for variables produced by analysis of 2a-2c criteria for target area for 2000-2001 season. The values in each of the columns in the format 'x1,x2,x3' represents the mean value (x1), the non-seed mean value (x2) and the seed mean value (x3). Units as in Table C1.

2000-2001 season	Season	November	December	January	February	March	April
600mb mean wind speed	14, 13, 16	9, 8, 13	16, 16, 17	12, 11, 14	17, 17, 16	11, 11, 14	15, 15, 16
600mb mean wind direction	222, 219, 231	222, 215, 261	228, 224, 241	228, 222, 261	177, 181, 170	269, 260, 293	162, 155, 208
600mb mean temperature	-12.8,-11.8,-16.0	-8.5, -7.2, -16.6	-14, -12.9, -16.9	-13.4, -12.8, -17	-14.1, -13.2, -15.4	-12.6, -11.4, -16	-9.1, -8.3, -14.8
600mb max snow mr	0.16, 0.12, 0.32	0.16, 0.14, 0.26	0.08, 0.04, 0.22	0.09, 0.06, 0.26	0.19, 0.14, 0.26	0.19, 0.14, 0.33	0.29, 0.27, 0.44
600mb max ice mr	0, 0, 0	0, 0, 0	0, 0, 0	0, 0, 0	0, 0, 0	0, 0, 0	0, 0, 0
600mb max cloud water mr	0.12, 0.06, 0.29	0.09, 0.07, 0.23	0.08, 0.02, 0.27	0.04, 0.01, 0.2	0.16, 0.08, 0.29	0.15, 0.08, 0.33	0.16, 0.14, 0.31
650mb mean wind speed	10, 10, 12	7, 7, 10	12, 11, 13	9, 9, 11	12, 12, 12	9, 8, 11	11, 11, 13
650mb mean wind direction	207, 207, 207	211, 205, 249	211, 209, 216	238, 237, 245	153, 161, 141	251, 238, 285	152, 145, 199
650mb mean temperature	-9.9, -9.1, -12.4	-5.2, -3.9, -13.3	-11.5, -10.7, -13.8	-11, -10.5, -13.7	-11, -10.5, -11.7	-9.4, -8.4, -12.3	-5, -4.2, -10.9
650mb max snow mr	0.17, 0.11, 0.37	0.17, 0.14, 0.34	0.1, 0.04, 0.28	0.1, 0.06, 0.32	0.19, 0.13, 0.29	0.2, 0.13, 0.41	0.28, 0.24, 0.53
650mb max ice mr	0, 0, 0	0, 0, 0	0, 0, 0	0, 0, 0	0, 0, 0	0, 0, 0	0, 0, 0
650mb max cloud water mr	0.17, 0.11, 0.35	0.13, 0.1, 0.31	0.13, 0.07, 0.32	0.09, 0.05, 0.3	0.21, 0.13, 0.33	0.27, 0.22, 0.4	0.17, 0.12, 0.45
700mb mean wind speed	6, 5, 8	4, 4, 6	6, 5, 9	4, 4, 7	7, 6, 7	5, 4, 7	7, 7, 8
700mb mean wind direction	166, 163, 176	177, 172, 212	156, 152, 169	193, 193, 198	132, 133, 130	191, 177, 231	147, 142, 181
700mb mean temperature	-6.7, -6.1, -8.5	-1.9, -0.7, -9.6	-8.7, -8.3, -10.2	-8.5, -8.2, -9.9	-7.7, -7.5, -8	-6, -5.2, -8.3	-0.9, 0, -6.8
700mb max snow mr	0.12, 0.07, 0.27	0.13, 0.11, 0.26	0.07, 0.03, 0.22	0.07, 0.04, 0.24	0.13, 0.08, 0.21	0.14, 0.08, 0.28	0.18, 0.15, 0.41
700mb max ice mr	0, 0, 0	0, 0, 0	0, 0, 0	0, 0, 0	0, 0, 0	0, 0, 0	0, 0, 0

700mb max cloud water mr	0.06, 0.04, 0.14	0.05, 0.04, 0.1	0.06, 0.03, 0.12	0.04, 0.02, 0.12	0.09, 0.05, 0.15	0.09, 0.08, 0.14	0.05, 0.03, 0.2
750mb mean wind speed	3, 3, 5	3, 3, 4	3, 3, 5	3, 2, 4	4, 3, 4	3, 3, 4	5, 5, 5
750mb mean wind direction	148, 153, 134	163, 165, 151	143, 147, 130	166, 171, 136	129, 134, 121	159, 160, 157	144, 146, 131
750mb mean temperature	-4.0, -3.7, -5.2	1.1, 2.2, -6.3	-6.6, -6.4, -7.2	-6.5, -6.5, -6.7	-5.1, -5.2, -4.9	-3.1, -2.5, -4.7	2.9, 3.8, -3.3
750mb max snow mr	0.04, 0.02, 0.1	0.04, 0.03, 0.11	0.03, 0.01, 0.09	0.02, 0.01, 0.09	0.05, 0.03, 0.08	0.03, 0.02, 0.09	0.06, 0.04, 0.18
750mb max ice mr	0, 0, 0	0, 0, 0	0, 0, 0	0, 0, 0	0, 0, 0	0, 0, 0	0, 0, 0
750mb max cloud water mr	0, 0, 0.11	0, 0, 0	0, 0, 0	0, 0, 0	0, 0, 0	0, 0, 0	0, 0, 0.1

Table C3. Mean values for variables produced by analysis of 2a-2c criteria for target area for 2007-2008 season. The values in each of the columns in the format 'x1,x2,x3' represents the mean value (x1), the non-seed mean value (x2) and the seed mean value (x3). Units as in Table C1.

2007-2008 season	Season	November	December	January	February	March	April
600mb mean wind speed	16, 16, 17	15, 15, 13	17, 17, 17	18, 17, 20	16, 16, 17	16, 16, 15	16, 16, 15
600mb mean wind direction	219, 214, 233	233, 232, 252	212, 216, 192	227, 229, 222	244, 244, 244	211, 203, 233	189, 165, 254
600mb mean temperature	-13.5, -12.4, -16.9	-8.1, -7.4, -18.9	-15.1, -14.9, -16.1	-16.8, -16.3, -17.8	-15.1, -13.8, -16.7	-14.1, -13.3, -16.3	-11.7, -9.9, -16.6
600mb max snow mr	0.16, 0.1, 0.35	0.04, 0.02, 0.33	0.2, 0.16, 0.35	0.21, 0.14, 0.37	0.18, 0.1, 0.27	0.18, 0.1, 0.41	0.16, 0.07, 0.39
600mb max ice mr	0, 0, 0	0, 0, 0	0, 0, 0	0, 0, 0	0, 0, 0	0, 0, 0	0, 0, 0
600mb max cloud water mr	0.11, 0.05, 0.28	0.04, 0.02, 0.26	0.12, 0.09, 0.26	0.12, 0.05, 0.25	0.16, 0.06, 0.29	0.12, 0.05, 0.3	0.1, 0.03, 0.29
650mb mean wind speed	12, 12, 12	11, 11, 10	13, 13, 13	13, 12, 15	12, 11, 13	11, 11, 11	11, 12, 10
650mb mean wind direction	202, 196, 219	214, 211, 270	191, 195, 173	200, 207, 183	221, 221, 221	207, 194, 242	178, 149, 257
650mb mean temperature	-10.6, -9.7, -13.4	-5.1, -4.5, -14.8	-12.7, -12.7, -12.8	-14.1, -14, -14.3	-12.4, -11.6, -13.4	-11.0, -10.5, -12.6	-8.2, -6.5, -13
650mb max snow mr	0.17, 0.1, 0.38	0.04, 0.02, 0.39	0.22, 0.18, 0.39	0.23, 0.15, 0.4	0.2, 0.1, 0.32	0.18, 0.1, 0.4	0.15, 0.06, 0.41
650mb max ice mr	0, 0, 0	0, 0, 0	0, 0, 0	0, 0, 0	0, 0, 0	0, 0, 0	0, 0, 0
650mb max cloud water mr	0.15, 0.09, 0.32	0.05, 0.04, 0.26	0.17, 0.14, 0.3	0.16, 0.09, 0.31	0.21, 0.12, 0.31	0.17, 0.1, 0.34	0.14, 0.06, 0.35
700mb mean wind speed	7, 6, 8	6, 6, 7	7, 7, 8	7, 6, 10	7, 6, 8	6, 6, 7	6, 6, 7
700mb mean wind direction	162, 153, 188	169, 164, 263	159, 158, 161	149, 154, 138	171, 159, 187	160, 146, 199	165, 138, 239
700mb mean temperature	-7.5, -6.7, -9.7	-1.5, -1, -10.5	-9.8, -9.9, -9.4	-11.2, -11.4, -10.8	-9.3, -9, -9.8	-7.9, -7.4, -9	-4.8, -3.2, -9.2
700mb max snow mr	0.13, 0.07, 0.27	0.03, 0.01, 0.27	0.17, 0.14, 0.3	0.17, 0.12, 0.3	0.14, 0.08, 0.22	0.13, 0.07, 0.28	0.11, 0.04, 0.3
700mb max ice mr	0, 0, 0	0, 0, 0	0, 0, 0	0, 0, 0	0, 0, 0	0, 0, 0	0, 0, 0

700mb max cloud water mr	0.06, 0.03, 0.12	0.01, 0.01, 0.08	0.07, 0.06, 0.13	0.07, 0.03, 0.14	0.08, 0.05, 0.12	0.05, 0.04, 0.11	0.05, 0.02, 0.12
750mb mean wind speed	4, 4, 5	4, 4, 5	4, 4, 6	4, 3, 6	4, 3, 5	4, 4, 5	4, 4, 4
750mb mean wind direction	140, 140, 140	138, 134, 208	133, 134, 131	127, 135, 110	138, 139, 138	140, 140, 143	161, 158, 172
750mb mean temperature	-4.8, -4.2, -6.6	1.9, 2.4, -6.5	-7.4, -7.6, -6.4	-9, -9.4, -8	-6.9, -6.9, -6.8	-5.3, -5.1, -5.9	-2, -0.6, -5.6
750mb max snow mr	0.05, 0.03, 0.1	0.01, 0, 0.09	0.07, 0.06, 0.14	0.07, 0.05, 0.11	0.05, 0.03, 0.08	0.05, 0.02, 0.11	0.04, 0.01, 0.11
750mb max ice mr	0, 0, 0	0, 0, 0	0, 0, 0	0, 0, 0	0, 0, 0	0, 0, 0	0, 0, 0
750mb max cloud water mr	0, 0, 0	0, 0, 0	0, 0, 0	0, 0, 0	0, 0.01, 0	0, 0, 0	0, 0, 0

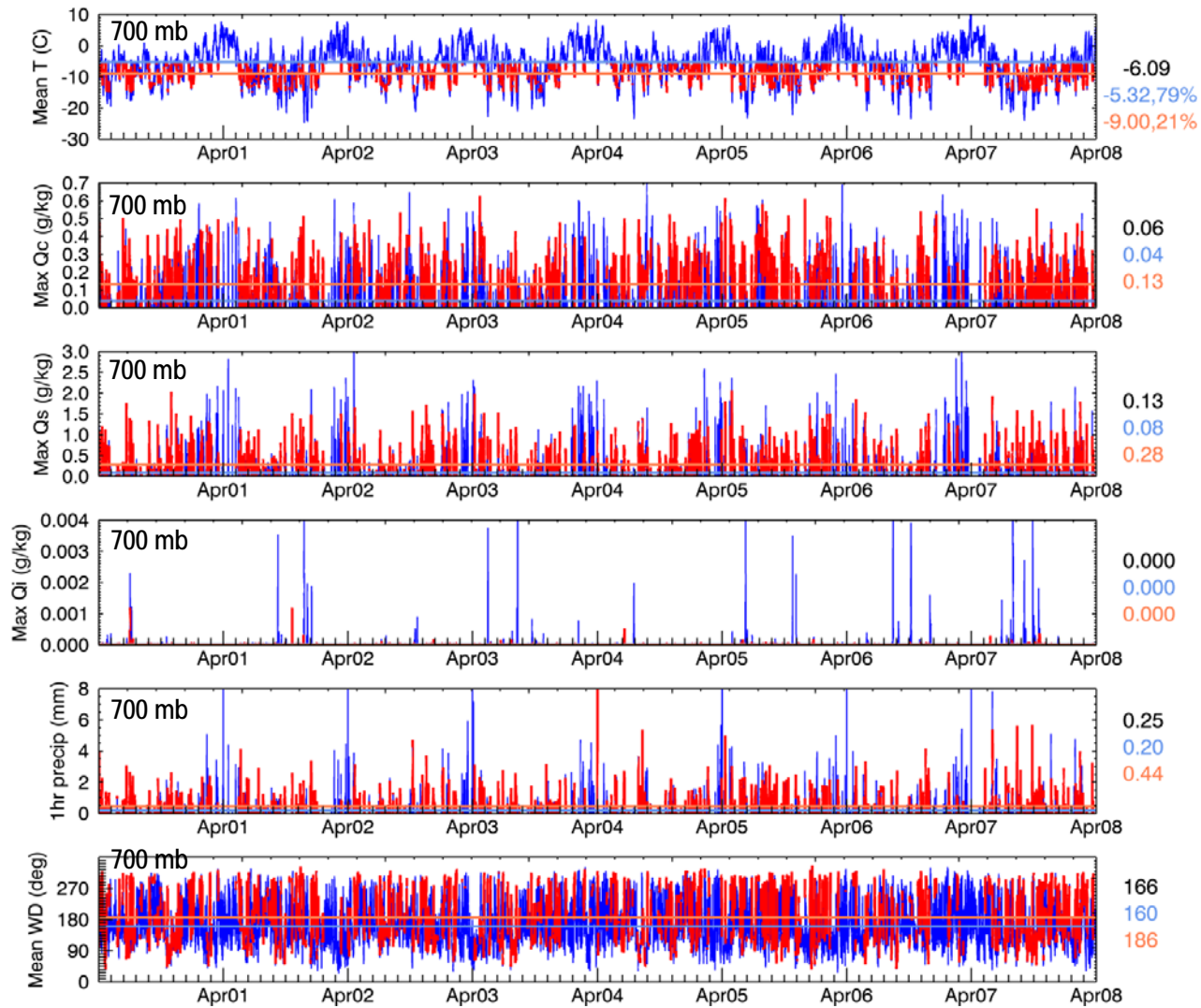


Figure C1. Mean temperature, maximum cloud water mixing ratio, maximum snow mixing ratio, maximum ice mixing ratio, 1-hour precipitation and mean wind direction at 700 mb for all seasons (Nov 2000 – Apr 2008). The numbers on the right side show the overall, non-seed, and seed mean values (top to bottom). The red trace indicates that the seeding criteria 2a-2c were met.

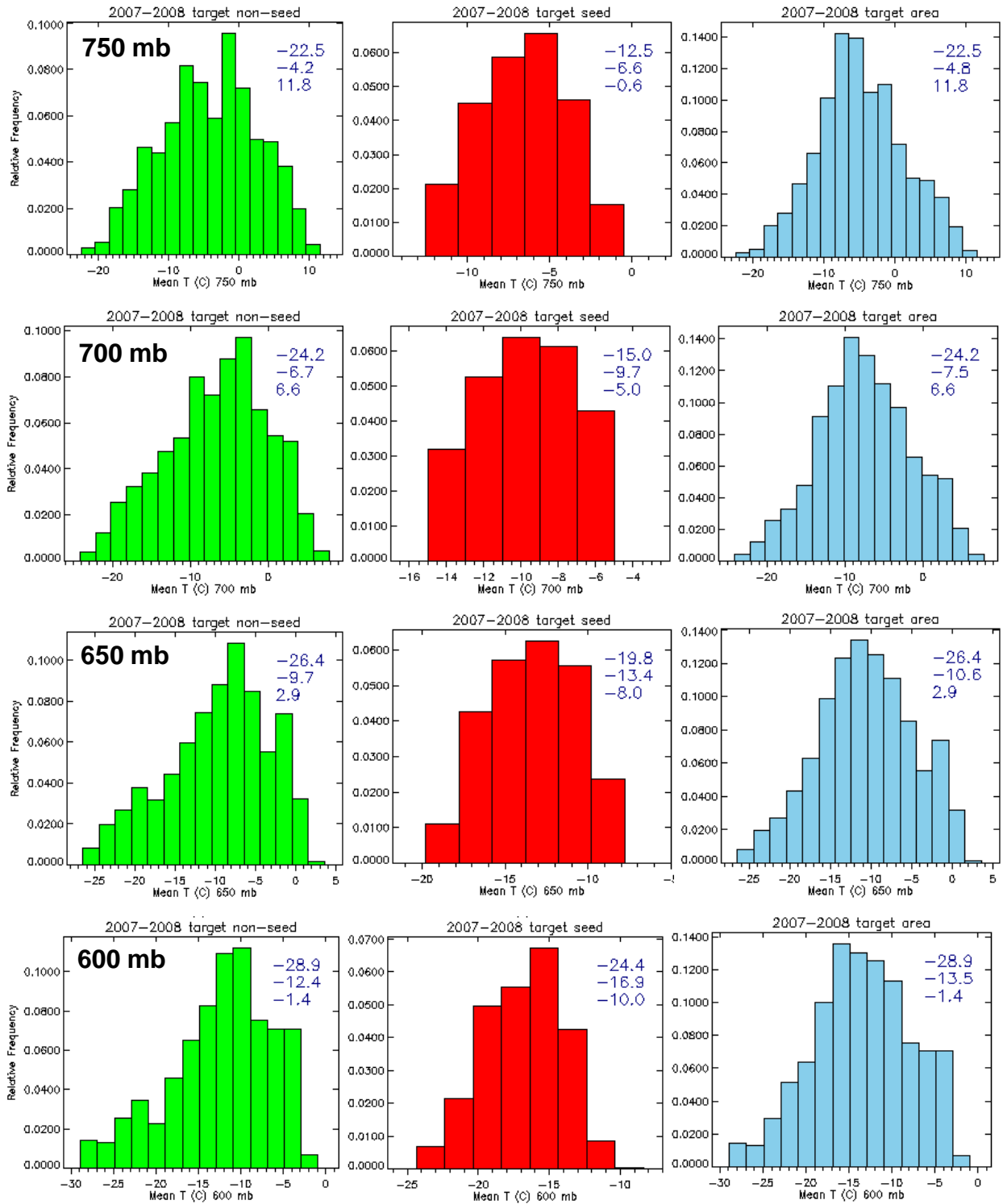


Figure C2. Mean temperature plots during the 2007-2008 season with non-seed cases (left), seed cases (middle), all days (right) at, top to bottom, 750, 700, 650, and 600 mb. The minimum, mean and maximum temperatures are printed in the upper right corner of each plot.

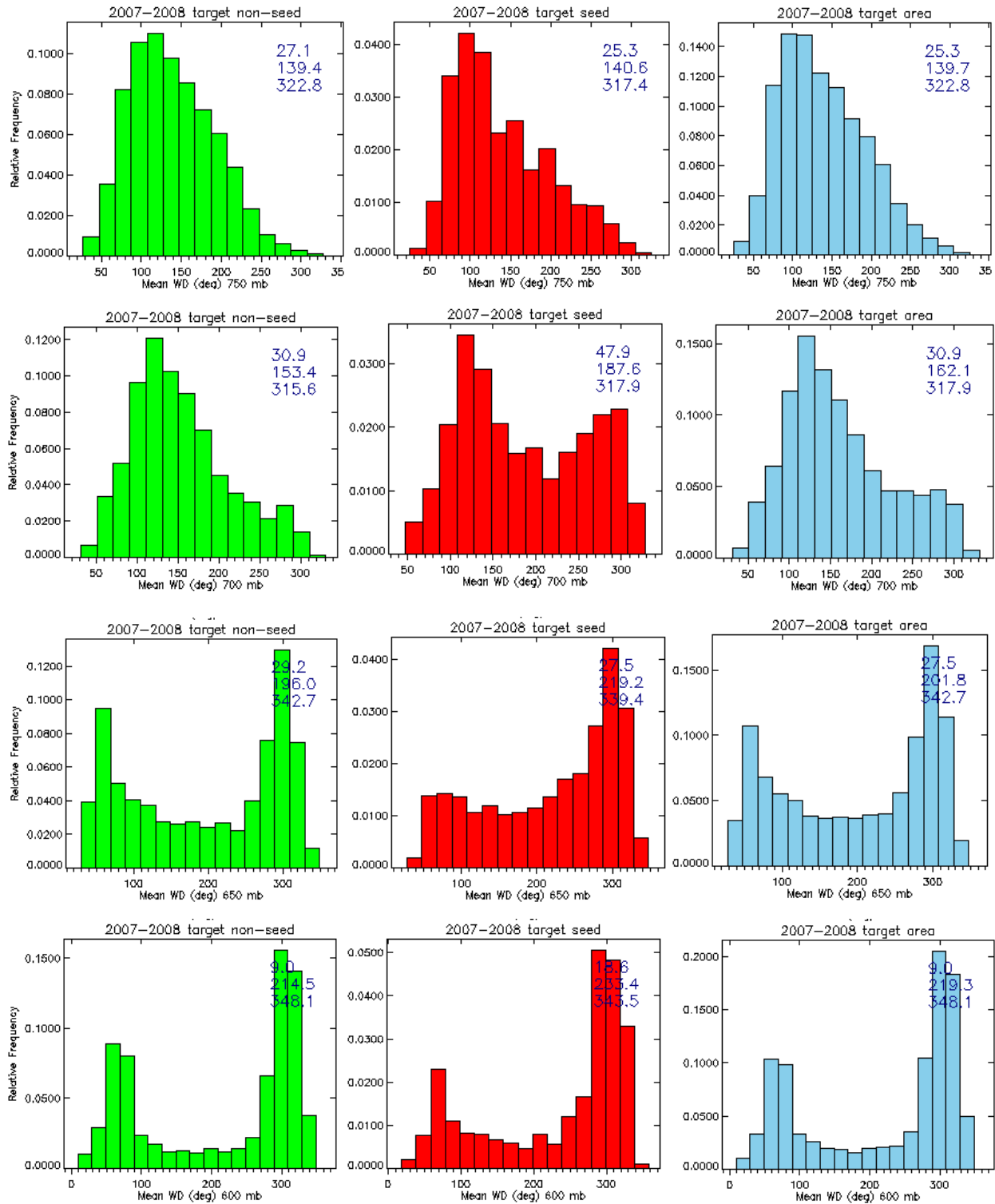


Figure C3. As in Figure C2 for wind direction during the 2007-2008 season.

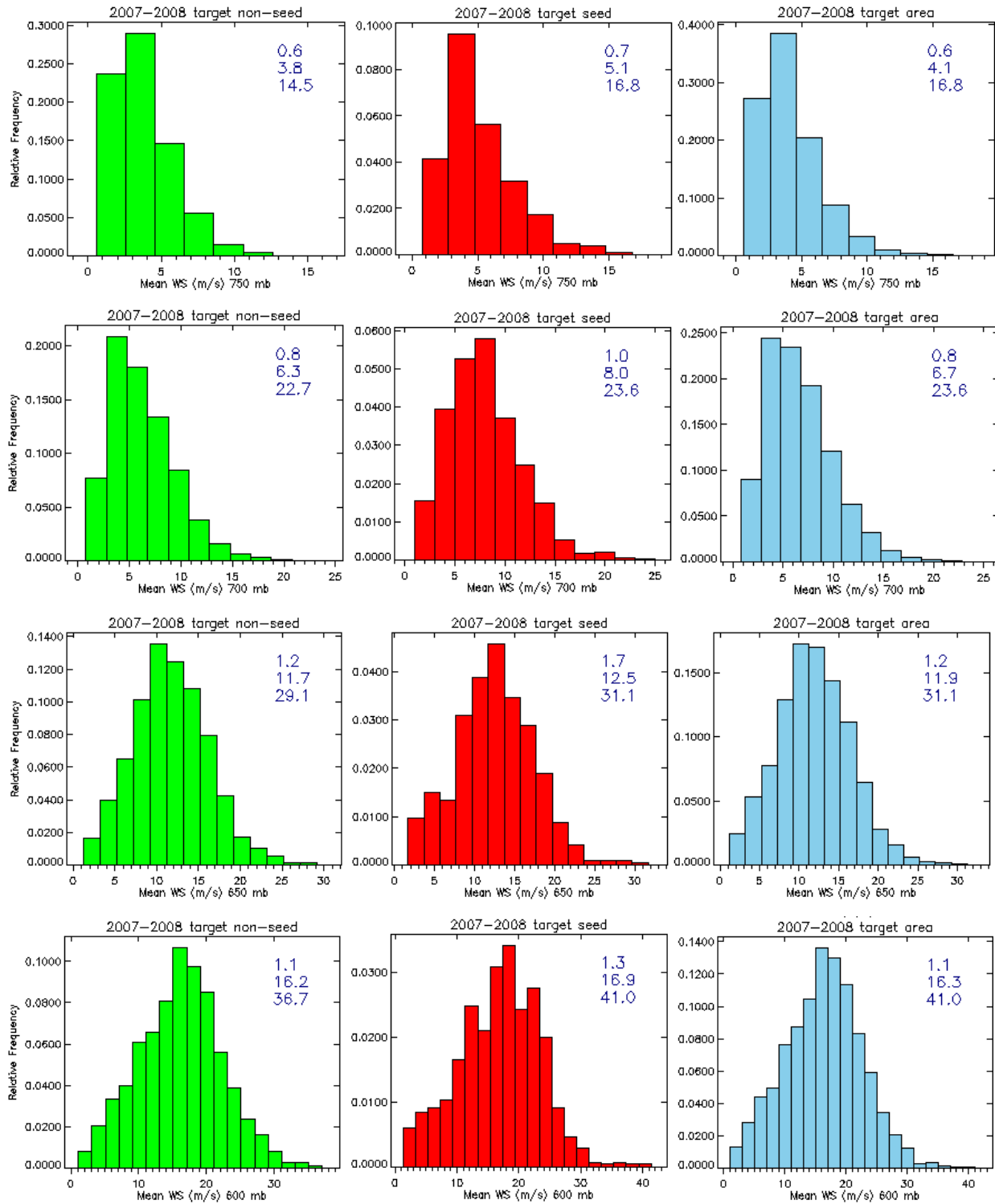


Figure C4. As in Figure C2 for wind speed during the 2007-2008 season.

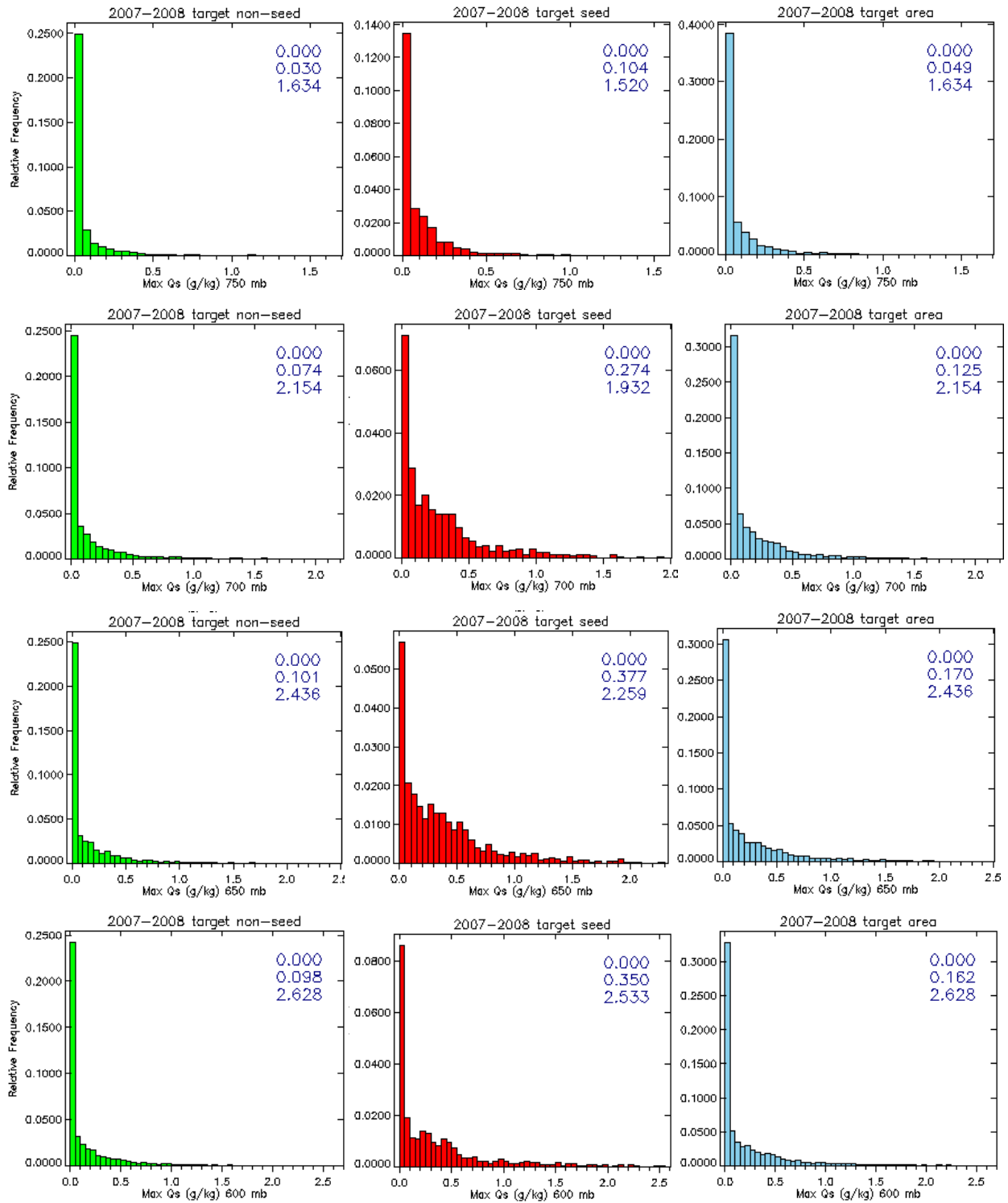


Figure C5. As in Figure C2 for snow mixing ratio during the 2007-2008 season.

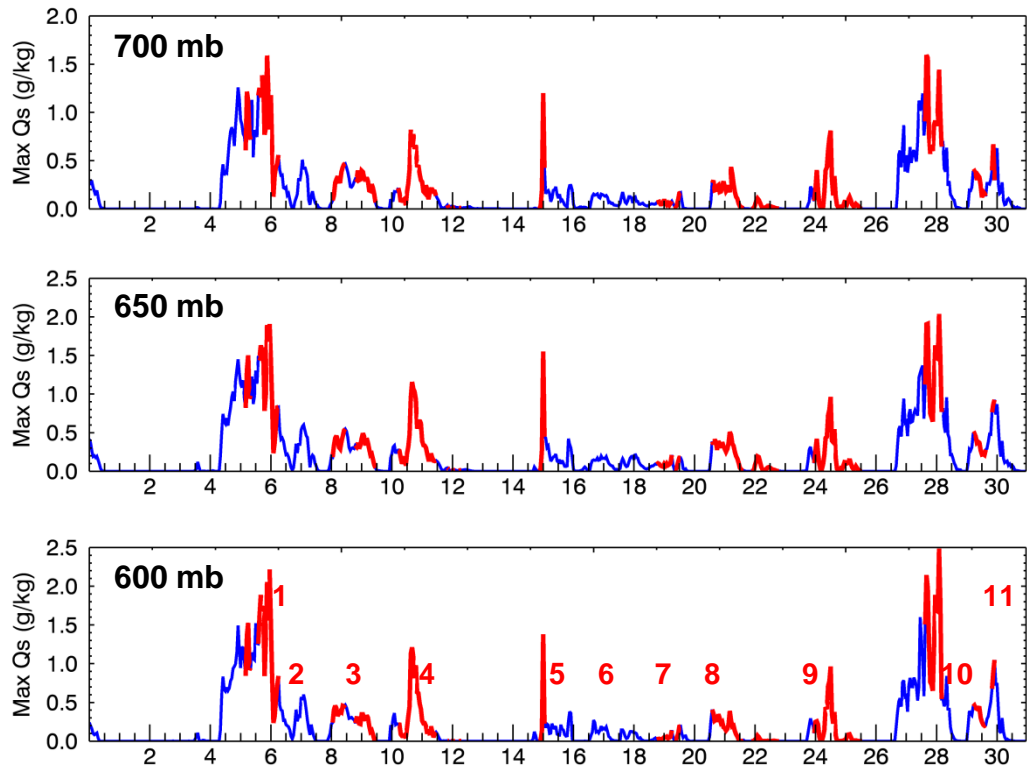


Figure C6. January 2008 maximum snow mixing ratio at 700, 650, and 600 mb.

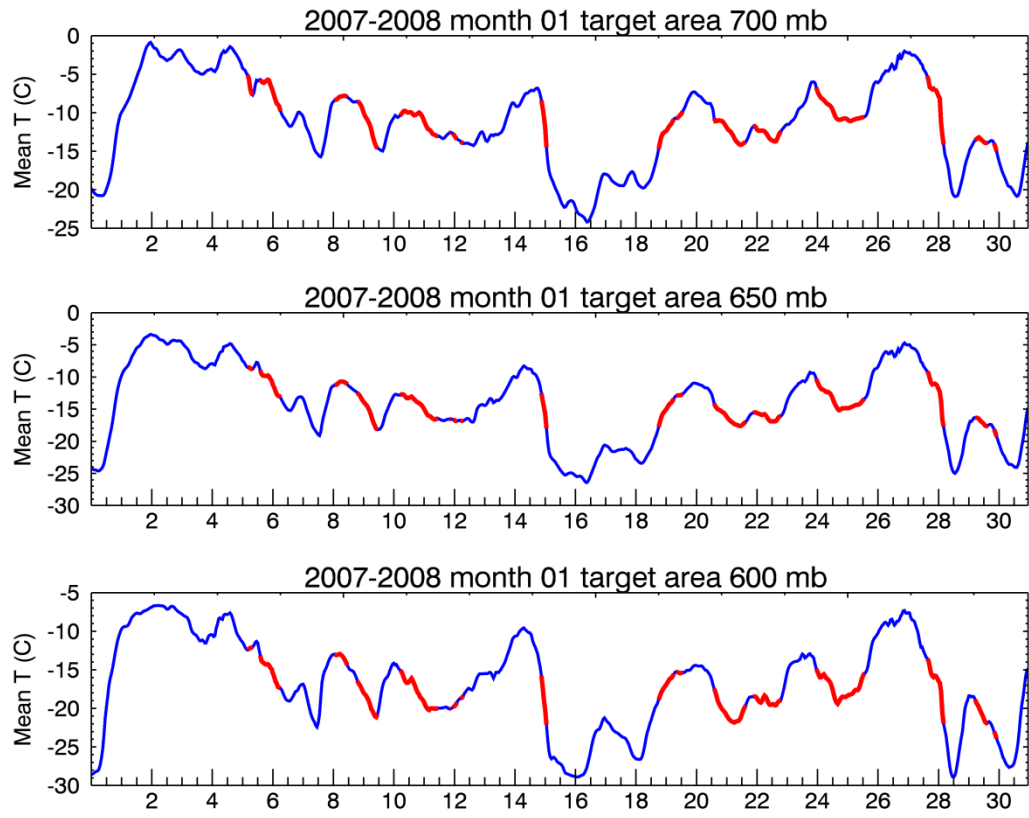


Figure C7. January 2008 mean temperature at 700, 650, and 600 mb.

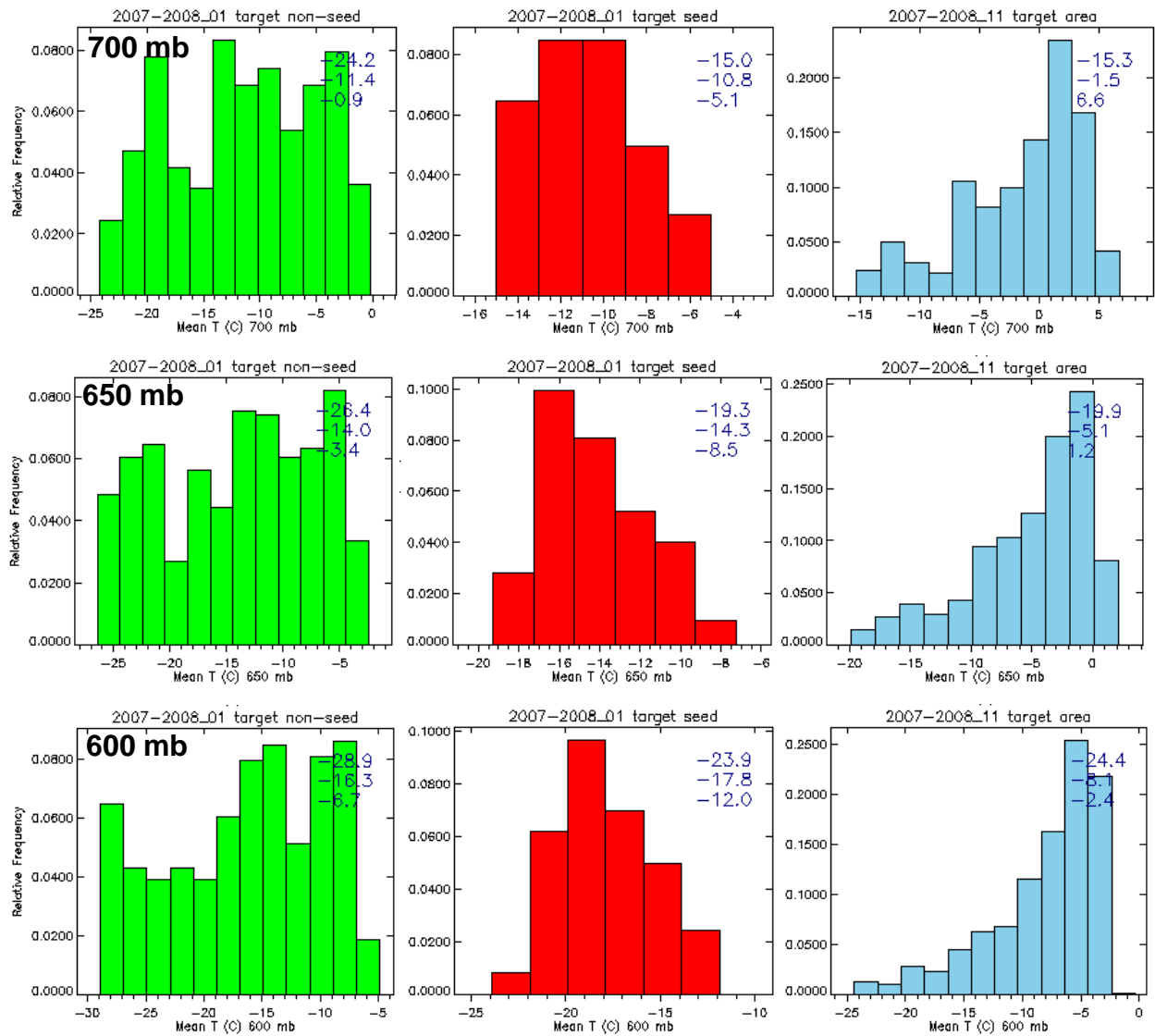


Figure C8. January 2008 histograms of mean temperature with non-seed cases (left), seed cases (middle) and all (right) days. The minimum, mean and maximum temperatures are printed on the upper right corner of each plot.

Climatology of seedable and non-seedable areas

The spatial analysis produces statistics on each grid point over the re-sampled domain. These statistics were produced for each month and each season starting November 2000 and ending April 2008. Table C4 shows a list of plots produced by this analysis. In this case, 12 plots were produced for each month and 3 plots for each season totaling 600 plots.

An example of spatial maps for the eight-year period (2000-2008) is shown for select variables in Figure C9. All the plots except mean temperature at 600 mb, which is above all ground grid points, show strong correlations to the topography.

Table C4. *Plots produced by analysis of 3a-3e criteria for re-sampled domain*

Contour plot type for re-sampled domain	month	season	units
10 m mean wind speed	✓		m/s
10 m mean wind direction	✓		degrees
600 mb mean temp	✓		°C
600 mb mean cloud water mixing ratio	✓		g kg ⁻¹
650 mb mean cloud water mixing ratio	✓		g kg ⁻¹
Snow water gain	✓	✓	in
Frequency when 10-m wind 280° < dir < 341°; speed < 17.9 m s ⁻¹	✓		hours
Frequency with no stable layers (stability criterion 2c not met)	✓		hours
Frequency when 600 mb -16.7 °C > temp > -26.7 °C	✓		hours
Frequency when cloud present at 650 mb or 600 mb	✓		hours
Frequency 3a-3e seed criteria satisfied	✓	✓	hours
Seed potential	✓	✓	%

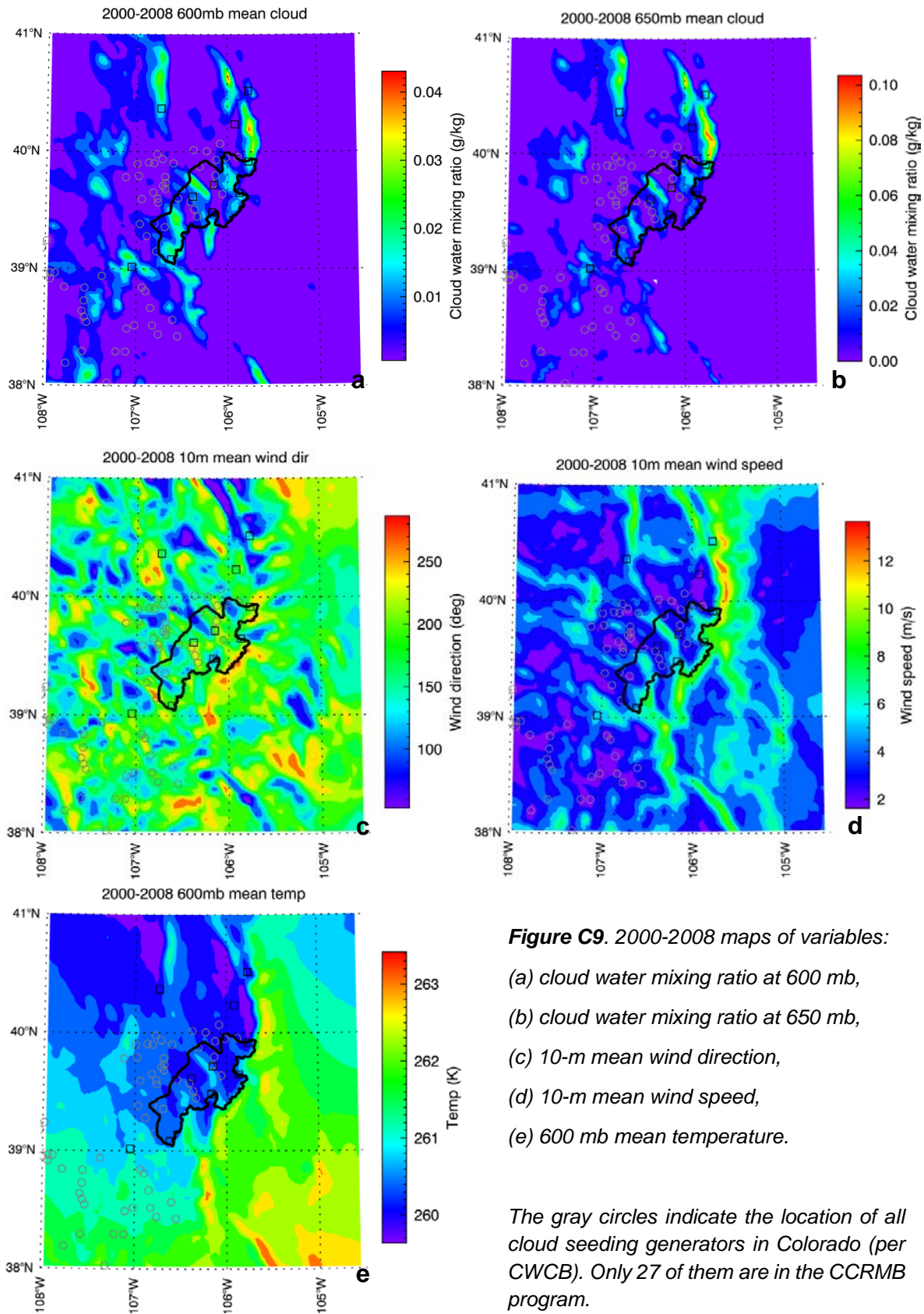


Figure C9. 2000-2008 maps of variables:

- (a) cloud water mixing ratio at 600 mb,
- (b) cloud water mixing ratio at 650 mb,
- (c) 10-m mean wind direction,
- (d) 10-m mean wind speed,
- (e) 600 mb mean temperature.

The gray circles indicate the location of all cloud seeding generators in Colorado (per CWCB). Only 27 of them are in the CCRMB program.

Appendix D: High-resolution WRF Model Setup

WRF model setup

- WRF version 3.5.1
- Two one-way nested domains consisting of a 4-km grid (318 × 268 grid points) and a 0.8-km grid (301 × 301 grid points)
- 51 vertical levels topped at 100 hPa (or mb)
- 36-hour simulation, starting from 28 January 2013, 0000 UTC
- Microphysics: Thompson scheme
- Convective scheme: none (explicitly resolved)
- PBL (planetary boundary layer – lowest levels): Yonsei University (YU) scheme
- Radiation: RRTMG scheme (a radiation transfer model)
- Surface layer: Revised MM5 surface layer scheme
- Land surface: Noah-MP land-surface model
- Forcing data: NARR (North American Regional Reanalysis data)
- Other features: MODIS (satellite) green fraction; terrain slope impact on radiation

Domain configuration

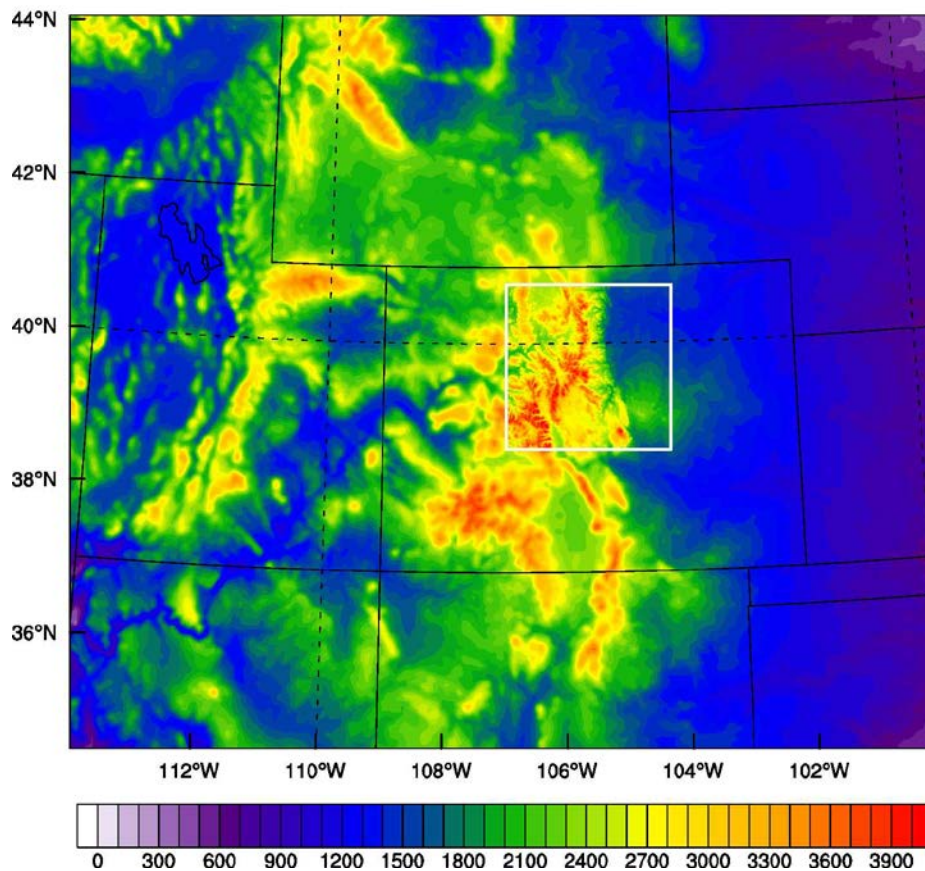


Figure D1. 4-km and nested 800-m domains – same as Figure 4.2.